

**Agricultural Features Recognition System Using UAV:
A Machine Learning Approach for Precision Agriculture**

January 2019

Pengbo GAO

Agricultural Features Recognition System Using UAV:
A Machine Learning Approach for Precision Agriculture

A Dissertation Submitted to
the Graduate School of Life and Environmental Sciences,
the University of Tsukuba
in Partial Fulfillment of the Requirements
for the Degree of Doctor of Philosophy in Bioresource Engineering
(Doctoral Program in Appropriate Technology and Sciences for Sustainable Development)

Pengbo GAO

Abstract

Unmanned Aerial Vehicle (UAV) significantly involved decision-making process through high resolution mapping in precision agriculture. To enable artificial intelligence in precision agricultural management using UAV, classification and recognition of features, precision application of pesticides, watering according to soil moisture content and object localization are very important for UAV system that built with smaller payload and limited battery life. The objectives of this research are first, to develop machine learning systems for recognizing the classifiers as spraying and nonspraying areas for precision application of fertilizer and pesticide; second, soil moisture distribution for precision irrigation management; and third, object localization to enable transportation logistics coordinated with UAV. To achieve the research objectives, the author developed the sensors networking system, Mutual Subspace Method (MSM) machine learning algorithm for recognizing the classifiers, data acquisition procedure from RGB and thermal cameras; and field reference data calibration procedures. The datasets were collected for the green onion, cabbage and carrots as regular winter crops for some randomly selected agricultural fields from Ibaraki prefecture. In addition, sensors data communication protocol also established between Electronic Platooning Vehicles (EPV) for coordination with UAV.

The MSM machine learning system has implemented that has the advantage of high computational speed with good accuracy for recognizing spray and nonspray areas for application in UAV-based sprayers in agricultural fields and orchards. Two classifiers, one for agricultural croplands and one for orchard areas, based on the MSM machine learning system were trained and tested with datasets of images to enable an autonomous spraying system for UAV. The field experiments were conducted in different types of fields to train and test the system in the selection of croplands and orchards using a commercial UAV (DJI Phantom 3 Pro) with an on-board 4K camera. The classifiers were sub-categorized to address spray and nonspray areas, and images were collected from low (5 m) and high (15 m) altitudes for croplands and orchards, respectively. The recognition system was divided into offline and online systems for recognition of classifiers. The offline recognition system shows the effectiveness of MSM systems for training and testing with datasets for croplands and orchards. In the offline recognition system, 70% accuracy was obtained for the cropland classifiers in recognizing spray and nonspray areas. In the case of orchards, the spray and nonspray

recognition accuracy was 77%. The online recognition system performance had higher recognition accuracy for low-altitude data (84%) than high-altitude data (68%). The computational time for the online recognition system was minimal, with an average of 0.004 s for classifiers reporting recognition of each of the frames. The high accuracy of the recognition system was obtained using the MSM and training and testing with datasets from three different types of selected agricultural fields. The developed machine learning system had a recognition accuracy of 70% using the classifiers, which can be implemented in an autonomous UAV spray system for recognizing spray and nonspray areas within the minimum computational requirements for real-time application.

The soil moisture content was estimated at the topsoil surface using thermal images and proposed a method to measure field moisture based on the radiometric calibration from thermal camera images. Indoor and outdoor experiments were conducted to confirm the accuracy of soil moisture detection from top surfaces of soil from collected samples at the different moisture levels during the indoor experiments. The monolithic analysis was conducted to find the correlation of soil moisture and the digital numbers of thermal images. The higher accuracy was obtained in the indoor ($R^2=0.85$) and outdoor ($R^2=0.79$) experiments. To develop a soil moisture map from the thermal camera, mosaic was performed using two types of features: ORB (Oriented FAST and Rotated BRIEF) and SURF (Speeded-Up Robust Features). The mosaic performances of ORB features and SURF features were compared for thermal images. SURF features could easily detect the features from thermal images with high accuracy of matching. The mosaic was done for multiple thermal images with SURF features using Python2.7® and OpenCV®. The average mosaic accuracy for two adjacent thermal images was 61.4% for ORB and 89.7% for SURF features.

The UAV-follower system was proposed with the autonomous EPV that could follow the UAV (map-based or target tracking). The experimental and simulation data were used to recognize ORB features using 3D RGB camera to reduce noise by eliminating the unnecessary features. Reducing unnecessary features are required to enable adaptive local navigation for UAV-EPV coordination. The simulation result showed that 36% of invalid features could be reduced using extended Kalman filter. In the navigation planer, the EPVs were in lined as leader-follower formation in road navigation to support transportation of agricultural products. The EPV platform was built to test recognition of features and 3D-based image acquisition, ORB features extraction from UAV had higher accuracy in edge detection for navigation planner.

Therefore, the core of this research contributed to develop the machine learning system for the classification to recognize features of spraying and nonspraying areas using MSM. Higher accuracy of recognition and robust computation time to recognize the spray and nonspray area could be implemented in the real time application of UAV-based autonomous sprayer. The calibration and mosaic of features for thermal images were conducted in indoor and outdoor experiments for soil moisture detection. Furthermore, the coordination between the UAV and EPV was proposed based on the ORB features for autonomous transportation logistics in the farm.

Keywords: *Precision Agriculture, Recognition System, Image Classifiers, Machine Learning System, Autonomous Navigation, UAV*

List of Contents

Abstract		i
List of Contents		iv
Nomenclature		viii
List of Tables		ix
List of Figures		x
Chapter 1	Introduction	1
1.1	Feature Recognition	1
1.2	Machine Learning System	1
1.3	Mapping and Sensing Systems	1
1.4	Application of Sensing System	2
1.5	Problem Statements	2
1.6	Research Questions	2
1.7	Research Objectives	3
1.8	Significance	3
1.9	Outlines of Thesis Structure	4
Chapter 2	Review of Literature	6
2.1	Studies Related to Feature Recognition System from the Images Takes from UAV to Complete Agricultural Operations	6
2.2	Studies Related to Machine Learning System	9
2.3	Studies related to Mapping and Sensing Systems	9
2.4	Studies Related to Application of Sensing System	10
2.5	Summary	14
Chapter 3	Development of Recognition System for Spraying Area	

	from UAV Using Machine Learning Approach	15
3.1	Background	15
3.2	Materials and Methods	17
	3.2.1 Mutual Subspace Method (MSM)	17
	3.2.2 Research Design for Classifiers and MSM	19
	3.2.3 Field Experiment for Training and Testing with Datasets	20
	3.2.4 Online Recognition System	23
	3.2.5 Online Recognition System	25
3.3	Results	26
	3.3.1 Offline Recognition Performance	26
	3.3.2 Online Recognition Performance	28
3.4	Discussion	32
3.5	Conclusions	33
3.6	Summary	33
Chapter 4	Thermal Images Acquisition with UAV for Soil Surface Moisture Monitoring	35
4.1	Background	35
4.2	Introduction	37
	4.2.1 ORB Features Detection and Matching	37
	4.2.2 SURF Features Detection and Matching	38
4.3	Materials and Methods	39
	4.3.1 Image Mosaic and Feature Detection for Estimating Soil Moisture	39
	4.3.2 Thermal Images Acquisition Platform	40
	4.3.3 Calibration Method	40
	4.3.4 Thermal Images Mosaicking with ORB Features	47
	4.3.5 Thermal Images Mosaicking with SURF Features	47
	4.3.6 Soil Moisture Distribution Map	48

4.4	Results	48
4.4.1	Soil Moisture Detection	48
4.4.2	Features Detection and Matching	49
4.4.3	Mosaicking of Thermal Images Using SURF Features	51
4.4.4	Mosaicking of RGB Images and Thermal Images of the Field	53
4.5	Discussion	54
4.5	Summary	54
Chapter 5	Development of UAV-Follower based Multi-task Robots System Using Features Recognition and Navigation Planner	56
5.1	Background	56
5.2	Materials and Materials	59
5.2.1	ORB-SLAM	59
5.2.2	Image Edge Detection	59
5.2.2.1	Sobel Operator	60
5.2.2.2	Robert's Cross Operator	61
5.2.2.3	Canny Edge Detector	61
5.2.2.4	Gaussian Filter	62
5.2.2.5	Edge Tracking by Hysteresis	62
5.2.3	Development of The Navigation System	63
5.2.4	Development of Autonomous Electrical Vehicle	64
5.2.5	Development of Autonomous Spraying System	64
5.2.6	Choice of Work Patterns	65
5.2.7	Plants Edge Detection Using Canny Edge Detector	66
5.2.8	Images Mosaicking for Local Mapping	66
5.3	Results	66
5.3.1	ORB Features Extraction and Matching	66
5.3.2	ORB-SLAM Simulation	67

5.3.3	Plants Edge Detection Using Canny Edge Detector	67
5.3.4	UAV Features Mapping for Developing Navigation Planner	69
5.4	Discussion	70
5.5	Summary	70
Chapter 6	Conclusions and Further Research	72
6.1	Development of a Machine Learning System with High Computational Speed for Recognizing Feature	72
6.2	Detection Soil Moisture Content from Thermal Images	72
6.3	Vision based Target Spray System from Autonomous Agricultural Vehicle	73
6.4	Further Research	73
6.4.1	Automated Field Moisture Determination using Wireless Sensor Network (WSN)	73
6.4.2	UAV and Multi-robot SWARM Application	74
6.5	Outlook of Future Agriculture	74
	Acknowledgements	75
	References	76

Nomenclature

PCA	Principal Component Analysis
KPCA	Kernel Principal Component Analysis
SM	Subspace Method
MSM	Mutual Subspace Method
KMSM	Kernel Mutual Subspace Method
ORB	Oriented FAST and rotated BRIEF feature
SURF	Speeded Up Robust Features
P	Reference Subspace Registered as Dictionary
Q	Input Subspace Obtained from the Input Data
C	Covariance Matrix from k Feature Vectors
M	Number of Image Sequence
N	Number of Image Sequence
X	n-dimensional Input Patterns
K_{ij}	Gaussian Kernel Function
C	Center of Mass of the Patch
d	Dimensionality of the Subspace Used for Recognition
s	A Free Parameter of Gaussian Kernel
u_i	Eigenvectors in the Reference Subspace P
v_i	Eigenvectors in the Input Subspace Q
f_i	Image Vector
\vec{x}_i	k Feature Vectors
θ	Angle of eigenvectors P registered as a dictionary and the eigenvectors Q from the Input Data
φ_i	i-th k-dimensional Orthogonal Normal Vector
\mathcal{R}^n	n-dimensional Feature Space
atan2	The Quadrant-Aware Version of Arctan
$p(x)$	The intensity of p at a point x
R_θ	The Corresponding Rotation Matrix
$L_{xx}, L_{xy}, L_{yx}, L_{yy}$	The convolution of the second-order derivative of gaussian with the image $I(x, y)$ at the point x
G_x	Value for the first derivative in the horizontal direction
G_y	Value for the first derivative in the horizontal direction

List of Tables

Table 3.1.	Training and Testing of detests classified into two categories for offline and online recognition systems	21
Table 3.2.	Accuracy analysis for offline recognition system	24
Table 3.3.	Offline classifiers recognition and accuracy analysis	27
Table 3.4.	Online classifiers recognition and accuracy analysis	27
Table 3.5.	Online classifier recognition and accuracy analysis	32
Table 4.1.	Data of Indoor Soil Moisture Detecting Using Sensor Unit	43
Table 4.2.	ORB features recognition	50
Table 4.3.	ORB features matching accuracy	50
Table 4.4.	SURF features recognition	51
Table 4.5.	SURF features matching accuracy	51
Table 5.1.	ORB features extraction and selected using EKF	67

List of Figures

Figure 2.1.	Spectrum representation including	7
Figure 2.2.	Field and crop features involved in the rule-set algorithm as affected by the image object scale	8
Figure 2.3.	Thermographic image-laser point cloud registration workflow	10
Figure 2.4.	Control environment of the developed system	10
Figure 2.5.	Visual processing and servo control system	11
Figure 2.6.	Imaging geometry of target	12
Figure 2.7.	Block diagram of visual servo system	12
Figure 2.8.	Vision- based segmentation scheme and decision process	13
Figure 2.9.	Workflow for individual detection and classification procedure	13
Figure 3.1.	Subspace method (SM)	17
Figure 3.2.	Comparison between two sets of images using MSM	18
Figure 3.3.	Research framework establishing the classifiers and the MSM	20
Figure 3.4.	Training and Testing Datasets for building the classifiers for recognizing spray area and non-spray area	23
Figure 3.5.	Image sets in classifier recognition in the learning and recognition phases for MSM application	24
Figure 3.6.	Online recognition system for decision of spraying based on MSM classifiers	26
Figure 3.7.	Online recognition performance of classifiers of cropland from 5 m height	30
Figure 3.8.	Online recognition performance of classifiers of orchard from 15 m height	31
Figure 4.1.	Thermal imagery to determine the soil moisture from infrared information	35
Figure 4.2.	Typical example of images camera to RGB images and thermal imagery	36
Figure 4.3.	Image mosaic and feature detection for estimating soil moisture	40

Figure 4.4.	Indoors experiment	41
Figure 4.5.	Outdoors experiments	41
Figure 4.6.	Outdoors field experiments	41
Figure 4.7.	Soil Moisture Sensor Unit	42
Figure 4.8.	Soil Samples and Thermal Image	43
Figure 4.9.	Soil Moisture Change Monitoring System and Thermal Images	46
Figure 4.10.	Landmark and Images Acquisition System	46
Figure 4.11.	RGB Image and Thermal Image Captured by UAV	47
Figure 4.12.	Relation of soil moisture and digital number of thermal imagery indoors experiment	48
Figure 4.13.	Relation of soil moisture and digital number of thermal imagery outdoors experiment	49
Figure 4.14.	The Relation of Soil Moisture and Thermal Image Value	49
Figure 4.15.	ORB features matching of thermal images (Features matching errors, 320x240)	50
Figure 4.16.	SURF features matching of thermal images	51
Figure 4.17.	Mosaic of features in thermal imagery	52
Figure 4.18.	Mosaic of features in thermal imagery	52
Figure 4.19.	Multiple thermal images mosaicking using surf features	53
Figure 4.20.	Mosaicking of RGB Images of the Field	53
Figure 4.21.	Mosaicking of Thermal Images of the Field	53
Figure 5.1.	Statistics of employed person by agriculture and forestry of Japan	56
Figure 5.2.	UAV-Follower based autonomous spray system	57
Figure 5.3.	UAV-Follower based autonomous transportation system	58
Figure 5.4.	Flowchart to integrate UAV image and Electronic Platonic Vehicle (EPV) through Navigation Planner	58
Figure 5.5.	ORB – SLAM system overview	59
Figure 5.6.	Create 3D dense map using Octomap	63
Figure 5.7.	Development of autonomous electrical vehicle	64

Figure 5.8.	Development of Autonomous Spraying System	65
Figure 5.9.	Choice of work patterns	65
Figure 5.10.	ORB features extraction without selected using EKF	66
Figure 5.11	ORB features extraction and selected using EKF	67
Figure 5.12.	Road edge detection using Canny edge detector using EPV	68
Figure 5.13.	ORB features detected by ORB-SLAM system using ZED camera to navigate the EPV	68
Figure 5.14.	Simulation experiment results for navigation using ORB-SLAM using ZED camera system to navigate the EPV	69
Figure 5.15.	Images mosaicking for local mapping	69
Figure 5.16.	Images mosaicking of agricultural fields	70

Chapter 1

Introduction

Unmanned Aerial Vehicle (UAV) and Internet of Things (IoT) in agriculture got the importance last couple of years for information in agricultural decision-making process. The decision-making and its application work on the development sensors and communication protocols.

1.1 Feature Recognition: In the vision system and analysis processes, feature recognition has been outlined by the researcher from computer science and pattern recognition. The challenges in the agricultural features, which vary in each stages of crop growths such as recognizing the land type, soil type, road edges, plant canopy's and orchards, trees, structures, and semi-structure areas. In the industrial application, features are constant compare to agriculture. In agriculture, it is open loop systems where as industrial production as a closed loop system, the feature recognition has the feedback. While conducting fieldwork for feature recognition, it is hard to outline the numbers and minimize the categories. Therefore, the key features are one of the potential solutions to minimize the features in the field. The features recognitions have been addressed through the machine learning system recently to add up with artificial intelligence. The machinery learning system helps in decision-making process.

1.2 Machine Learning System: Machine learning is being implemented in the IoT platform to bring the decision with the confidences. The machine learning system could provide the decision according to the classifiers that we can train and test to get the accuracy while conducts operations. The UAV provides the images and frames continuously during operation. The recognition accuracy of classifiers needs computational flexibility with minimum time involvement.

1.3 Mapping and Sensing Systems: The feature recognition and machine learning system have further implication in the mapping system development using the different sensors platform. The reflectance-based sensors have the advantages of non-destructive measurement than compare to the resistance sensors. The reflectance sensors got the wide variety of Infrared application starting NIR and SWIR ranges. One of that is thermal camera, which comes the

Infrared filters to get the moisture information. The sensing system application is the challenging part for getting information using UAV and spray according to the information feature recognition, classifier identification of spray and non-spray areas.

1.4 Application of Sensing System: The sensing system based on the feature recognitions, classifiers identifications and Simultaneous Localization and Mapping (SLAM) could help in spraying system, which is lack of presently. The autonomous application with enabling SLAM and UAV-based mosaic information, which identify the key features, classifiers of target spraying could help prescription application to minimize the pesticides, herbicides in the crop lands and orchards.

1.5 Problem Statements

The feature recognition in agricultural works in real-time using UAV is a challenging to employ the precision management through machine learning system. Unlimited features needs to classify and minimize for the robust application. Machine learning requires training of key features for robust application of spray and nonparty areas, determination of wet conditions, soil moisture distributions, coordination of robotic vehicle and UAV follower system to accomplishment multiples task in agricultural works. On the other hand, Japanese and worldwide agricultural labor forces are decreasing significantly. The labor forces need to replace through multiple coordinated robotic system, which have adaptive local mapping system to help the farm owner through multiple work accomplishments. As the UAV costs are drastically reduce, it has the potential to coordinate multi-task robot system in agricultural farm with lower cost. In the multi-task system, UAV-based leader requires to have robust training system and navigation planner. To accomplish a navigation planer, UAV-based transportation vehicle and small mounted sprayer could work out in combination with sensor distortions.

1.6 Research Questions

The feature recognition and real-time training system needs to work out to implement agricultural navigation planning scheme. It needs start from the very beginning while UAV used to map in the agricultural land for multiple crops. Different crop has the different features. Therefore, the proposed research requires designing as follows:

1. How to develop a robust agriculture feature recognition system using UAV from lower and higher altitudes for identification of nonspray area to enable precision fertilizer application in short time?
2. What could be the possible way using UAV to detect soil moisture in the crop field for precision irrigation management?
3. How to develop a vision based local navigation planer using UAV to complete the multiple tasks inside the farm such as spraying, transportation of products and scouting in the field?

1.7 Research Objectives

Therefore, the purpose of this research is illustrated on the basis of three above mentioned challenging research questions: robust feature recognition, machine learning system, mapping and sensing system and application of sensing system through a local navigation scheme. The objectives are as follows:

1. To develop a machine learning system that has the advantage of high computational speed with good accuracy for recognizing spray and nonspray areas for application in UAV-based sprayers for precision application of fertilizer to crops and orchards.
2. To detect soil moisture content information from thermal image features taking from UAV platform for precision application of irrigation management.
3. To develop vision-based multi-task navigation planner system for target spraying, transportation of products using autonomous agricultural vehicle.

1.8 Significance

Agricultural operations have two major challenges to deal: first, the uncertainty and second, time specificity. The uncertainty deals with open loop agricultural system where feedback has not been established. The precision application of pesticides, irrigation is very much important according to the identification of features that can be recognized from the UAV images. The robust recognition and filtering are required in a real time application. The real-time application could be utilized in the arid land zone detection for precise application of irrigation to deal with water stress and spray herbicides in the spray area to minimize the weed infestation. To recognize the spray and nonspray areas, a machine learning system is needed that requires minimum computational time with good accuracy to identify and nonspray areas to minimize the application and waste of herbicides. UAV along with autonomous small robot have the

advantages of multi-task robot application as the leader follower applications. This multi-task robot will help in accomplishment of tasks and aid in labor in the rural farms with adaptive local mapping and navigation planner.

1.9 Outlines of Thesis Structure

The thesis is organized into six chapters with cognitive summary and the list of contents. Each of the chapter is designed based on the objective, its significance, methods, results, discussion and summary.

Chapter 1 is discussed the significance of the UAV application and machine learning system for the feature detection. The ORB feature and SURF feature classified. The importance's of feature detection, accuracy assessments and finally UAV-based feature recognition system is outlined briefly to orient the thesis objective originality and significance of research. The objectives are noted to achieve the goal of this research.

Chapter 2 is discussed on the reviews based on the feature detections process, some of the recent research contributions on feature recognition system, machine-learning system and map-based sensing systems are reviewed. The application of this soil moisture distribution is been a long challenges in this part of the world.

Chapter 3 briefly highlights the contemporary research focuses on the machine learning systems, deep learning about the training of and testing of the datasets for the for spraying and nonspray areas for the proposing a spraying control and minimizing the fertilizer application in the nonspray area from UAV or drone. The UAV limitation about the flight duration and pay load still a challenge, therefore, a fast and robust system is required to accomplish the work in the field. An RGB camera was used to collect the images from low and high latitude to train and test the datasets.

Chapter 4 reported on the thermal image processing system to detect the moisture content on the field based on the thermal features. In the thermal imagery compare to ORB, SURF feature are works well. The ground calibration, thermal camera calibration and indoor and outdoor experiments are reported to fit the regression-based relation between the soil moisture contents and feature recognition. The SURF features are reported with better accuracy in the mosaic system.

Chapter 5 discussed vision-based system, which is adapted in the small vehicle robot with human guidance leader and robot-based follower. UAV guided multi-task robot could serve as the assisted marker of leader and autonomies of vehicle in future agriculture to aid in the labor force. The small sprayer system is scheduled to attach in our further researches. In addition, the feature-based recognition and mosaic information on RGB images are reported based on SLAM application, canny's edge detection.

Chapter 6 is designed to conclude overall research summary in a cognitive way. How this research helps in the scientific community. Specially UAV-based application in spray and non-spray, thermal imagers-based sensing system for water stress area identification. The application efficiency can be expressed and small unit of leader follower-based system is reported about multiple robots.

In the following sections, the details of problem statement, original research points and methods of conducting the research, results and discussion are presented.

Chapter 2

Review of Literature

The main purpose of this chapter is to provide a brief review of the past research works which are related to the present study. It is always beneficial for the researcher to consult available literature to assess the past stock of knowledge with the hope of receiving future guidelines for conducting further research in the particular area. The following section presents the most common and relevant studies which have been conducted in the past at home and abroad. Literature reviewed in this study is available from different libraries and websites. The following studies undertaken so far at home and abroad are reviewed in this chapter.

2.1 Studies Related to Feature Recognition System from the Images Takes from UAV to Complete Agricultural Operations

J. Torres-Sánchez et al., 2015 reviewed that in site-specific management in agriculture for detecting the vegetation in herbaceous crops at the early season is a first and important step prior to addressing counting plants for monitoring proper germination, or identification of weeds for early season site specific weed management. The present research work develops an innovative thresholding OBIA algorithm based on the Otsu's method, and studies how the results of this algorithm are affected by the different segmentation parameters (scale, shape and compactness). The image segmentation scale parameters affected the histogram of the vegetation index, that had changes in the automatic estimation of the optimal threshold value for the vegetation indices. The other parameters also involved in the segmentation procedure and showed minor influence while conducting classification accuracy.

TelmoAdão et al., 2017 reviewed that traditional imagery based on the RGB and/or NIR sensors. The RGB and NIR has the potential and applied in many agricultural forestry to researches. In regards to application, the spectral range spectral range and precision are required profile materials and organisms that only hyperspectral sensors can provide. Hyperspectral imagery have gone the developments and consistently resulting in lighter and high spectral signature sensors that can currently be integrated in UAS for research and industrial application. The hyperspectral sensors' ability for measuring hundreds of bands

raises complexity when considering the sheer quantity of acquired data, whose usefulness depends on both calibration and corrective tasks occurring in pre and post-flight stages (**Figure 2.1**). With the goal of simplifying hyperspectral data processing—by isolating the common user from the processes’ mathematical complexity—several available toolboxes that allow a direct access to level-one hyperspectral data are presented.

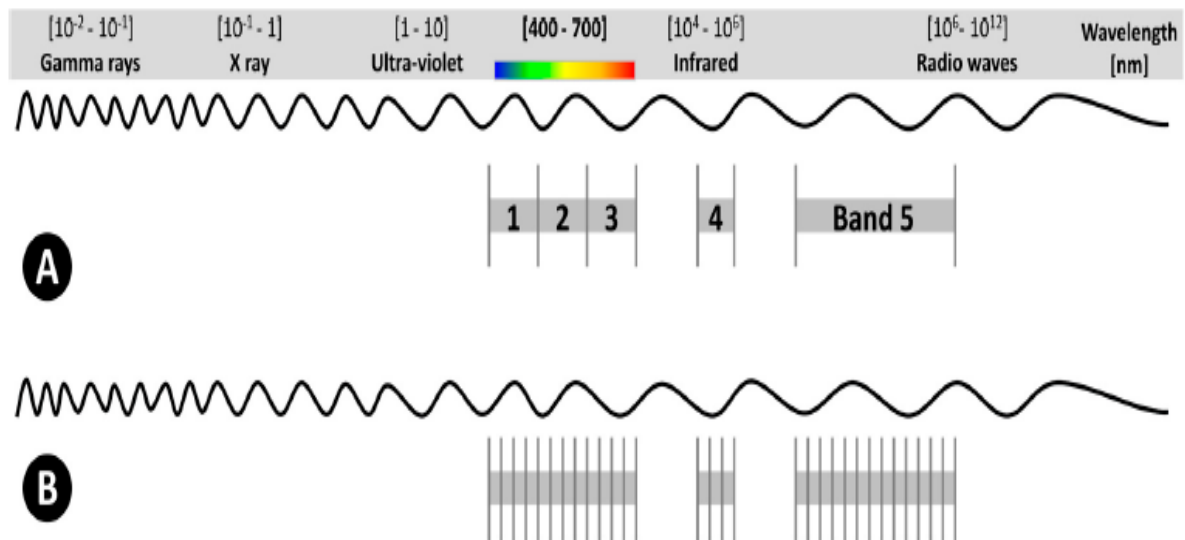


Figure 2.1. Spectrum representation including: (A) Multispectral example, with 5 wide bands; and (B) Hyperspectral example consisting of several narrow bands that, usually, extends to hundreds or thousands of them (image not drawn to scale)

Hitoshi Sakano et al., 2005 proposed a new object recognition algorithm called the kernel mutual subspace method (KMSM). The authors theoretically derived a new object recognition algorithm called the kernel mutual subspace method by applying the kernel nonlinear principal component analysis, which is known as a powerful nonlinear principal component analysis method, to the mutual subspace method. When the proposed technique was applied to an individual identification problem based on facial images, it was apparent that the relationship between the degrees of freedom of the object motion and the subspace dimensionality indicating a high recognition rate. Moreover, this procedure could be consistently explained through experiments that used the proposed method, which did not differ significantly from the conventional method at the highest precision. They also showed that the proposed technique could be effective for large-scale recognition problems and that its recognition dictionary has a more compact structure.

J.M. Peña-Barragán et al., 2012 examined a list of color-infrared images captured from the new generation of remote platforms known as unmanned aerial vehicles (UAV), specifically a quadrotor, was tested for site-specific weed management applications. An object-based image analysis (OBIA) procedure was developed by combining several scenes, contextual, hierarchical and object-based features in a looping structure (**Figure 2.2**). The procedure integrates several features from the crop-field patterns: i) field structure, such as field limits and row length, ii) crop patterns, such as row orientation and inter-row distance, and iii) plant (crop and weeds) characteristics, such as spectral properties (NDVI values) and plant dimensions; as well as iv) hierarchical relationships based on different segmentation scales, and v) neighboring relationships based on distance, position and angle between objects.

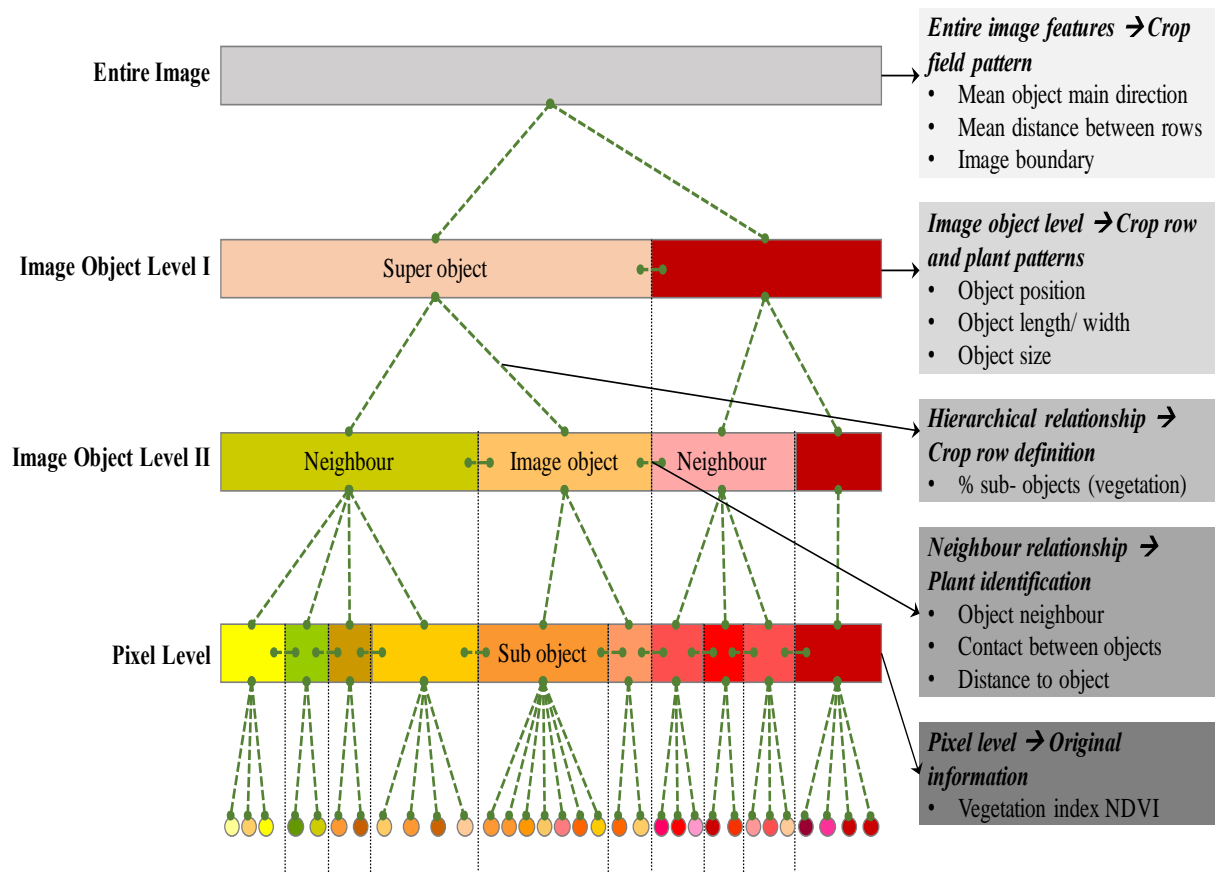


Figure 2.2. Field and crop features involved in the rule-set algorithm as affected by the image object scale

S. Lagüela et al., 2011 explored that infrared thermography is generally used in energy efficiency studies moisture detection and building inspections studies for heat losses. Laser scanning technology can be an optimal complement for the thermographic measurement,

because it provides the metric information that allows the quantification of the thermal studies if the clouds of points are texturized with thermographies. In this paper a methodology for registering thermographies in clouds of points is explained, with the following steps: initially, processing the metric calibration of the thermal camera, secondly, register of thermographies in the cloud of points based on control points, and finally, processing the textured cloud of points to obtain rectified thermographies, with no optical distortions.

2.2 Studies Related to Machine Learning System

Calvin Hung et al., 2014 proposed an alternative learning-based approach using feature learning to minimize the manual effort required. Authors apply this system to the classification of invasive weed species. Small UAVs are suited to this application, as they can collect data at high spatial resolutions. Authors also apply feature learning to generate a bank of image filters that allows for the extraction of features that discriminate between the weeds of interest and background objects. They evaluated the approach to weed classification on three weeds of significance in Australia namely water hyacinth, tropical soda apple and serrated tussock. Results showed that collecting images at 5-10 m resulted in the highest classifier accuracy, indicated by F1 scores of up to 94%.

2.3 Studies Related to Mapping and Sensing Systems

D. González-Aguilera et al., 2012 described a new approach to multi-sensor registration of infrared images and 3D-laser scanner models, based on the extraction of common features in the IR image and the range image obtained from a laser-scanner 3D-point cloud. The workflow developed in this research allows the automatic registration of two different sensors with completely different characteristics, including fields of view, spatial resolution and spatial position (**Figure 2.3**).

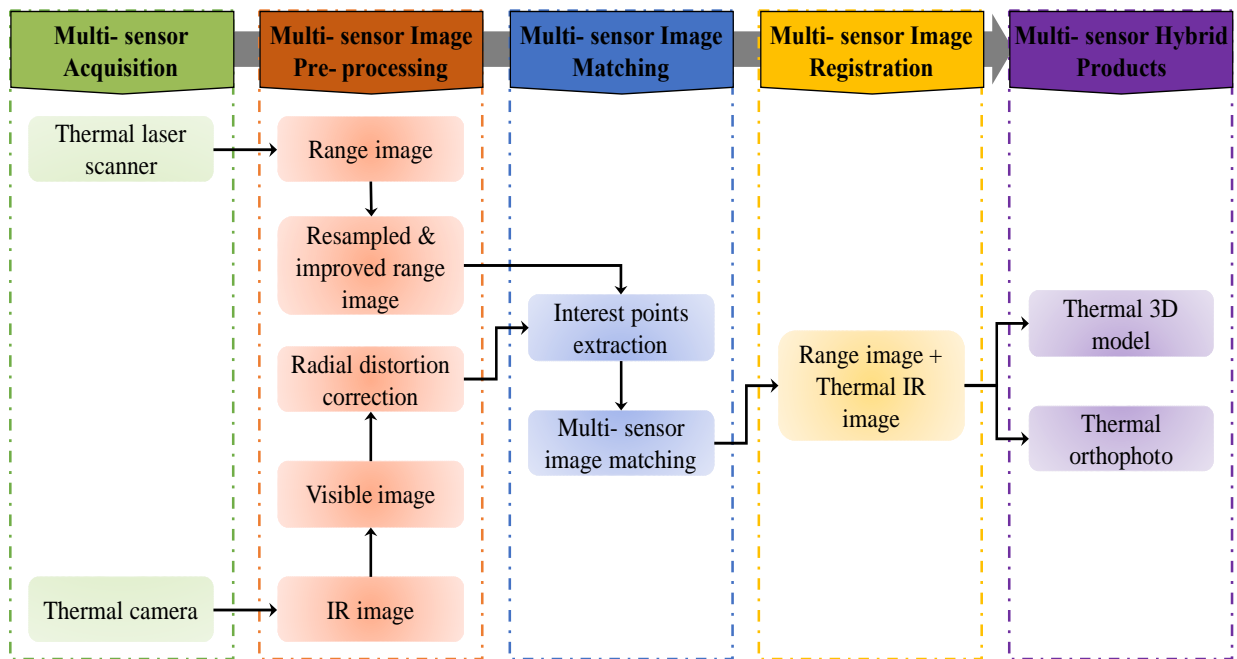


Figure 2.3. Thermographic image-laser point cloud registration workflow

2.4 Studies Related to Application of Sensing System

Natraj et al. 2014 presented a new application of laser rangefinder sensing to agricultural spraying vehicles (Figure 2.4). The current generation of spraying vehicles uses automatic controllers to maintain the height of the sprayer booms above the crop.

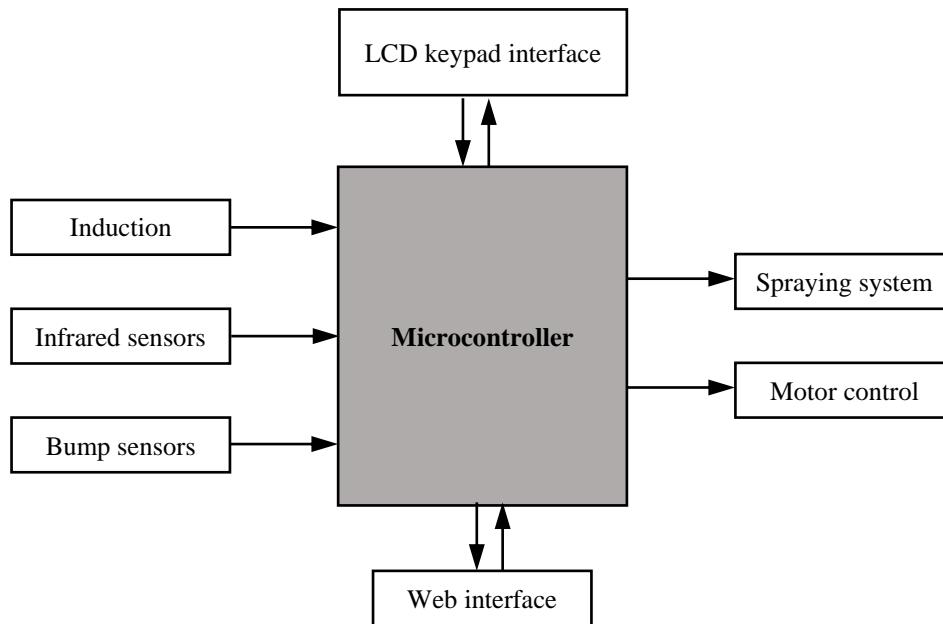


Figure 2.4. Control environment of the developed system

Adrian Carrio et al., 2017 examined that deep learning is recently showing outstanding results for solving a wide variety of robotic tasks in the areas of perception, planning, localization and control. Its excellent capabilities for learning representations from the complex data acquired in real environments make it extremely suitable for many kinds of autonomous robotic applications. In parallel, Unmanned Aerial Vehicles (UAVs) are currently being extensively applied for several types of civilian tasks in applications going from security, surveillance, and disaster rescue to parcel delivery or warehouse management. In this research, a thorough review has been performed on recent reported uses and applications of deep learning for UAVs, including the most relevant developments as well as their performances and limitations. In addition, a detailed explanation of the main deep learning techniques is provided.

Alberto Tellaeche et al., 2008 explored an automatic computer vision-based decision support system for the detection and differential spraying of weeds in corn crops (**Figure 2.5**). The method is designed for post-emergence of herbicide applications. In this research, weeds and corn plants display were similar spectral signatures and the weeds appeared irregularly distributed within the crop's field. The proposed strategy involves two processes namely image segmentation and decision making (**Figure 2.6**). Image segmentation combines basic suitable image processing techniques in order to extract cells from the image as the low-level units. Each cell is described by two area-based measuring relationships between crop and weeds. The decision making determines the cells to be sprayed based on the computation of a posterior probability under a Bayesian framework (**Figure 2.7**).

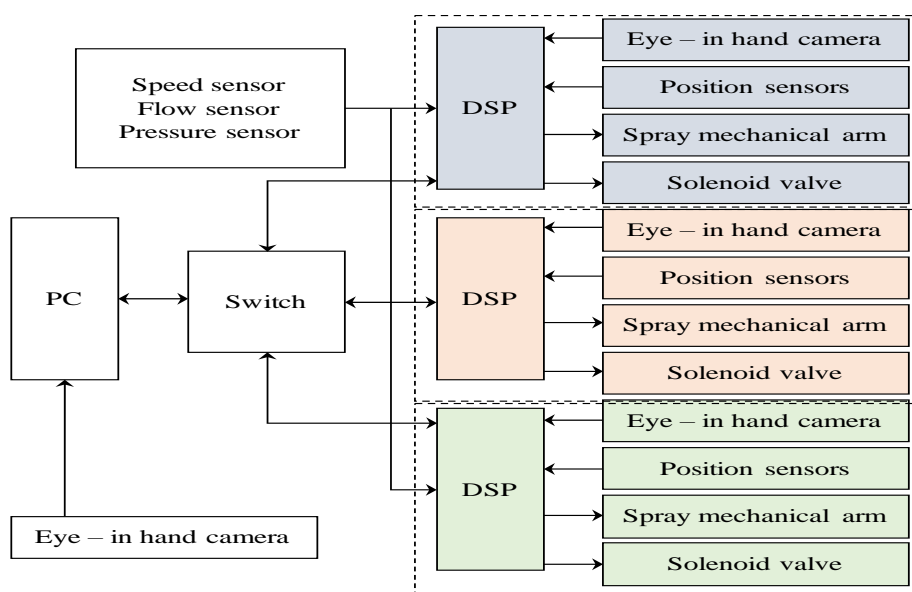


Figure 2. 5. Visual processing and servo control system

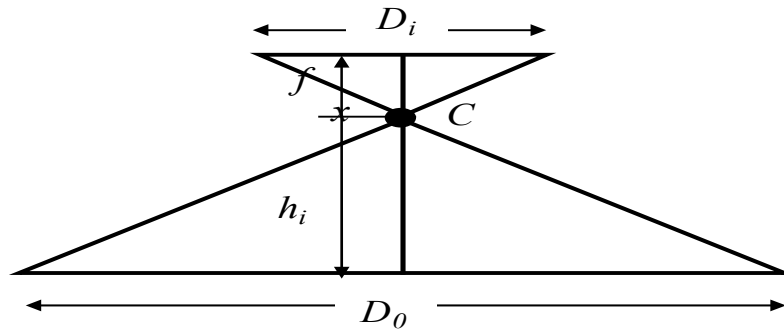


Figure 2.6. Imaging geometry of target

Where C : camera projection centre, f : focal length D_0 : actual diameter of MEC h_i : distance between crop canopy and camera and D_i : image diameter of MEC

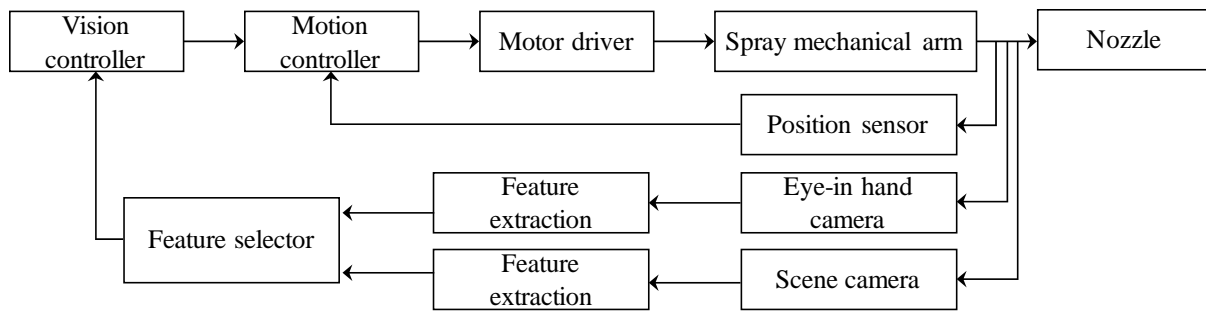


Figure 2.7. Block diagram of visual servo system

Olli Nevalainen et al., 2017 investigated the overall of a UAV-based photogrammetry and hyperspectral imaging system for individual tree detection and tree species classification in boreal forests (**Figure 2.8**). Eleven test sites were selected with 4151 reference trees representing various tree species and developmental stages were collected in June 2014 using a UAV-based onboard remote sensing platform. This system is equipped with a frame format with hyperspectral and a RGB camera. Dense point clouds were measured photogrammetrically using high resolution RGB images with a 5 cm point interval. Spectral features were obtained from the hyperspectral image blocks based on radiometric block adjustment with the help of in-flight irradiance observations. In this study a spectral and 3D point cloud features were used in the classification experiment. The best results were found at Random Forest and Multilayer Perceptron (MLP) model analysis with overall accuracies of 95 % and an F-score value of 0.93. The accuracy of individual tree identification varies 40-

95% depending on the characteristics of the area and cloud level. Results were promising, indicating that hyperspectral 3D remote sensing was operational from a UAV platform even in very difficult conditions (**Figure 2.9**).

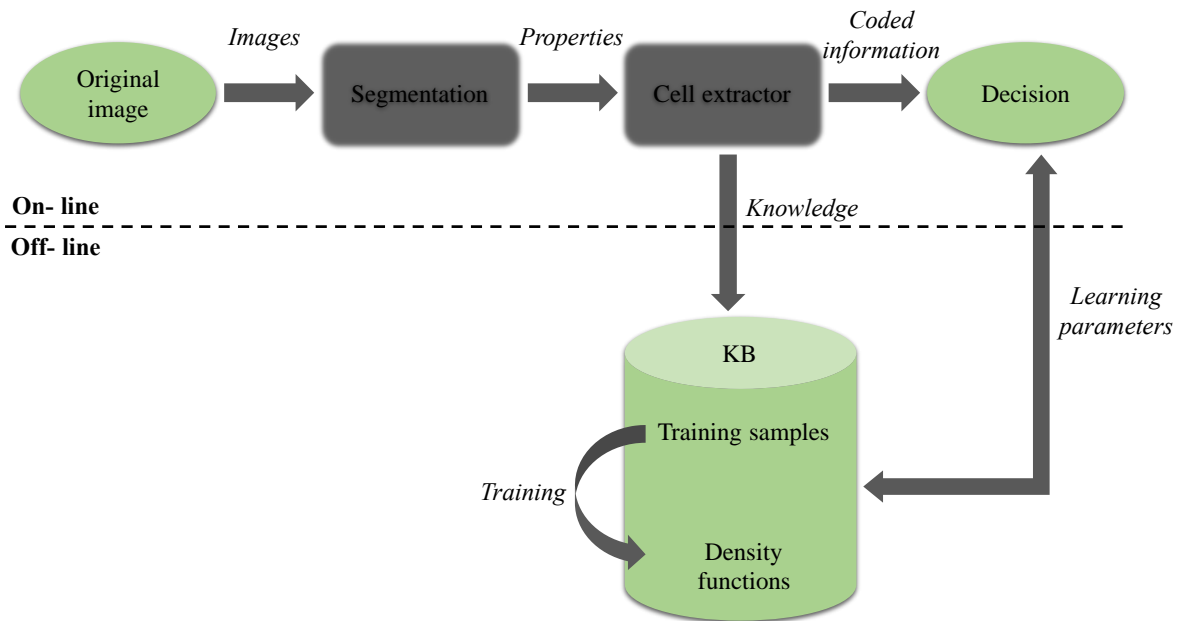


Figure 2.8. Vision- based segmentation scheme and decision process

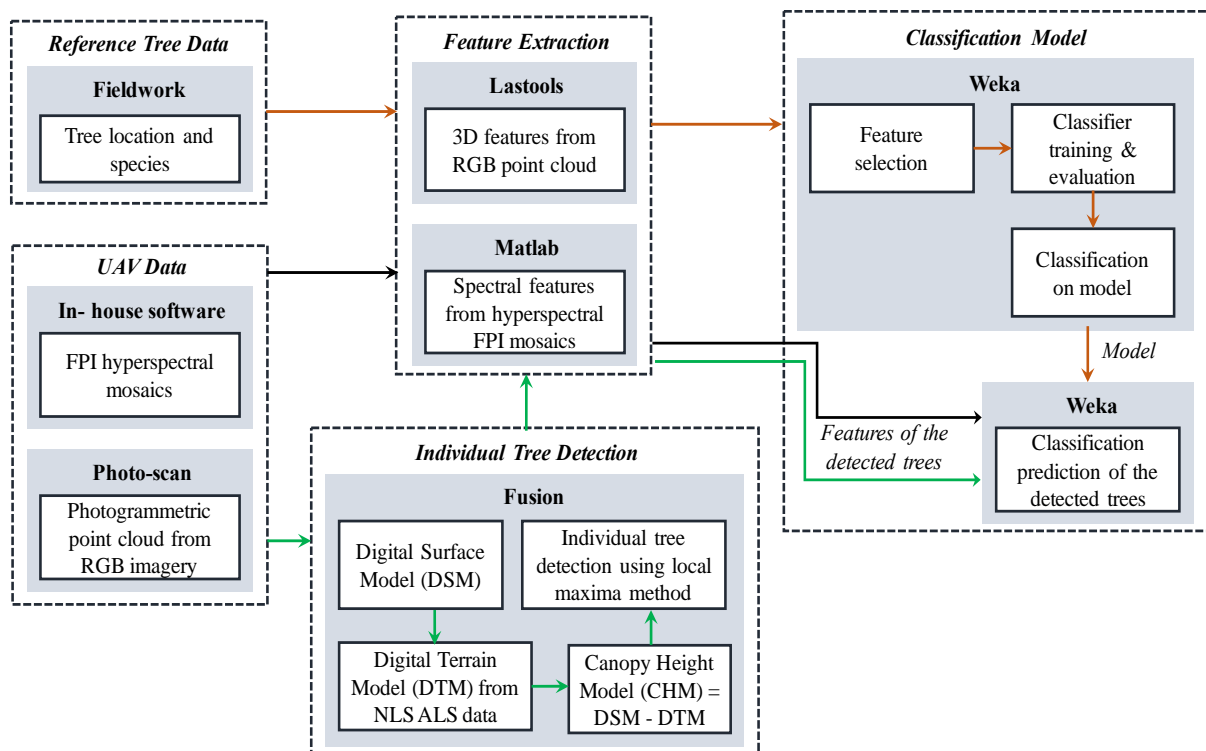


Figure 2.9. Workflow for individual detection and classification procedure

Jos'e Mart'nez-Carranza et al., 2015 defined and experimented visual simultaneous localization and mapping (SLAM) system according to visual features. It has emerged as one of the best systems for estimating the 6D camera pose for building a 3D map of the observed scene. This method is well-known as ORB-SLAM system and one of the main features is to use the same visual binary descriptor called ORB. Another task of ORB-SLAM combines local and graph based global bundle adjustment for enabling scalable map generation through real-time performance. The author examines an implementation of autonomous flight for a low-cost micro aerial vehicle (MAV), where ORB-SLAM is used as a visual positioning system that feeds a PD controller that controls pitch, roll and yaw. They found implementation has potential and could soon be implemented on a bigger aerial platform with more complex trajectories to be flown independently.

2.5 Summary

A careful review of the literature suggests that most of the studies had objectives not similar to those of the proposed study. The findings from the proposed research are expected to generate a set of meaningful and new research policy in the precision agricultural research. Shrinking by 22 percent in 2014, significant shortage of agricultural labor shortages is threatening the Japanese agricultural productivity. The circumstance highly motivates the automated smart transformation, which creates a high demand in the Japanese rural farms. To meet with the environmental standard and increasing productivity at Japanese agricultural farm aim at developing integrated autonomous system for crop plantation. The UAV-based features recognition to recognize spray non-spray area for precision application of fertilizer is one of the new approaches with Mutual Sub Space Method (MSM) machine learning system. Precision irrigation management requires the soil moisture information, wetness of canopy. In the proposed research, uses thermal imagery to find out the soil moisture information and ground reference data calibration have high impacts in agriculture. Furthermore, the features recognitions and UAV-based multi-task coordinated vehicle is one of the leading-edge concepts that is significantly differ from the previous contributions. In our best knowledge, this is the first attempt to coordinate multi-task robot simultaneous operation with UAV and electronic platonic vehicles for shared agricultural operations in the farm. In the following chapters, feature recognition system using MSM, soil moisture detection system and UAV-based multi-task robots and navigation planner will be introduced.

Chapter 3

Development of Recognition System for Spraying Area from UAV Using Machine Learning Approach

3.1 Background

With the development of UAV technologies, the use of UAV is rapidly expanded to different applications such as aerial photography to monitor vegetation, surveying mapping and scouting with wireless networking (Zhang, Y.; Chen, D.; et al. 2018). UAVs have the potential in agricultural applications and have an ideal solution to enable precision agriculture compared to aerial mapping and satellite remote sensing. Not only is the use of UAVs more efficient, but also more cost-effective compared to aerial or high-resolution commercial satellite data sets. It helps farmers to monitor crops in real-time and provides high-resolution images of the field and canopy for crop growth and production. High-resolution and machine vision images are used for identification of weeds and non-weeds areas using ground-based conventional sprayers (Hung, C.; Xu, Z.; et al. 2014, Rebetz, J.; Hector F.; et al. 2016). In recent advancements, the sprayers are attached to the UAV system to spray in the field. However, as the payload of the UAV with sprayer cannot make it heavier, therefore, it becomes difficult to fly with large quantities of liquid chemicals while flying in the field. The broadcasting of spray liquids needs to be very efficient in spraying to agricultural crops and stop spraying in the non-crop's areas. In the similar way, the orchard spray system needs to fly in a higher altitude to spray chemical on the top of the canopy. Higher payloads of chemicals in the tank have also the problem. The larger tank size requires more power and safety concerns while flying. It is very important to recognize the spray area as well as above the orchards and non-orchards area to ensure precision application of spray chemicals. For autonomous UAV-based spraying systems, the recognition of crop and orchards area is significantly important. A machine learning system is required prior to enable an autonomous spraying system to understand spraying spots and non-spraying spots from operational environments of UAV. The ground-based vehicle has the application of an image processing system (Peteinatos, G.; et al. 2014, Lee, D. H.; Lee, Kyou S.; et al. 2012).

Most of the researches have the datasets collection and machine-learning system were limited. Some of the research has reported the aerial application of spraying targets is reached only 50% from less than 1 m altitude (Pimentel, D. and Burgess M., 2011). In our best knowledge, the UAV-based sprayers introduced to the market and largely started to use in the mountains and

crop areas for enabling spray with precision. Most of the commercial UAVs with sprayers are operated with regulations in many countries. As the technology tends to be autonomous system onwards, it is likely to be UAV spray system must have high potentials for autonomous spraying applications. However, the UAV cannot fly for a long time due to limited power supply. To increase longer flight time, UAV manufacturer improves endurance by increasing battery capacity and reducing total weight of UAV. However, for reducing the weight, the higher payload was difficult. In this regard, needs to improve the application efficiency of chemicals to the spray area from a distant altitude. The height of the operation greatly influences the systems; a faster coverage required using minimum time for croplands for the orchards. Therefore, to increase the efficiency in precision spraying, a robust machine learning system is required for recognizing crop field and orchard areas with good accuracy.

Several machine learning systems have been introduced in the ground-based sprayers using deep learning, neural network and Bayesian classifiers (Carrio, A.; Sampedro, C.; et al. 2017, Majidi, B. and Bab-Hadiashar A., 2005, Tellaeche, A.; Xavier P.; et al. 2005). Most of the machine learning systems had higher complexity of data training and time requirements for real time application. While flying UAV, the time of flying is also very limited. Furthermore, the carrying liquid chemicals to the on-board UAV is also limited. To overcome this limitation, it is very important to introduce a machine learning system to recognize spraying and no spraying areas in real-time with good accuracy. In our previous research, we have experienced, the Mutual Subspace Method (MSM) has the higher potential to recognize features and actions of tracking with accuracy more than 80% in real time. Furthermore, MSM and KMSM along with Hankel matrix were implemented for machinery operator's action recognition in 0.07 sec (Yan Z., Pengbo G., Tofael A., 2018). Mutual subspace method has been used for action recognition of human face tracking action recognition of vision recognition society (Maeda K., Watanabe S., 1985, Fukui, K. and Yamaguchi O., 2005, 13. Fukui, K. and Yamaguchi O., 2007). Therefore, the MSM has the high capability in machine learning system to recognize the action and features in agricultural environments. In the spraying application from the on-board UAV, the recognition of features with minimum time and high accuracy can be done using MSM. In this research, we attempted to minimize the spraying chemicals amount while spraying in the field with limited carrying capacity of agricultural chemical using in crop fields and orchards.

Objective

To develop a machine learning system for recognizing the features of spraying and nonspraying areas for applying UAV-based sprayers in agricultural croplands and orchards. It is expected that MSM machine learning systems can be employed, offering advantages of low computational complexity and good accuracy in feature recognition systems for real-time applications.

3.2 Materials and Methods

3.2.1 Mutual Subspace Method (MSM)

The MSM was introduced to the field of pattern recognition, a well-known method for object recognition based on image sets (Maeda K., Watanabe S. 1985). It is an extension of the

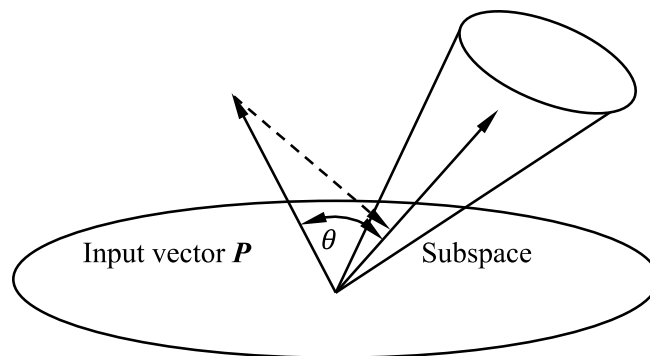


Figure 3.1. Subspace method (SM)

Subspace Method (SM) by classifying a set of input pattern vectors into several classes based on multiple canonical angles between the input subspace and class subspaces (**Figure 3.1**). The input subspace is generated from a set of input patterns as class (Watanabe, S. and Pakvasa N. 1985). The SM has high performance in pattern recognition, it was developed independently named as CLAFIC and multiple similarity method (Iijima, T., et al. 1974) respectively. It classifies an input pattern vector into several classes based on the minimum distance or angle between the input pattern vector and each class subspace, where a class subspace corresponds to the distribution of pattern vectors of the class in high dimensional vector space (Fukui, K. and Yamaguchi, O. 2014). We considered that the input vector \mathbf{P} and m class subspaces belong to k -dimensional vector space, the similarity is defined by the length or the minimum angle between the input vector \mathbf{P} and i -th class subspace, where the length of \mathbf{P} is often normalized to 1.0. The angle-based similarity can be derived as follows:

$$\cos^2 \theta = \sum_{i=1}^d \frac{(\mathbf{P} \cdot \boldsymbol{\varphi}_i)^2}{\|\mathbf{P}\|^2} \quad (3.1)$$

where d is the dimension of the class subspace and $\boldsymbol{\varphi}_i$ is the i -th k -dimensional orthogonal normal vector (PCA). The kPCA is an extension of PCA using kernel method for nonlinear applications (Scholkopf B.; Smola A., et al., 1998). Firstly, the conventional PCA operates by diagonalizing the covariance matrix C from k feature vectors \bar{x}_j ($a = 1, 2, \dots, k$) in an n -dimensional feature space \mathcal{R}^n ,

$$C = \frac{1}{k} \sum_{j=1}^k (\bar{x}_j \cdot \bar{x}_j^T) \quad (3.2)$$

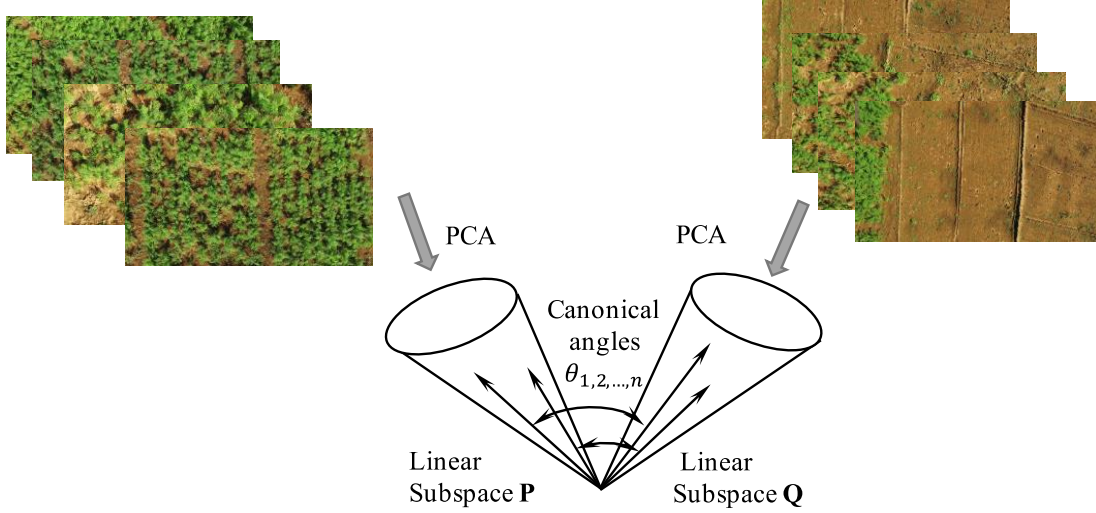


Figure 3.2. Comparison between two sets of images using MSM

it gives an eigen decomposition of the covariance matrix by PCA to obtain the principal components \bar{v}_i ($i = 1, 2, \dots, k$) of the distribution:

$$\lambda \bar{v} = C \bar{v} \quad (3.3)$$

However, we assume that all data here is calculated from the data centroid. This principal component describes the direction of the largest data variation under a linear approximation [15]. The above characteristic equation can be transformed as follows:

$$\lambda \bar{x} = \left[\frac{1}{k} \sum_{j=1}^k (\bar{x}_j \cdot \bar{x}_j^T) \right] \bar{v} \quad (3.4)$$

$$= \frac{1}{k} \sum_{j=1}^k (\bar{x}_j \cdot \bar{x}_j^T) \bar{v} = \frac{1}{k} \sum_{j=1}^k (\bar{x}_j \cdot \bar{v}) \bar{x}_j \quad (3.5)$$

Since \bar{v} is in $\{x_1, \dots, x_k\}$, we obtain:

$$\lambda (\bar{x}_a \cdot \bar{v}) = \bar{x}_a \cdot C \bar{v} \quad (3.6)$$

To solve the problem of recognition rate falls substantially when the compared pattern distributions have a highly nonlinear structure, the kPCA was applied with MSM for improving the recognition performance. The MSM has compared the small variations of the training data and recognition target data, to obtain a powerful recognition technique when the data

distribution can be linearly approximated, which is applied when multiple data can be used as recognition target image inputs. In the subspace method, a subspace that has d-dimensional vectors is selected according to a criterion such as the cumulative contribution rate from the eigenvectors, which are obtained using Principal Component Analysis (PCA) on the entered images. Then, the similarity between subspaces is defined according to the angle θ of eigenvectors $P = \{\vec{\mu}_i\}$ registered as a dictionary and the eigenvectors $Q = \{\vec{v}_j\}$ obtained from the input data (**Figure 3.2**).

According to the formula of (3.1), the angle θ between subspaces is given as the maximum eigenvalue:

$$\cos \theta = \max_{\vec{\mu}_i \in P} \max_{\vec{v}_j \in Q} \vec{\mu}_i^T \vec{v}_j \quad (3.7)$$

Where $\vec{\mu}_i^T \vec{\mu}_i = \vec{v}_j^T \vec{v}_j = 1$, $\vec{\mu}_i^T \vec{\mu}_j = \vec{v}_i^T \vec{v}_j = 0$, $i \neq j$, $0 < i, j \leq d$, and d is the dimensionality of the subspace used for recognition.

3.2.2 Research Design for Classifiers and MSM

The classifiers are required to be established before the MSM application. The MSM research approach involves two steps: offline and online recognition systems. The offline recognition system was used to validate the model and the accuracy of the recognition of classifiers (**Figure 3.3**). The online recognition system was proposed to understand the computational times to enable in the real-time system. In offline recognition, videos must be captured using the UAV and converted through a JPG converter. For offline recognition, selected images were taken for training and testing the classifiers from different datasets of crops and orchards. For online recognition, a new video stream was captured. From the stream video, 1 frame was chosen out of 20 frames from a new video stream. Considering the restricted computational time required by a real-time system, RGB images were converted to the gray scale. While testing using the online recognition system, a sliding window was used to obtain 4 consecutive frames, and PCA was applied using the subspace method. In the subspace method, multiple images were required, and we noted that 4 frames were optimal for use in the subspace method.

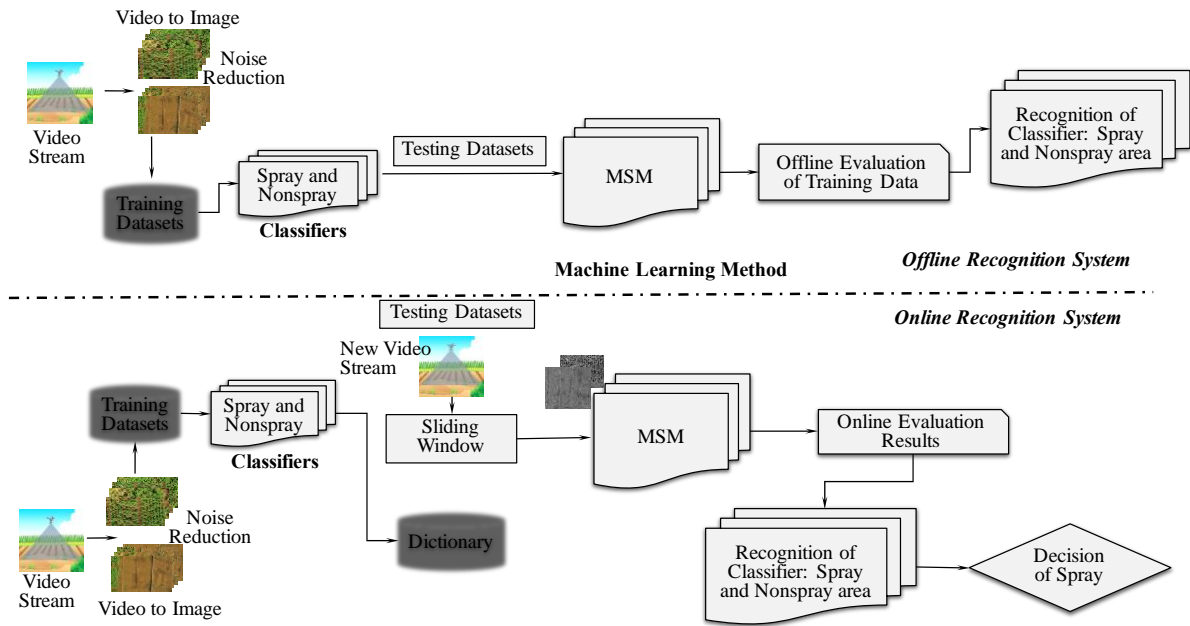


Figure 3.3. Research framework establishing the classifiers and the MSM

In the following sections, details of field experiments for training and testing different datasets and the offline and online recognition systems are described.

3.2.3 Field Experiment for Training and Testing with Datasets

To implement the MSM for feature recognition, different crops, and orchards are required for training the subspace patterns and verifying the recognition accuracy. While selecting the datasets for training, image acquisition at close range is preferable for agricultural croplands. On the other hand, for orchards, a high altitude allows the canopy to be covered in a minimum time. Generally, close-range spraying can effectively reduce the drift and waste of chemicals. However, UAV sprayer payload and battery operational time are major concerns in enabling autonomous spraying. In this study, two working patterns are defined depending on the flying height. The corresponding work areas are described as follows: for cropland (i.e., carrot, cabbage, and onions), plant height was less than 5 m, and image acquisition was performed using a UAV from a height of 5 m. In the case of orchards or plantations (i.e., chestnut, persimmons, and tall trees). We considered the height of orchards to be less than 15 meters, and thus, the acquisition of images was conducted from a height of 15 m from the ground (**Table 3.1**). Two classifier datasets were collected for cropland spray area recognition: one dataset for spray areas (carrot, cabbage, onions) and another dataset for nonspray areas (inner farm roads, ridges, bare soil). Similarly, two classifier datasets (spray and nonspray areas) were also collected for orchards: one dataset for orchard areas (chestnuts and persimmon) and

another dataset for trees that included structured areas (farm houses, green house structure, farm buildings). The classifier datasets were captured using a commercial UAV (DJI Phantom 3 Pro) with an onboard 4K camera with 1/2.3" CMOS and FOV 94° 20 mm f/2.8 lens. The 4K videos were collected and converted to images using a JPG converter at the preprocessing stage. The images were collected in the morning from 10 AM to 12 PM to ensure uniform lighting while the UAV flew over the croplands and orchards. Days with clear skies were generally chosen for collecting the videos by flying the UAV. The classifiers were segmented from the videos according to flight heights for croplands and orchards (Table 1). Three field experiments were conducted with the UAV in three randomly selected zones; a rural farm with a combination of croplands and orchards (L1), a farm with different croplands with orchards (L2) and a research farm with croplands and orchards (L3) (**Figure 3.4**). MATLAB 2015a® (MathWorks, California) was used to develop the user interface and training and testing datasets for offline and online recognition systems.

Table 3.1. Training and testing with datasets classified into two categories for offline and online recognition systems

Targets	Data sets		Training image numbers		Testing image numbers	
	Spray	Nonspray	Offline (Spray + Nonspray)	Online (Spray + Nonspray)	Offline (Spray + Nonspray)	Online
Carrot	120	120	First half (60+60)	All (120+120)	Last half (60+60)	New video (89)
Cabbage	198	198	First half (99+99)	All (198+198)	Last half (99+99)	New video (298)
Onion	107	107	First half (53+53)	All (107+107)	Last half (54+54)	New video (204)
Chestnut	97	97	First half (48+48)	All (97+97)	Last half (49+49)	New video (180)
Persimmon	94	94	First half (47+47)	All (94+94)	Last half (47+47)	New video (210)
Trees and Structures	118	118	First half (59+59)	All (118+118)	Last half (59+59)	New video (141)



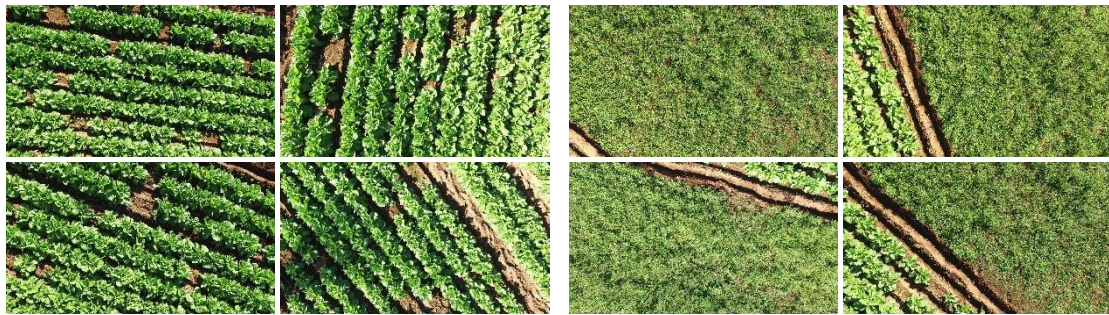
(a) L1: Cropland: Carrot, Spray Area

(b) L1: Cropland: Nonspray Area



(c) L1: Orchard: Chestnut, Spray Area

(d) L1: Orchard: Nonspray Area



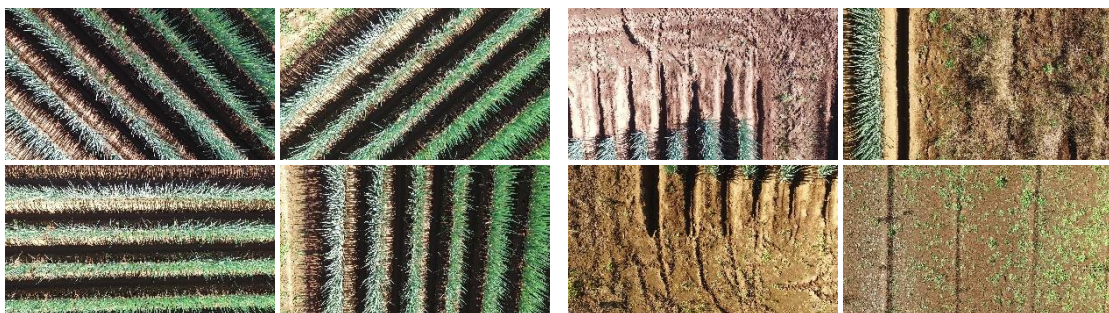
(a) L2: Cropland: Cabbage, Spray Area

(b) L2: Cropland: Nonspray Area



(c) L2: Orchard: Persimmon, Spray Area

(d) L2: Orchard: Nonspray Area



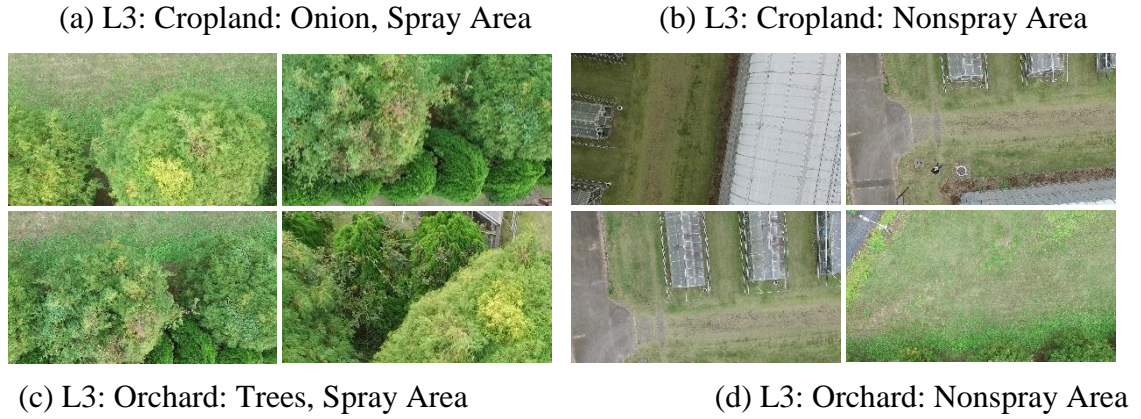


Figure 3.4. Training and testing datasets for building the classifiers for recognizing spray areas and nonspray areas

3.2.4 Offline Recognition System

The offline recognition system consisted of learning and recognition phases. The learning phase was started by collecting training image datasets of each class $m \in \{1, \dots, M\}$ and inputting them into the system. For offline experiments of each land type, we used one of the videos with the first half for training and the last half for testing. The recognition phase was confirmed to begin once the learning phases of the classifiers using scene sequences were completed (**Figure 3.5**). Then, PCA was applied to establish the linear subspace as a reference subspace for each class. The training phase was completed in three stages. First, all the collected testing images of $I_j \in \{1, \dots, J\}$ were input into the system, and each I had frames of $\{f_1, \dots, f_n\}$. Second, the PCA was applied to establish the linear subspace for testing the subspace for each class I_j . Finally, the canonical angles between the current testing subspace and each reference subspace were calculated. The current image was assigned to the class with whom it shared the smallest canonical angles, which indicated that it had the highest similarity when referenced to the training datasets. In an offline experiment setting, the UAV was flown in 5 m above the cropland. The first half of images for training (99 images, spray and 99 images, nonspray) and the last half of images for testing (99 images, spray and 99 images, nonspray) were selected for cabbage fields (**Table 3.1**). The first half of images for training (53 images, spray and 53 images nonspray) and the last half of images for testing (54 images, spray and 54 images, nonspray) were selected for onion fields. Similarly, the first half of images for training (60 images, spray and 60 images nonspray) and the last half of images (60 images, spray and 60 images, nonspray) were selected for testing carrot fields. A height of 15 m was chosen for flying over orchard areas to collect the first half of images for training (48 images, spray and

48 images, nonspray) and the last half of images for testing (49 images, spray and 49 images, nonspray) for chestnut trees. Again, the first half of images for training (47 images spray and 47 images, nonspray) and the last half of images for testing (47 images, spray and 47 images, nonspray) were used in the case of persimmon fields. Finally, the first half of images for training (59 images, spray and 59 images, nonspray) and the last half of images for testing (59 images, spray and 59 images, nonspray) were used for trees and structures. The accuracy analysis of offline recognition system was compared with the true positive and true negative values (**Table 3.2**). For further confirmation, the extended datasets were considered to check the recognition accuracy of classifiers using MSM.

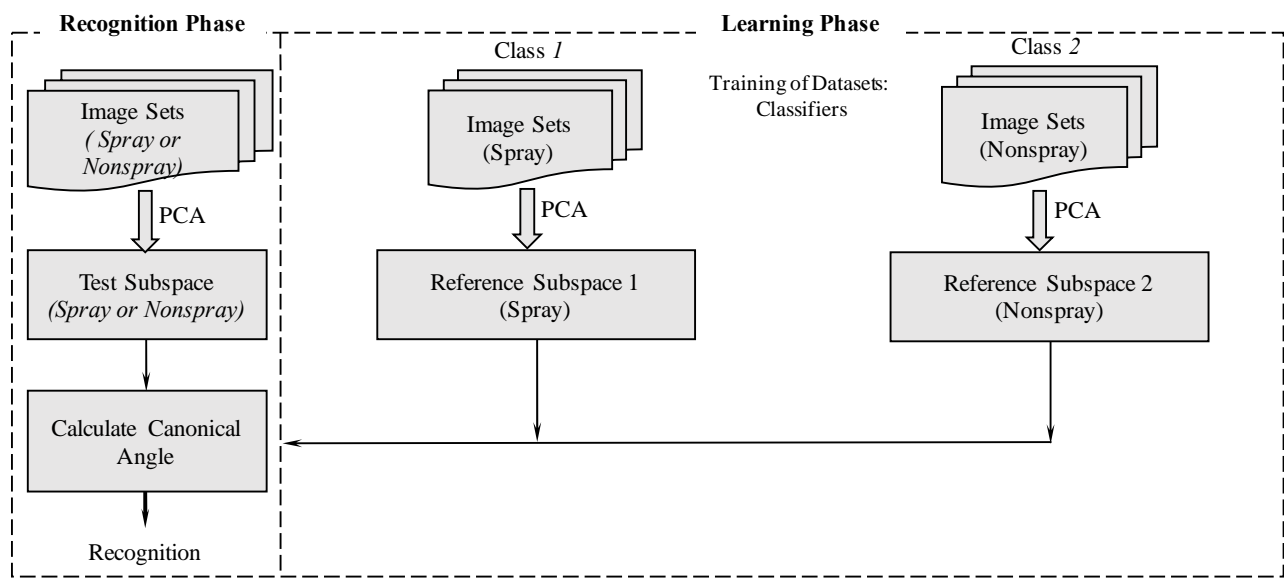


Figure 3.5. Image sets in classifier recognition in the learning and recognition phases for MSM application

Table 3.2. Accuracy analysis for the offline recognition system

		True condition (offline recognition)		
		Spray	Nonspray	Σ Total
Predicted condition (tested by recognition phase)	Spray	True Positive	False Positive	Total Positive
	Nonspray	False Negative	True Negative	Total Negative
Accuracy		$Accuracy = \frac{\Sigma True Positive + \Sigma True Negative}{\Sigma Total}$		

3.2.5 Online Recognition System

The subspace patterns were trained during the offline recognition process. These patterns were used for the online recognition development of classifiers. A sliding window was used to select 4 images that were converted to 4 vectors through resizing and reshaping. The gray scale images were resized to 8x8 and reshaped to 1 column vector using MATLAB®. A test subspace was generated using PCA for creating a matrix from the vectors. The online recognition progress was completed in the following stages. First, each video from each target crop or orchard was preprocessed, and one image was extracted from every 20 frames. Among the extracted images, there were several frames captured that did not belong to either class during takeoff and landing or that included other plants during entry and exit. Such images were marked as noise images and removed to improve recognition accuracy. In the experiment, two datasets were collected for each target land. For the online experiment, we used all of the frames (removed noise) from one of the videos as training, and we used another video for testing (the video was not directly read; rather, the video was extracted to image frames, and noise was removed). In the second step, we classified the set of sequential images using the MSM classifier. Finally, the spray areas were recognized based on the training datasets (**Figure 3.6**). In the datasets, 198 images (spray) and 198 images (nonspray) were collected from a 5 m height for training, and a reference subspace was built for use in the online experiment for cabbage. In case of testing, a new video was taken where one frame was selected out of 20 frames. There was a total of 298 frames used for testing for cabbage. Similarly, 107 images (spray) and 107 images (nonspray) were selected for training in online experiments. The new video stream was used with a total of 204 images for onion. In the case of carrot, 120 images (spray) and 120 images (nonspray) were used for training, and a new video stream with 89 images was used for testing the datasets. For orchard categories from a height of 15 m, two classifiers were trained using 97 images (spray) and 97 images (nonspray); 94 images (spray) and 94 images (nonspray); 118 images (spray) and 118 images (nonspray) for chestnut, persimmon and trees, respectively. For testing the datasets of each target, a new video stream was taken with a total of 180 images extracted for chestnut, 210 images for persimmon and 141 images for trees.

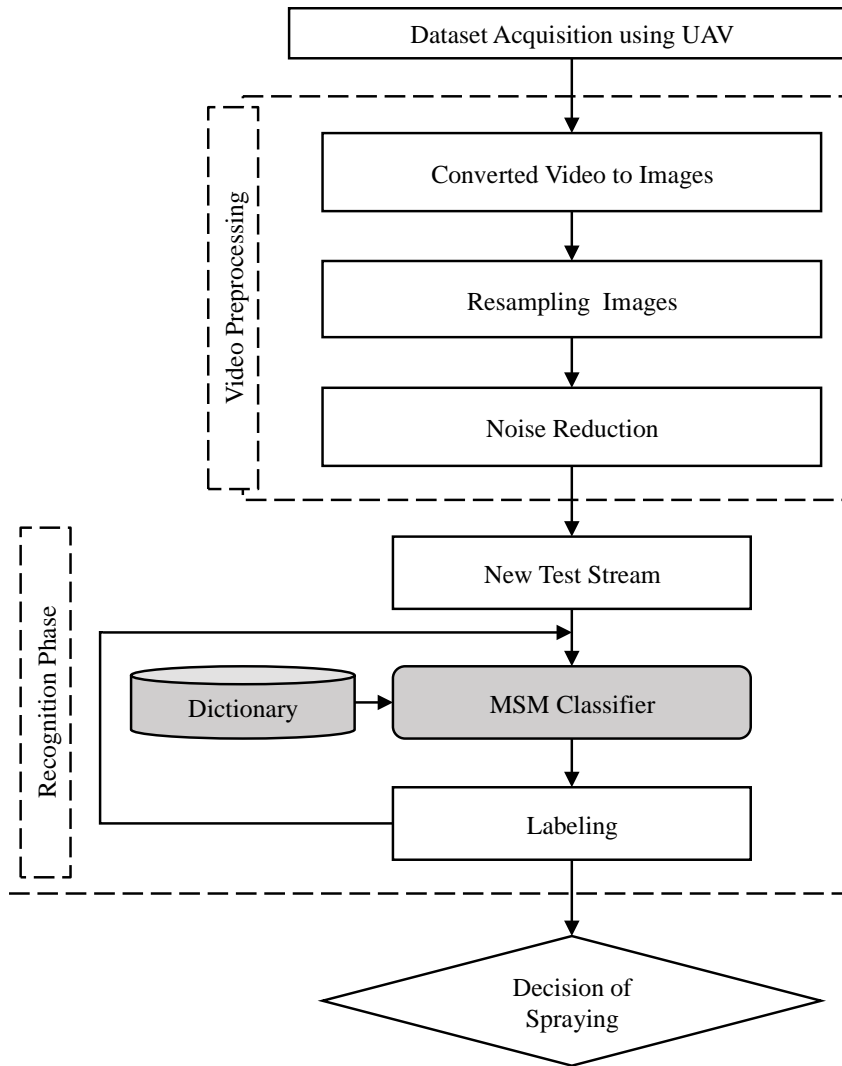


Figure 3.6. Online recognition system for classification of spraying based on MSM classifiers

3.3 Results

3.3.1 Offline Recognition Performance

In the offline recognition system, the accuracy was 80.5% in the cropland classifiers for spray and nonspray area recognition in the first experimental areas (L1). In the case of orchards, the spray and nonspray area recognition was 75% (**Table 3.3**). In the second experimental area (L2), the recognition accuracy was 70.4% and 86.1% for croplands and orchards, respectively. Finally, mixed crop and orchard areas (L3) were chosen for offline recognition by classifiers. The recognition accuracy was 72.3% and 70% for croplands and orchards, respectively. The overall accuracy was 74.3% (croplands) and 77% (orchards) for the L1, L2 and L3 locations, which had a combination of croplands and orchards (**Table 3.3**). Wide crop canopy or orchards had the advantage of higher recognition by classifiers. The high accuracy of the recognition

system was obtained using the MSM for training and testing the datasets from the three different types of experimental fields.

Table 3.3. Offline classifier recognition and accuracy analysis

		Location (Croplands, Orchards)	Work patterns Classifiers	True condition (offline recognition)			
				Cropland		Orchard	
				Spray	Nonspray	Spray	Nonspray
Predicted condition (Tested by the recognition phase)	L1	Spray	74	21	35	9	
		Nonspray	16	79	13	31	
		Accuracy	80.5%		75%		
	L2	Spray	38	11	41	2	
		Nonspray	18	31	10	33	
		Accuracy	70.4%		86.1%		
	L3	Spray	56	0	37	18	
		Nonspray	31	25	15	40	
		Accuracy	72.3%		70%		

(L1: a farm with a combination of croplands and orchards, L2: a farm with different croplands with orchards, L3: a research farm with croplands and orchards)

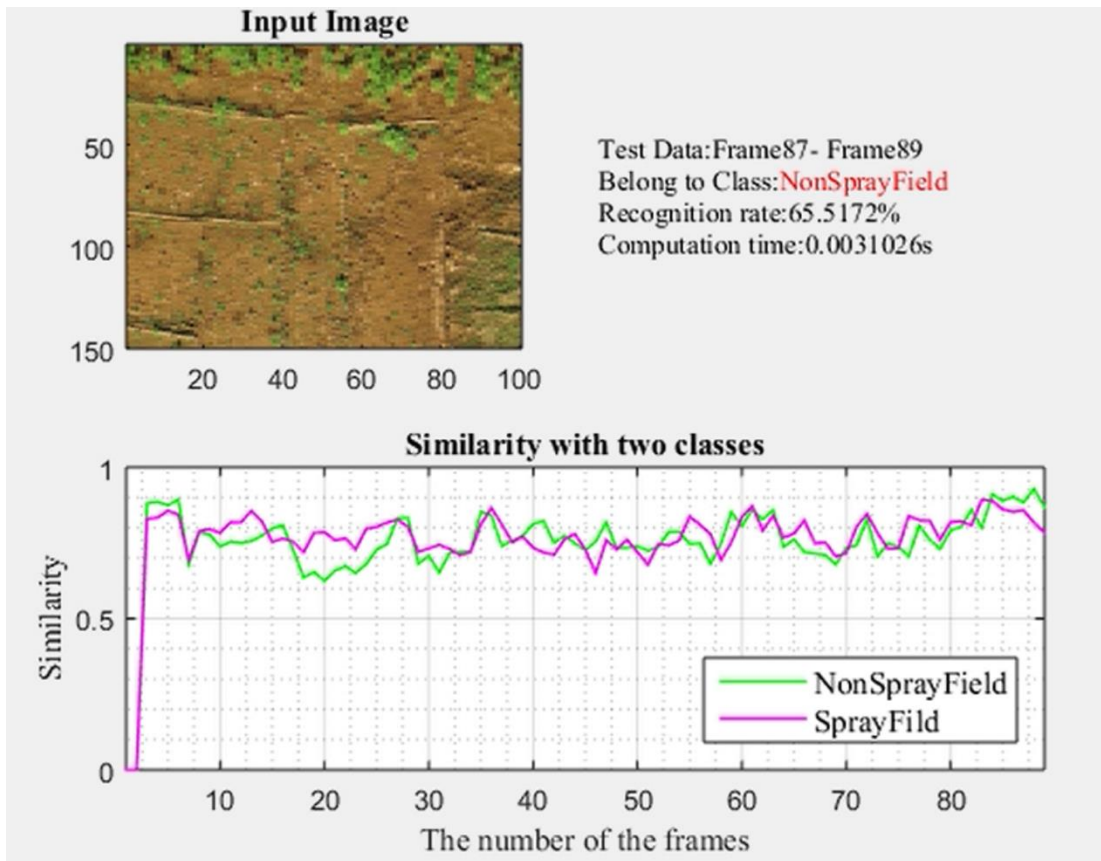
Table 3.4. Extended datasets for training and testing of classifiers using offline recognition system

Croplands and Orchards	Data sets		Training image numbers	Testing image numbers	Accuracy
	Spray	Nonspray	Offline	Offline	
Carrot	256	256	First half (128+128)	Last half (128+128)	73.79%
Cabbage	440	440	First half (220+220)	Last half (220+220)	81.25%
Onion	210	210	First half (105+105)	Last half (105+105)	66.32%
Chestnut	224	224	First half (112+112)	Last half (112+112)	77.31%
Persimmon	248	248	First half (124+124)	Last half (124+124)	70.94%
Trees and Structures	216	216	First half (108+108)	Last half (108+108)	64.58%

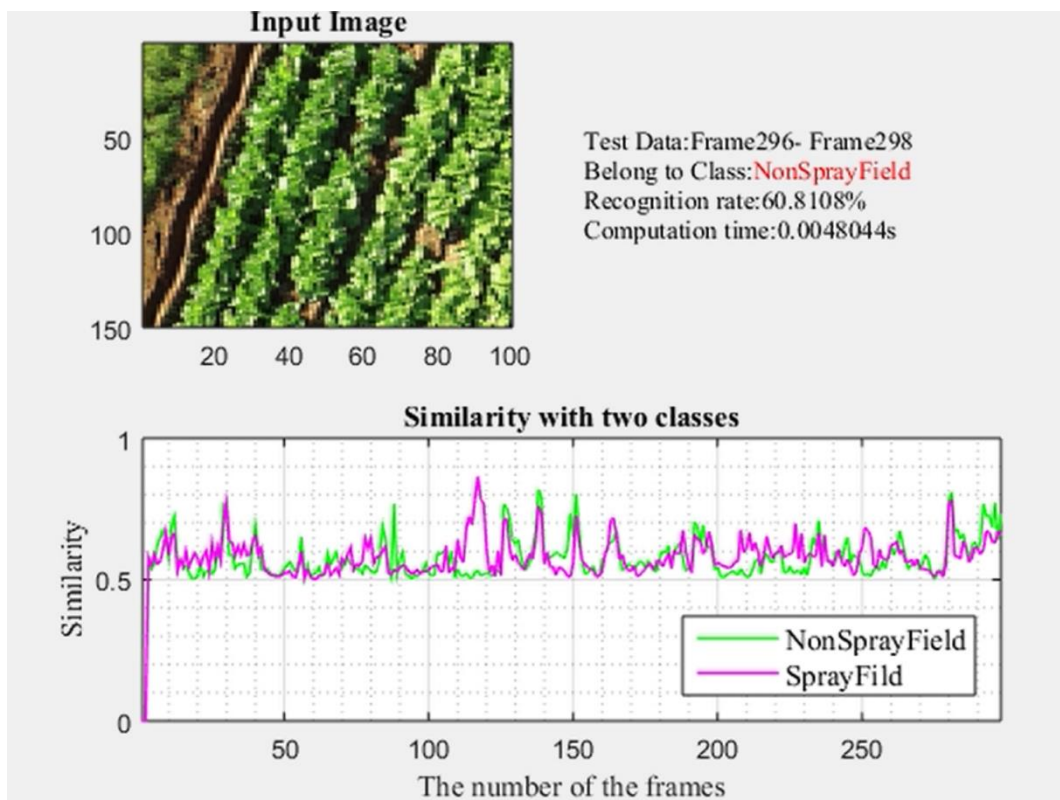
Further confirmation, frame numbers were increased for training and testing of datasets, whether there were significant differences in recognition accuracy of classifiers. Extended datasets confirmed the accuracy of MSM method did not change much even if the frames were increased to double for testing and training of datasets in offline recognition system (**Table 3.4**).

3.3.2 Online Recognition Performance

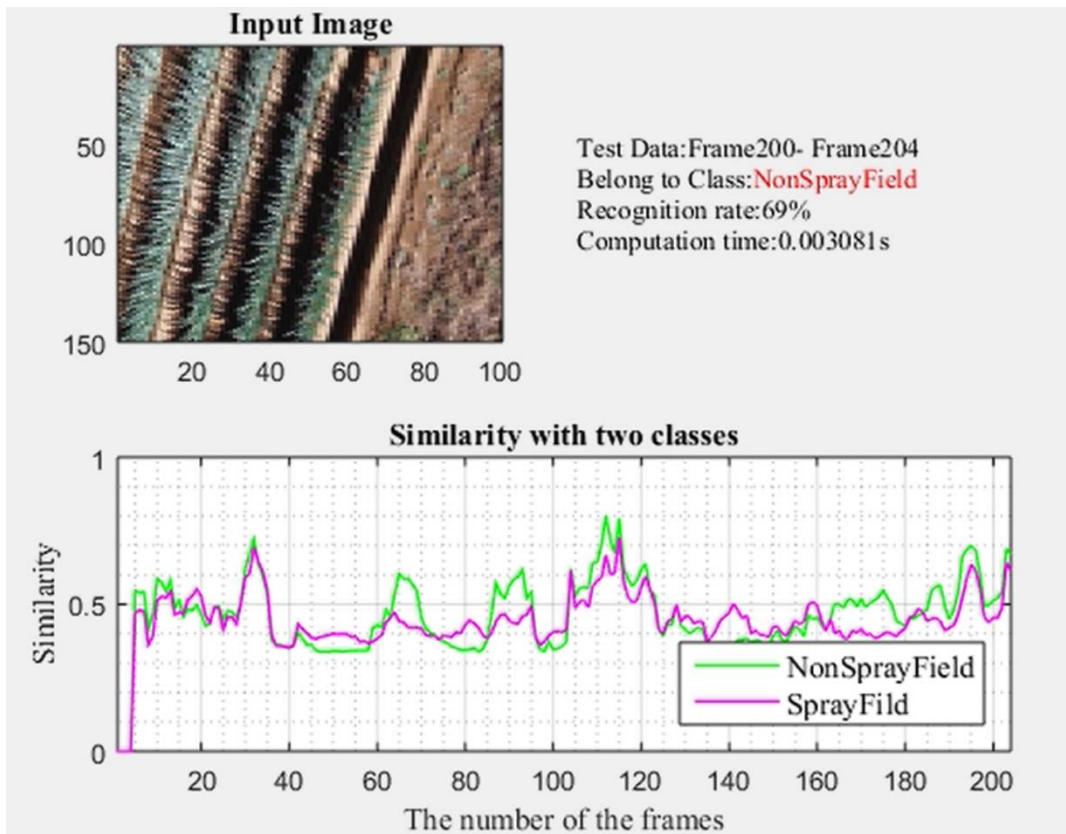
The developed user interface had the advantage of online information that included the current cropped image, the tested image sets using a sliding window, the predicted category, the recognition rate (the correct classifications were known during the test), the computational time, and the similarity plot. For the cropland classifiers, the UAV was flown at a 5 m height, and the recognition rate was observed to be 65.5% for L1 experimental areas. The computational time was only 0.0031 s for classifier recognition (**Figure 3.7a-c**). The flying height was 15 m for orchard classification, and recognition was observed at 69.1% with a computation time of 0.0031 s for each classifier. In the second experimental flying areas (L2), the recognition accuracy of classifiers for noted spray and nonspray areas was 60.8% and 82.2% for croplands and orchards, respectively. The computational time was only 0.0031 s for recognition by the classifiers, and orchard classifier recognition also required only 0.0031 s for each classifier (**Figure 3.8a-c**). In the third experimental location (L3), the online recognition rate by classifiers reached 69% in 0.0048 s for each classifier and 71.7% in 0.0031 s for each classifier in croplands and orchards, respectively. The online recognition system had an average accuracy of 65.1% and 75.1% for croplands and orchards, respectively, with a recognition time of 0.0031 s (**Table 3.5**).



(a) Cropland: Carrot

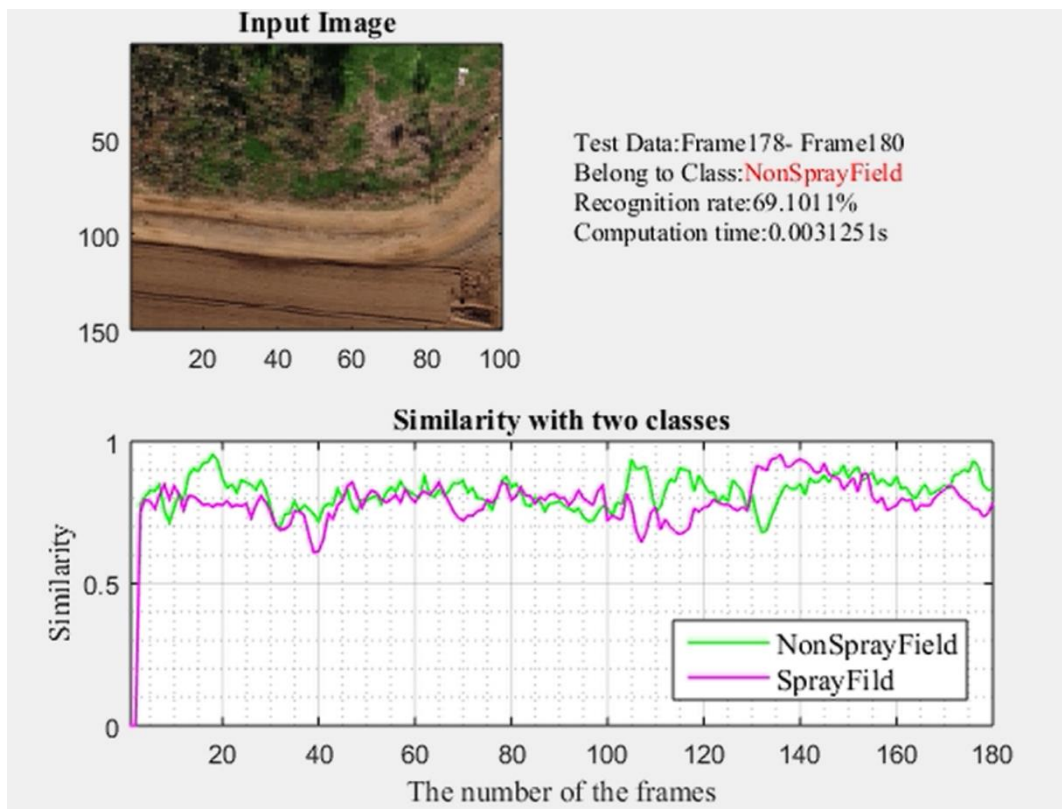


(b) Crop field: Cabbage

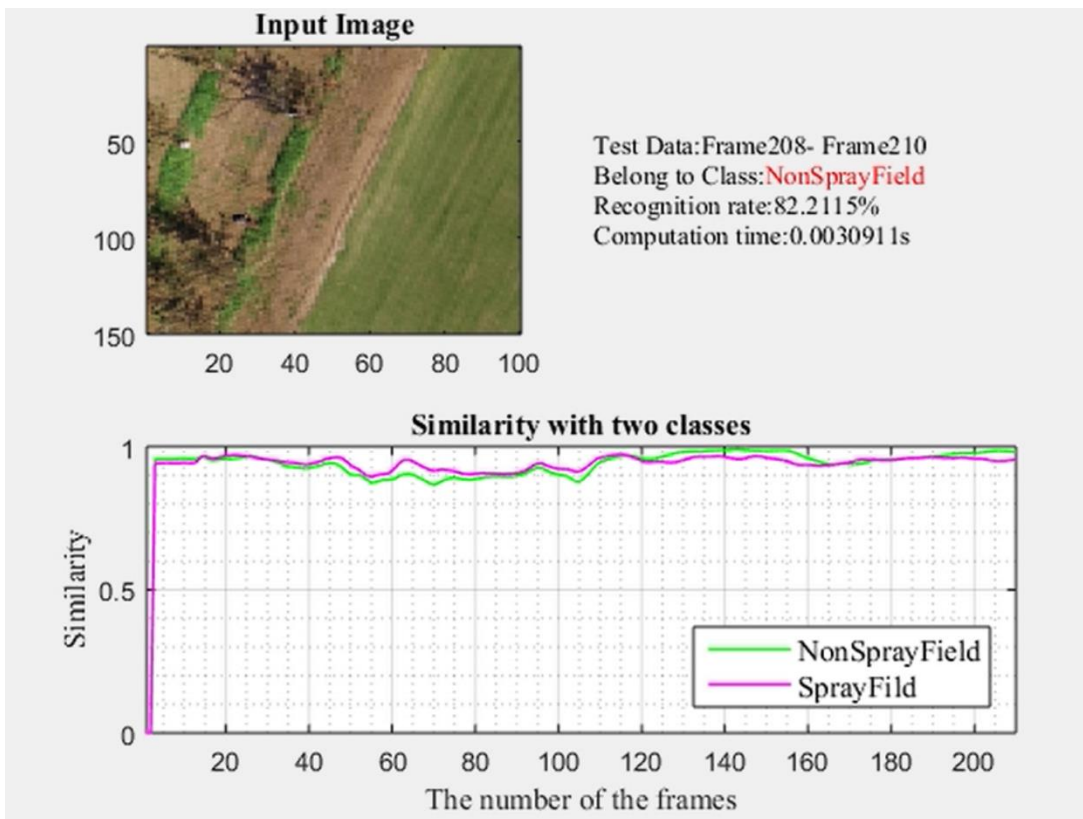


(c) Cropland: Onions

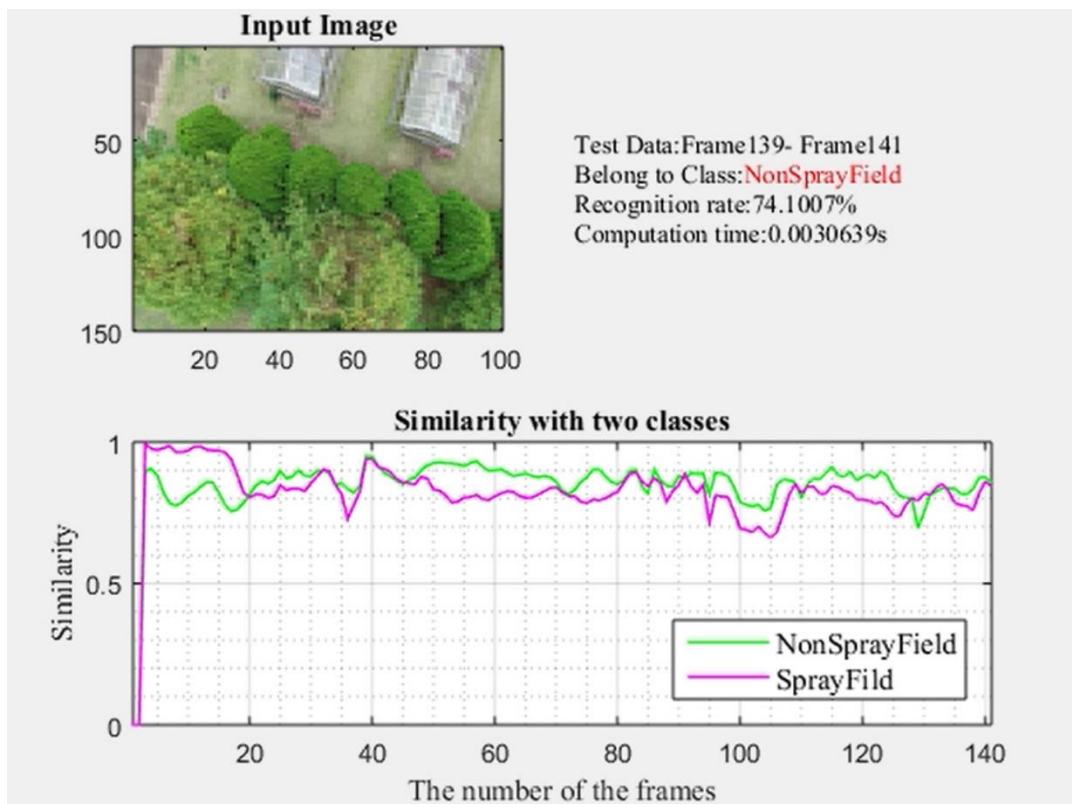
Figure 3.7. Online recognition performance of a classifier of croplands from a 5 m height



(a) Orchard: Chestnut



(b) Orchard: Persimmon



(c) Orchard: Trees and Structures

Figure 3.8. Online recognition performance of a classifier of orchards from a 15 m height

Table 3.5. Online classifier recognition and accuracy analysis

Crop/Land	Flying Height (m)	Accuracy (%)	Recognition time of classifier (s)
Carrot	5	65.51	0.0031
Cabbage	5	60.88	0.0048
Onion	5	69.00	0.0031
Chestnut	15	69.10	0.0031
Persimmon	15	82.21	0.0031
Trees and Structures	15	74.10	0.0031

3.4 Discussion

The field experiments were conducted in different types of fields to increase dataset variety for the selection of spray and nonspray areas inside the croplands and orchards. The offline recognition system shows the MSM effectiveness for training and testing the datasets for croplands and orchards. The classifiers were used for croplands and orchards and were limited to being trained and tested on datasets acquired in the late fall season. The MSM has the flexibility to increase the number of classifiers, which may increase the computational time requirement. As UAV spraying is performed at higher speeds, we tend to focus on minimizing the computation time to reduce the computational burden for decision making to recognize the spray and nonspray areas in croplands and orchards. UAVs operating at high speed with limited battery life and a small payload of liquid chemicals demand high computational speed and fast operation with good recognition accuracy. With this consideration, the online recognition system provided some advantages, although its accuracy was not as high as that of the offline recognition system. The system needs further training data to increase accuracy, especially for the identification of croplands less than 5 m high and orchard areas from 15 m high. In the online experiment setting, similar environments resulted in increased recognition, while adding different categories of orchards reduced recognition. It was very challenging to test the datasets from a fast UAV operating speed at a high altitude. Classifiers were trained and tested on datasets acquired from three different locations to confirm the recognition accuracy. However, complex canopy systems were not present in the features. This MSM system had a limitation in recognizing classifiers in complex canopies of crops or orchards. We could not collect images of complex canopy crops, and we assume that in such canopy systems, upward and

downward image acquisition is required to identify the spray and nonspray areas under different lighting conditions. Lighting is a key point that needs to be carefully considered, especially interception through the canopy. It would be ideal to train the UAV features of spray and nonspray areas on a large field to obtain higher accuracy in precision applications ranging from usual to complex canopies of crops. Further studies are required to deal with such complexity of canopies, very large datasets in different lightening conditions, the processing of images to remove noise using extended Kalman filters in onboard UAV systems.

3.5 Conclusions

A machine learning system was developed using MSM for images collected by a UAV in different types of farm fields and orchards. The machine learning system was developed to train and test two classifiers, one for agricultural croplands and one for orchard areas, on different datasets to distinguish spray and nonspray areas for the development of autonomous spraying systems in the future. Images were collected from low (5 m) and high altitude (15 m). The accuracy of the offline recognition system was found to be 74.4% and 77% for low- and high-altitude systems, respectively. On the other hand, the online recognition system performance had an average accuracy of 65.1% and 75.1% for low-altitude and high-altitude image acquisition systems, respectively. The computation time for online recognition systems was observed to have a minimum of 0.0031 s (on average) for reporting classifier recognition. The developed machine learning system for recognizing classifiers of spray and nonspray areas can be implemented in the autonomous UAV spray system in real time. In our future experiments, we will improve the training and testing system by incorporating an artificial neural network (ANN) and deep learning to develop a UAV-based autonomous spraying unit for croplands and orchards.

3.6 Summary

The machine learning system was developed using MSM for images collected by a UAV in different types of farm fields. The machine learning system was developed to train and test the datasets for two classifiers of agricultural croplands and orchard areas for enabling autonomous spraying system in future. The classifiers were sub categorized as spray and non-spray areas. Datasets images were collected from low (5 m) and high altitude (15 m) respectively. The offline recognition system was noted as 70.4% and 80.5% for low and high-altitude systems respectively. On other hand, the online recognition system performance was reported with higher accuracy of 80% from low altitude and 71% from higher altitude image acquisition

systems. The computation time for online recognition system was observed minimum with an average 0.004 s for reporting recognition of each of the frame for classifiers. The developed machine learning system for recognizing the classifiers can be implemented in the autonomous UAV spray system for recognizing spray and non-spray within the minimum computation in real-time. In our future experiment, we will implement this machine learning system to develop autonomous spraying system for croplands and orchards. Furthermore; precision irrigation is one major concern to save water and unnecessary clogging. To enable the precision irrigation management, this is very important to know the soil moisture information. In the following chapter, UAV-based soil moisture information system will be discussed along with g calibration system.

Chapter 4

Thermal Images Acquisition with UAV for Soil Surface Moisture Monitoring

4.1 Background

Soil moisture detection including canopy water content assessment is necessary for any crops. This part of the research attempted to develop soil moisture detection using UAV imagery. In the UAV imagery for detecting the soil moisture, thermal imaging and thermal videos are most commonly chosen. The radiation in the long-infrared range of the electromagnetic spectrum (9–14 μm) are usually detected by thermal cameras and produce radiation images, which called thermograms. A thermal image or thermographic image is actually a visual display of the infrared energy emitted, transmitted and reflected by the object. (Figure 4.1).

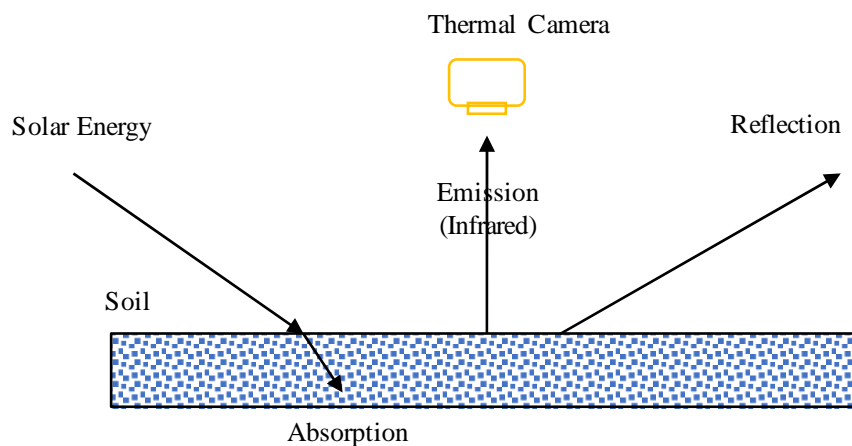


Figure 4.1. Thermal imagery to determine the soil moisture from infrared information

The field could contain different infrared energy due to the difference of soil moisture contents. Soil moisture could be found by detecting infrared energy using thermal camera. The thermal IR imagery got importance in agricultural sector due to recognizing of surface temperature of soil and plant canopy. The moisture content information can be indirectly measure through the canopy feature analysis or soil features analysis. The features mosaic got significance importance in agricultural researches. UAV based thermal camera have the opportunity to sense the temperature and soil moisture information (Figure 4.2).

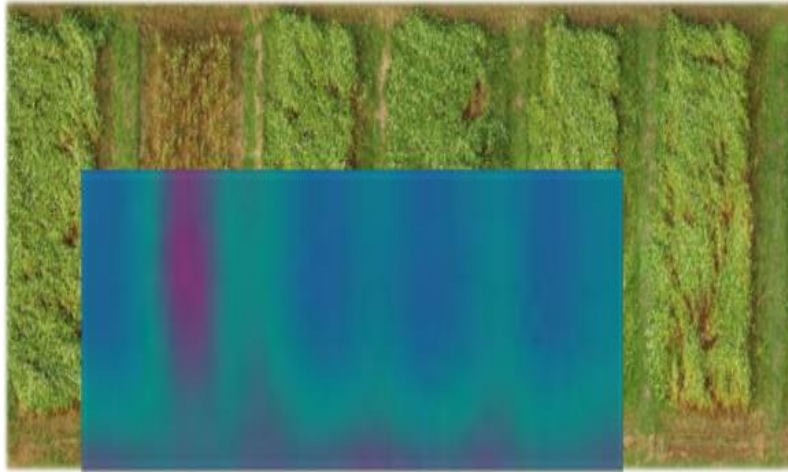


Figure 4.2. Typical example of images camera to RGB images and thermal imagery

It is very important to measuring soil moisture in agricultural production process and can help farmers manage irrigation system more effectively. Understanding the soil moisture contents of field, farmers can not only reduce water consumption during grow crops, but also improve the yield and quality of crops by precision management of soil moisture during key plant growth stages. There kinds of methods to measure field moisture, such like using soil moisture sensors, satellite remote sensing method, thermal infrared analyzing method, and thermal camera with UAV method. Soil moisture sensors could achieve continuously and real-time detection with high accuracy. But it needed to spend a lot of labor force and resources for setting the sensors. It could estimate soil moisture using satellite microwave remote sensing due to the large difference of dielectric properties between the of wet and dry soil. But it could not provide real-time monitoring because of satellite limitation (Yang, et al., 2015). Thermal infrared remote sensing method could collect the data from LANDSAT or ASTER. The problems of this method are non-real time and low resolution. Thus, to collect high-resolution thermal imaging images for analyzing the soil moisture in real time using thermal camera from UAV becomes research hotspot.

Objective

In this part of thesis, it attempted to develop the way to measure field moisture using thermal image collected by UAV. To estimate of surface soil moisture from thermal images and proposed a method to measure field moisture using thermal images acquisition by UAV.

4.2 Introduction

4.2.1 ORB Features Detection and Matching

A feature is a property that can be measured, or an observed characteristic of a phenomenon was defined in machine learning and pattern recognition (Bishop, Christopher, 2006). The key step for effective algorithms in pattern recognition, classification and regression is to choose the features, which should be informative, discriminating and independent. Different from features of numeric, strings and graphs which belong to structural features are used in syntactic pattern recognition. The concept of "feature" is related to that of explanatory variable used in statistical techniques such as linear regression. In the study, different features were analyzed for the thermal images (ORB features and SURF features). Oriented FAST and rotated BRIEF (ORB) features is a fast-robust local feature detector. The ORB features could be applied for object recognition or 3D reconstruction in computer vision tasks, which is based on the Features from Accelerated Segment Test (FAST) keypoint detector and the visual descriptor Binary Robust Independent Elementary Features (BRIEF). It could provide a fast and efficient replacement compare to SIFT features (Ruble, E.; Rabaud, V., 2011).

ORB Feature has the advantages of resistant to noise and rotation invariant and is capable of being used for performance in real-time. To improve the image-matching applications, to perform panorama stitching and patch tracking using low-power devices without GPU acceleration, and to reduce the time of standard PCs for detecting feature-based objects. Compare to SIFT this descriptor performs equally well on these tasks (and better than SURF). ORB uses the intensity centroid which simply measured corner orientation. It assumes that the intensity of the angle deviates from its center and that the vector can be used to estimate the direction. First, the moments of a patch are defined as:

$$m_{pq} = \sum_{x,y} x^p y^q I(x, y) \quad (4.1)$$

the centroid (the mass center of the patch) could be found:

$$C = \left(\frac{m_{10}}{m_{00}}, \frac{m_{01}}{m_{00}} \right) \quad (4.2)$$

From the corner's center -O to the centroid could be constructed as a vector, \overrightarrow{OC} . The orientation of the patch could be simplified as:

$$\theta = \text{atan2}(m_{01}, m_{10}) \quad (4.3)$$

where atan2 is the quadrant-aware version of \arctan . The descriptor that obtaining rotation invariance could be computed when calculated the orientation of the patch and rotate it to a canonical rotation.

The BRIEF descriptor is a bit string description of an image patch constructed from a set of binary intensity tests. Assume that p is a smoothed image patch, a binary test τ is defined as:

$$\tau(p; x, y) := \begin{cases} 1 & : p(x) < p(y) \\ 0 & : p(x) \geq p(y) \end{cases} \quad (4.4)$$

where $p(x)$ and $p(y)$ is the intensity of p at a point x or y . The feature is defined as a vector of n binary tests:

$$f_n(p) = \sum_{1 \leq i \leq n} 2^{i-1} \tau(p; x_i, y_i) \quad (4.5)$$

Here a Gaussian distribution is applied around the center of the patch and the vector length $n = 256$.

BRIEF is steered by the orientation of key points. For any feature set of n binary tests at location (x_i, y_i) , a $2 \times n$ matrix was defined as:

$$S = \begin{pmatrix} x_1, \dots, x_n \\ y_1, \dots, y_n \end{pmatrix} \quad (4.6)$$

Depending on the patch orientation θ and the corresponding rotation matrix R_θ , the steered version S_θ of S could be constructed as:

$$S_\theta = R_\theta S \quad (4.7)$$

The steered BRIEF operator changes into:

$$g_n(p, \theta) := f_n(p) | (x_i, y_i) \in S_\theta \quad (4.8)$$

The correct set of points S_θ will be applied to compute its descriptor as long as the keypoint orientation θ is consistent across views.

4.2.2 SURF Features Detection and Matching

Speeded up robust features (SURF) commonly applied as local feature detector and descriptor that can be used for object recognition, 3D reconstruction or image registration, classification.

SURF uses an integer approximation of the determinant of Hessian blob detector to detect interest points. Its feature descriptor is depending on the sum of the Haar wavelet response around the interest point. It can be computed with 3 integer operations using a precomputed integral image. It is reported that the standard version of SURF is faster than SIFT and more robust against different image transformations than SIFT (Herbert B., Andreas E., Tinne T., 2008). The square-shaped filters are used as an approximation of Gaussian smoothing for SURF. It is much faster for filtering the image with a square using the integral image:

$$S(x, y) = \sum_{i=0}^x \sum_{j=0}^y I(i, j) \quad (4.9)$$

Using the integral image could evaluated the sum of the original image within a rectangle quickly based on evaluations at the rectangle's four corners. A blob detector based on the Hessian matrix is applied to find interest points from SURF. It used the determinant of the Hessian matrix to measure the local change around the point which is chosen based on the maximal determinant. Assume that a point $p = (x, y)$ in an image \mathbf{I} , the Hessian Matrix $\mathbf{H}(p, \sigma)$ at point p and scale σ could be wrote as:

$$H(p, \sigma) = \begin{pmatrix} L_{xx}(p, \sigma) & L_{xy}(p, \sigma) \\ L_{yx}(p, \sigma) & L_{yy}(p, \sigma) \end{pmatrix} \quad (4.10)$$

where $L_{xx}(p, \sigma)$, $L_{xy}(p, \sigma)$, $L_{yx}(p, \sigma)$ and $L_{yy}(p, \sigma)$ are the convolution of the second-order derivative of gaussian with the image $\mathbf{I}(x, y)$ at the point x . A 9×9 box filter of is similar to a Gaussian with $\sigma=1.2$ and corresponds the lowest level for blob-response maps.

4.3 Materials and Methods

For measuring field moisture content using thermal camera, soil samples were collected to analyses the digital data of thermal images to find out the relation with soil moisture. Monotectic analysis was chosen as the basic method. The image acquisition platform was designed to take the images from the UAV (Phantom3 Professional, DJI) (**Figure 4.3**). The UAV images were collected with thermal camera (FLIR Vue Pro 336) and on-board RGB camera (Flying height: 20m; Flying place: Tsukuba Plant Innovation Research Center T-PIRC).

4.3.1 Image Mosaic and Feature Detection for Estimating Soil Moisture

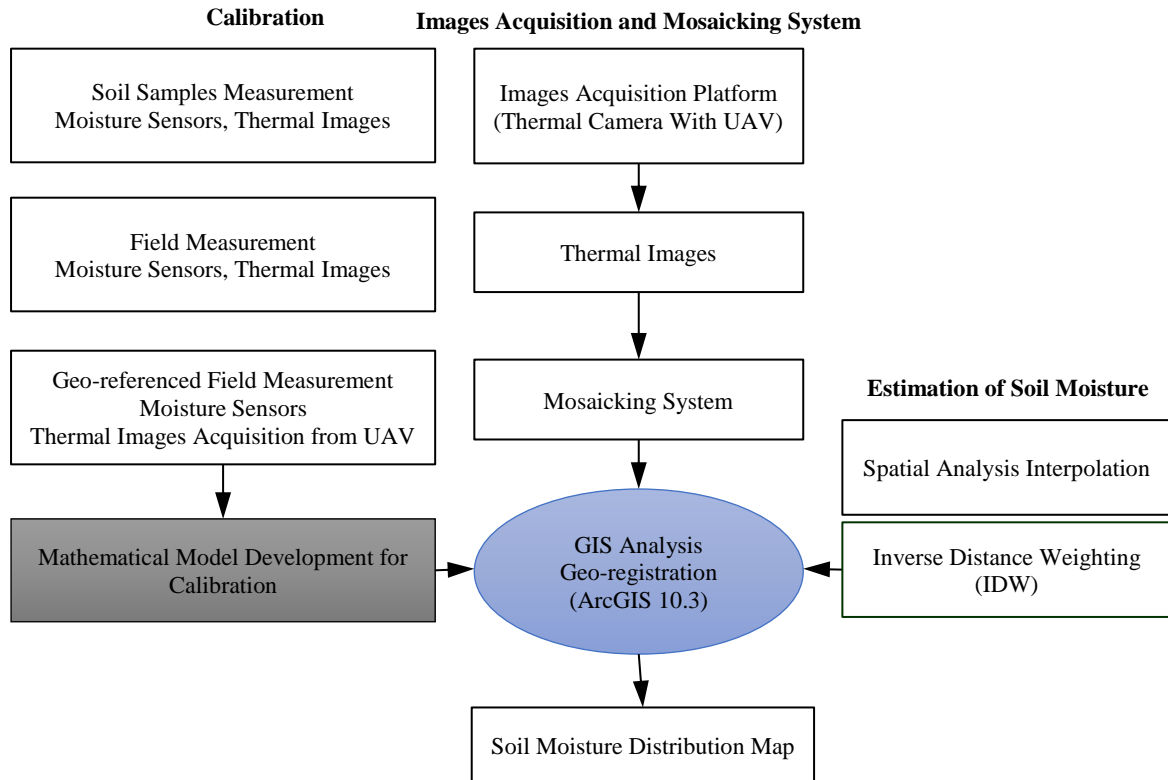


Figure 4.3. Image mosaic and feature detection for estimating soil moisture

The data of thermal images were 8-bit digital numbers about near-infrared wavelength. For recognizing the soil moisture from thermal images, firstly, the calibration for thermal camera to find out the relation about the soil moisture and thermal images. And then, a UAV equipped with thermal camera and RGB camera was used for datasets acquisition. At last, for showing the moisture distribution, we uploaded the data into the software of ArcGIS 10.3 for making soil moisture distribution map.

4.3.2 Thermal Images Acquisition Platform

The image acquisition platform was designed to capture the images from a commercial UAV (Phantom3 Professional, DJI). The UAV images were collected with thermal camera (FLIR Vue Pro 336) and on-board RGB camera (Flying height: 20m; Flying place: T-PIRC).

4.3.3 Calibration Method

4.3.3.1 Experiments of Testing Soil Moisture Using A Household Soil Moisture Detector

For measuring field moisture content using thermal camera, soil samples were collected to analyses the digital data of thermal images to find out the relation with soil moisture. Monotectic analysis was chosen as the basic method. 16 cups of soil samples were divided into

4 groups, and added into different amount of water (0, 50, 100, 150ml, soil weight: 350g, a moisture sensor was chosen for detecting the soil moisture directly in the same experiment (Indoor humidity: 38%, indoor temperature: 32°C) (**Figure 4.4**).

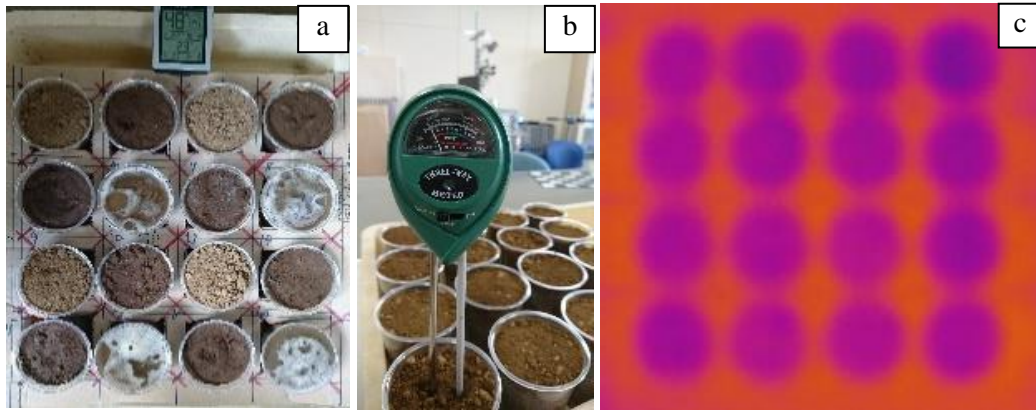


Figure 4.4. Indoors experiment

(a: Soil samples; b: Moisture sensor; c: Thermal image)



Figure 4.5. Outdoors experiments



Figure 4.6. Outdoors field experiments,
(a) Reference moisture sensor; (b) Thermal camera

Again, 16 cups of soil samples were divided into 2 groups, and added into different amount of water (25, 50, 75, 100, 125, 150ml, soil weight: 350g), tested 5 times at similar environment (Outdoor humidity: 43%, Outdoor temperature: 34°C) (**Figure 4.5**). Finally, chose different fields to detect the soil moisture and captured thermal images for testing the calibration system (**Figure 4.6**).

4.3.3.2 Soil Moisture Sensor Unit

A new soil moisture sensor unit was designed based on the IoT technologies and micro controlling board (**Figure 4.7**). This soil moisture sensor unit were made up with a soil moisture sensor as the main part to test the moisture content; a digital temperature and humidity sensor module was used for collecting the information of environment; the GPS module was selected for recording the location when test in the field; a wireless transmission module was chosen to send the data to a laptop for saving and analyzing and the LCD display was used to show the data in real-time.

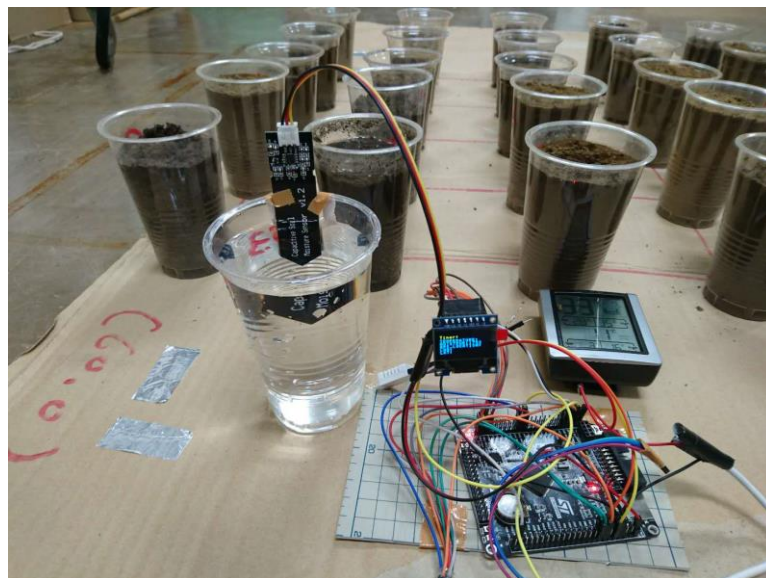


Figure 4.7 Soil Moisture Sensor Unit

4.3.3.3 Indoor Experiments with the Sensor Unit

In order to test the relation of the soil moisture and thermal image value, 25 plastic cups of soil were randomly added different amounts of water. After keeping for two hours, a thermal image

was captured with the thermal camera (Flir VUE Pro 336) (**Figure 4.8**), as well as the soil moisture content were detected twice of each sample (**Table 1**).

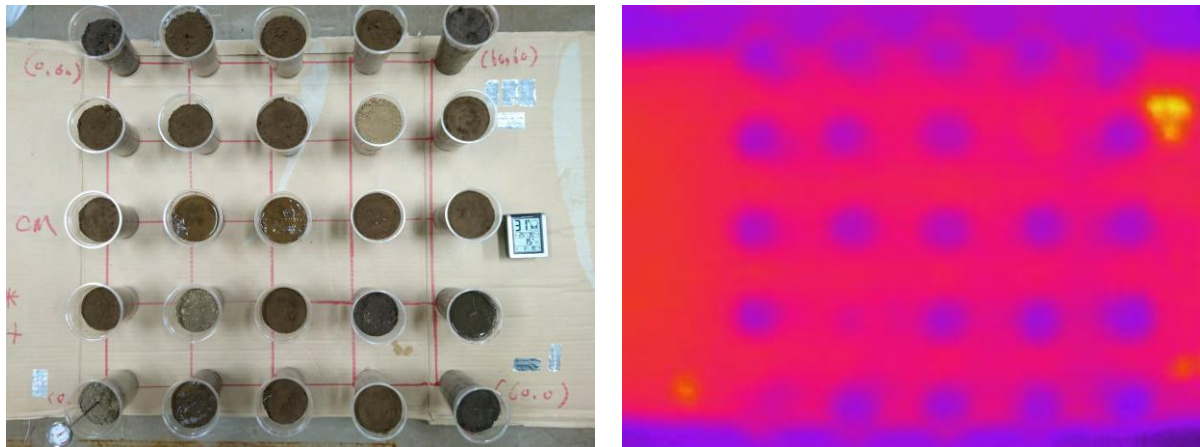


Figure 4.8. Soil Samples and Thermal Image

Table 1. Data of Indoor Soil Moisture Detecting Using Sensor Unit

Soil M	GPS LUN	GPS LAT	GPS TIME	AIR Temperature	AIR Humidity	Soil Temperature
3365	3607.1593	14005.7007	12:12:00	8.7	24.5	14.2
3365	3607.1591	14005.7004	12:12:00	9.1	24.9	
3267	3607.1552	14005.6963	12:12:00	10.4	0.7	12.9
3266	3607.1551	14005.6962	12:13:00	10.4	0.7	
3049	3607.156	14005.6952	12:13:00	10.3	0.7	12.4
3049	3607.1561	14005.6952	12:13:00	10.3	0.7	
2962	3607.1561	14005.6932	12:13:00	10	0.6	12.4
2962	3607.1562	14005.6929	12:13:00	10	0.6	
2249	3607.1529	14005.6897	12:14:00	10.1	0.8	12.1
2250	3607.1526	14005.6896	12:14:00	9.9	0.6	
1829	3607.1517	14005.6889	12:14:00	10.7	1.5	11.8
1822	3607.1517	14005.6888	12:14:00	10.7	1.5	
3104	3607.1516	14005.6883	12:14:00	9.9	0.9	13.3

3104	3607.1517	14005.6883	12:14:00	9.9	0.9	
1822	3607.1521	14005.6885	12:15:00	9.6	0.7	12.2
1817	3607.1521	14005.6885	12:15:00	9.5	0.6	
2600	3607.1524	14005.6887	12:15:00	9.8	1.1	12.1
2600	3607.1525	14005.6886	12:15:00	9.8	1.1	
2809	3607.1532	14005.6887	12:15:00	9.5	0.9	12
2802	3607.1532	14005.6888	12:15:00	9.4	0.9	
2590	3607.154	14005.6883	12:16:00	9.6	1.4	11.6
2590	3607.1543	14005.6882	12:16:00	9.6	1.4	
2893	3607.1552	14005.6854	12:16:00	9.2	1.1	11.9
2894	3607.1547	14005.6852	12:16:00	9.3	1.2	
2445	3607.1544	14005.6833	12:17:00	9.4	1.5	12
2445	3607.1544	14005.6833	12:17:00	9.4	1.5	
2793	3607.1535	14005.6836	12:17:00	9.6	1.8	12.1
2792	3607.1535	14005.6838	12:17:00	9.3	1.6	
2935	3607.1524	14005.6846	12:17:00	8.9	1.3	11.8
2933	3607.1522	14005.6847	12:17:00	8.7	1.2	
2889	3607.1527	14005.6853	12:18:00	9	1.6	11.8
2889	3607.1527	14005.6853	12:18:00	9	1.6	
2728	3607.1535	14005.6864	12:18:00	7.9	0.6	11.6
2723	3607.1535	14005.6865	12:18:00	7.8	0.6	
2949	3607.1535	14005.6876	12:19:00	7.6	0.5	12.2
2950	3607.1534	14005.6875	12:19:00	7.4	0.3	
3255	3607.1526	14005.6878	12:19:00	7.6	0.6	15.1
3265	3607.1523	14005.6877	12:19:00	7.6	0.6	
3139	3607.1518	14005.6879	12:19:00	6.9	25.5	11.6

3140	3607.1518	14005.688	12:19:00	6.8	25.5	
2454	3607.1508	14005.6895	12:20:00	6.4	25.1	11.8
2448	3607.1505	14005.6897	12:20:00	6.5	25.2	
1763	3607.1488	14005.6911	12:20:00	6.5	25.2	11.9
1763	3607.1487	14005.6917	12:20:00	6.7	25.4	
2523	3607.1486	14005.6935	12:20:00	7	0.1	12
2523	3607.1491	14005.6941	12:20:00	7	0.1	
2775	3607.1549	14005.6952	12:21:00	7.5	0.7	11.3
2775	3607.1551	14005.6951	12:21:00	7.5	0.7	
2111	3607.1555	14005.6924	12:21:00	7.3	0.5	10.9
2111	3607.1555	14005.6922	12:21:00	7.3	0.5	
1751	3607.1479	14005.6863	12:22:00	8.1	1.7	Water
1755	3607.148	14005.6865	12:22:00	8.1	1.8	
3464	3607.1492	14005.6878	12:22:00	7.5	2.1	Air
3465	3607.1497	14005.6882	12:22:00	7.2	1.9	

4.3.3.4 Soil Moisture Change Monitoring

In order to monitor the changing of soil moisture and test the relation, a 35 cm height flowerpot of soil sample was set and added water until saturated. The soil moisture content was collected, and a thermal image was captured automatically every 10 minutes (**Figure 4.9**).

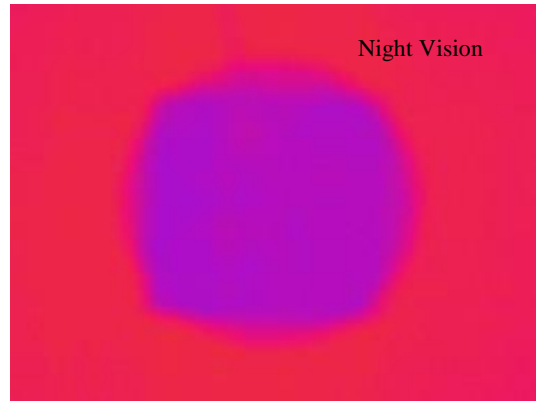
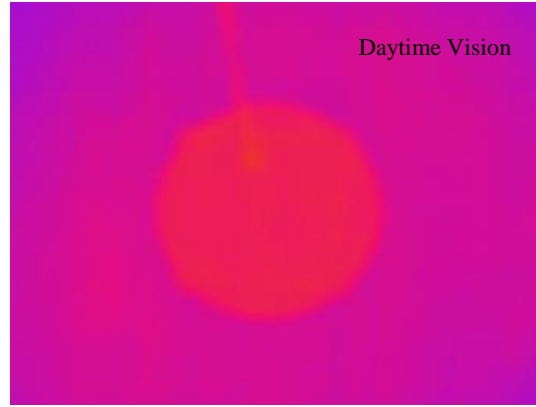


Figure 4.9. Soil Moisture Change Monitoring System and Thermal Images

4.3.3.5 Field Experiments



Figure 4.10. Landmark and Images Acquisition System

In order to test the calibration method, the field experiments were designed (**Figure 4.10**). At beginning, 16 landmarks were set up on the field and three times of soil moisture content were detected inside of the marks and recorded with the sensor unit. The UAV with thermal camera flired at the altitude of 5 m to capture the RGB images and thermal images and saved the data at TF cards (**Figure 4.11**).

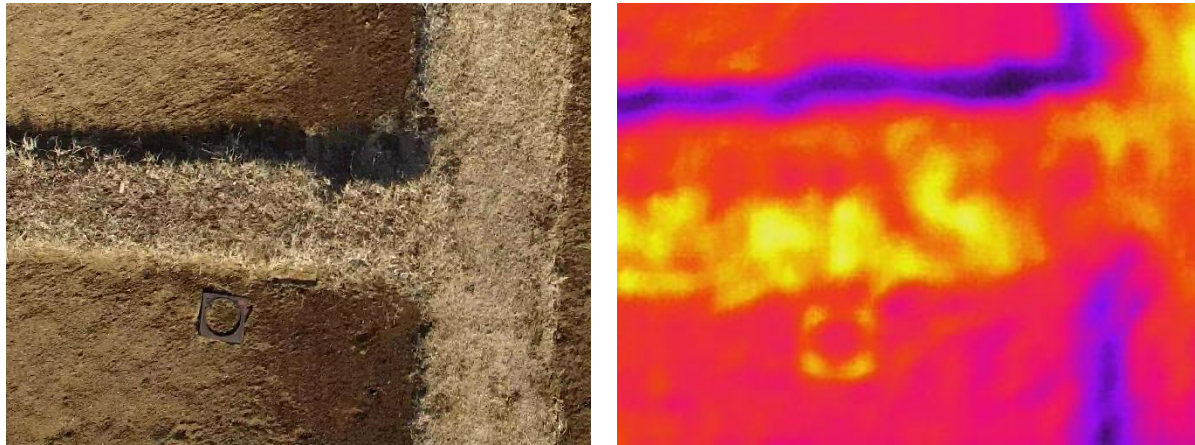


Figure 4.11. RGB Image and Thermal Image Captured by UAV

4.3.4 Thermal Images Mosaicking with ORB Features

The mosaicking system was tested with ORB features for multiple thermal images. It was programming in Python2.7® and OpenCV. The work progress was followed: Firstly, to identify the ORB features of each thermal images; and then matching the same ORB features of each images for recognizing the same area; and reduced the matching errors through Kalman filter; finally, clipping the overlap area and stitching images for a new image.

4.3.5 Thermal Images Mosaicking with SURF Features

The mosaicking system was developed with SURF features for multiple thermal images. The work progress was followed: Firstly, to identify the SURF features of each thermal images; and then matching the same SURF features of each images for recognizing the same area; and reduced the matching errors through Kalman filter; finally, clipping the overlap area and stitching images for a new image.

4.3.6 Soil Moisture Distribution Map

The soil moisture distribution map was created by the software of ArcGIS 10.3 (Esri, USA). The mosaicking images with multiple thermal images were georeferenced based, that contained the GPS information by setting up landmarks. After calibrated with the calibration method of soil moisture, we uploaded the image into the system and analyzing with spatial analysis interpolation and inverse distance weighting (IDW).

4.4 Results

4.4.1 Soil Moisture Detection

4.4.1.1 The Relation Detected by Household Moisture Detector

Soil moisture content had negative correlation with thermal energy (**Figure 4.12** and **Figure 4.13**).

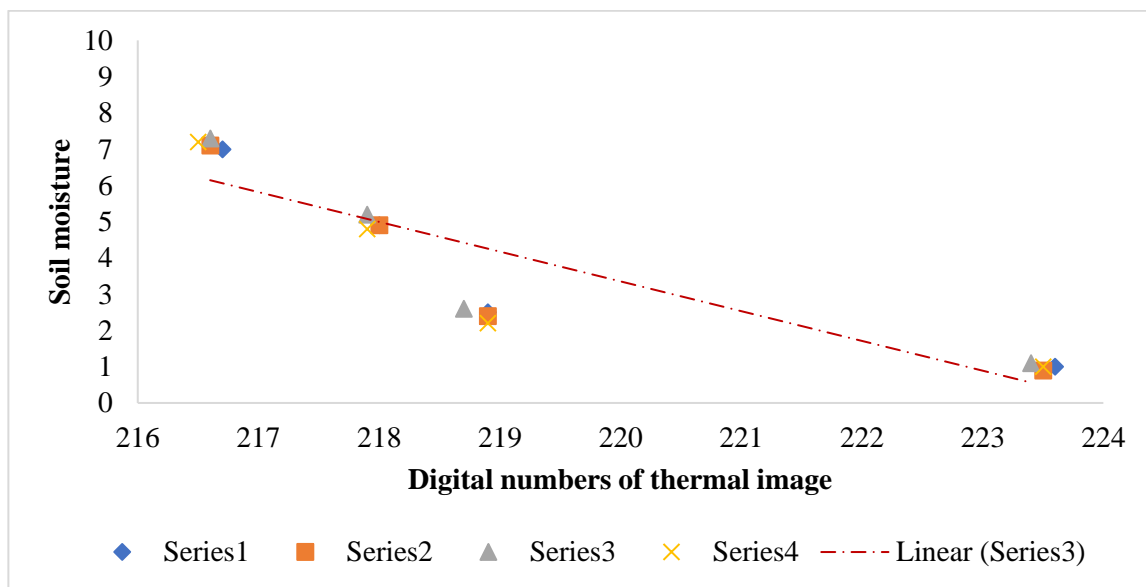


Figure 4.12. Relation of soil moisture and digital number of thermal imageries indoors experiment

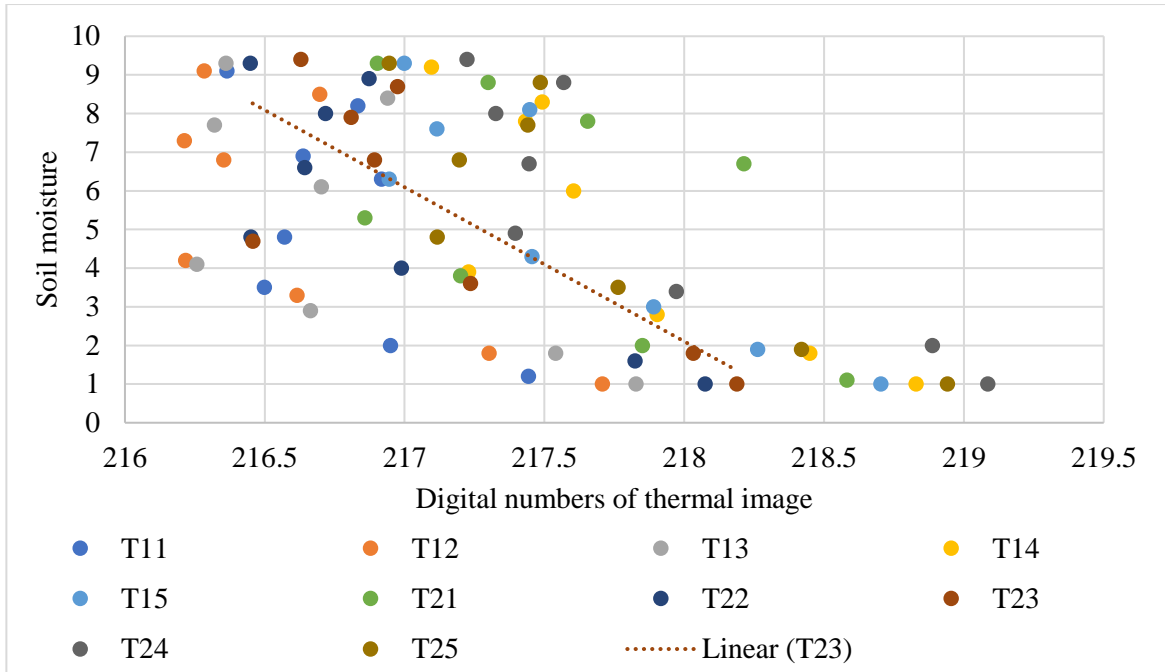


Figure 4.13. Relation of soil moisture and digital number of thermal imagery outdoors experiment

4.4.1.2 The Relation of Soil Moisture and Thermal Image Value

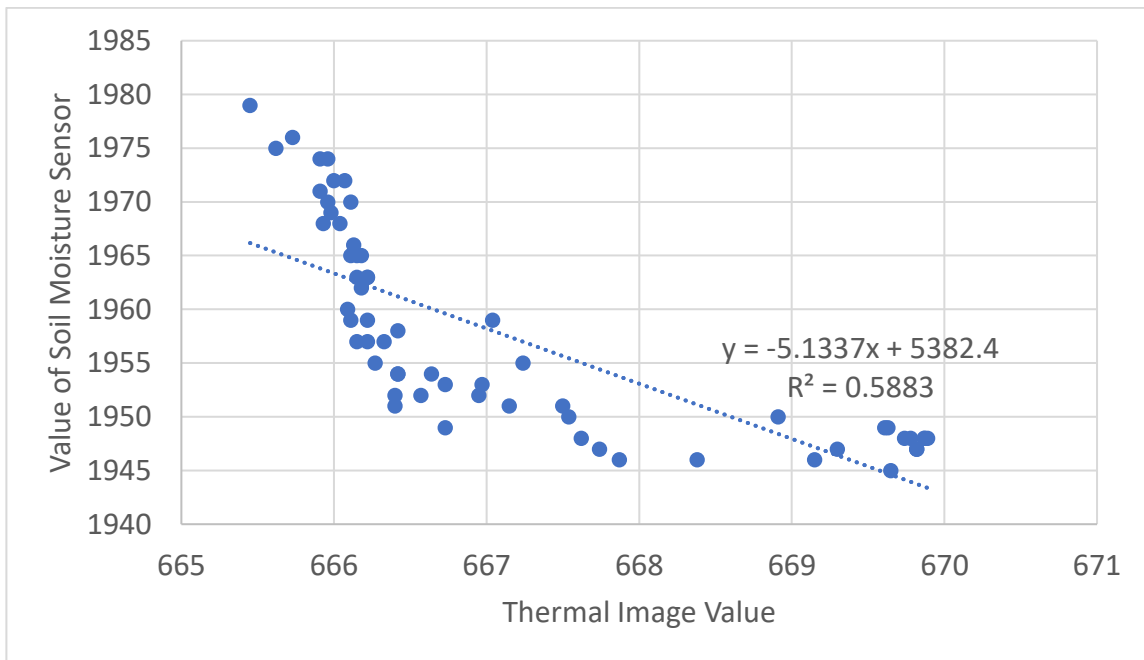


Figure 4.14. The Relation of Soil Moisture and Thermal Image Value

4.4.2 Features Detection and Matching

In this part, the ORB features were tested recognition for thermal images (**Figure 4.15**). One image could recognize 104 ORB features and 53 could be useful for matching after selected by extend Kalman filter (EKF) for reducing the noise; the other image could recognize 111 features and 57 could work for matching. Finally, 44 features could match, and 27 features were matching correctly, the matching accuracy was just 61.7% (**Table 4.2 and Table 4.3**).

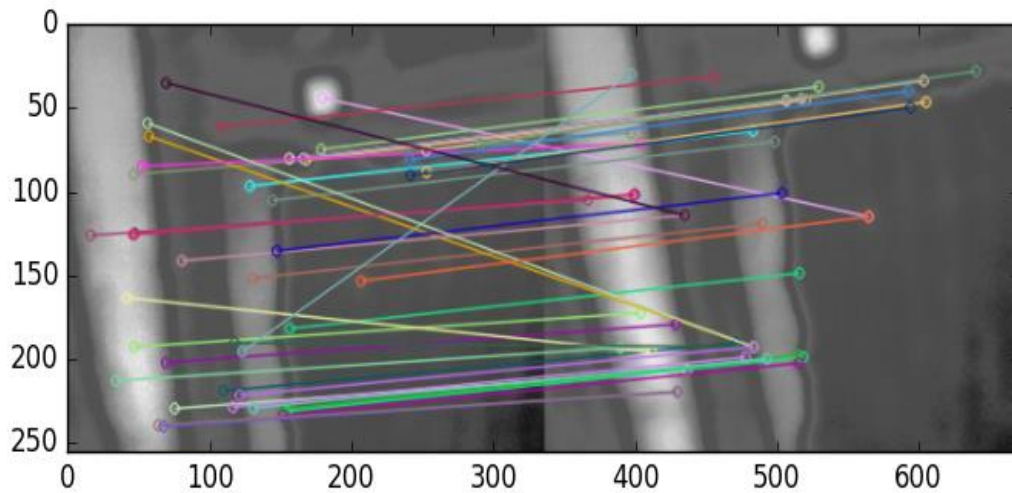


Figure 4.15. ORB features matching of thermal images (Features matching errors, 320x240)

Table 4.2. ORB features recognition

		Number of ORB Features	Selected ORB Features (EKF, k=2)
Thermal Camera	Image1	104	53
	Image2	111	57

Table 4.3. ORB features matching accuracy

	Matching Features	Matching Correctly	Matching Accuracy
Thermal Camera	44	27	61.4%

SURF features recognition for thermal images (**Figure 4.16**) could be recognized 481 SURF features and 249 could be useful for matching after selected by extend Kalman filter (EKF) for reducing the noise; the other image could recognize 524 features and 216 could work for matching. Finally, 186 features could match, and 167 features were matching correctly, the matching accuracy was 89.7% (**Table 4.4 and Table 4.5**).

Compare with the results of ORB features and SURF features, we found that the SURF features could work well for thermal images for features recognition and matching with multiple thermal images.

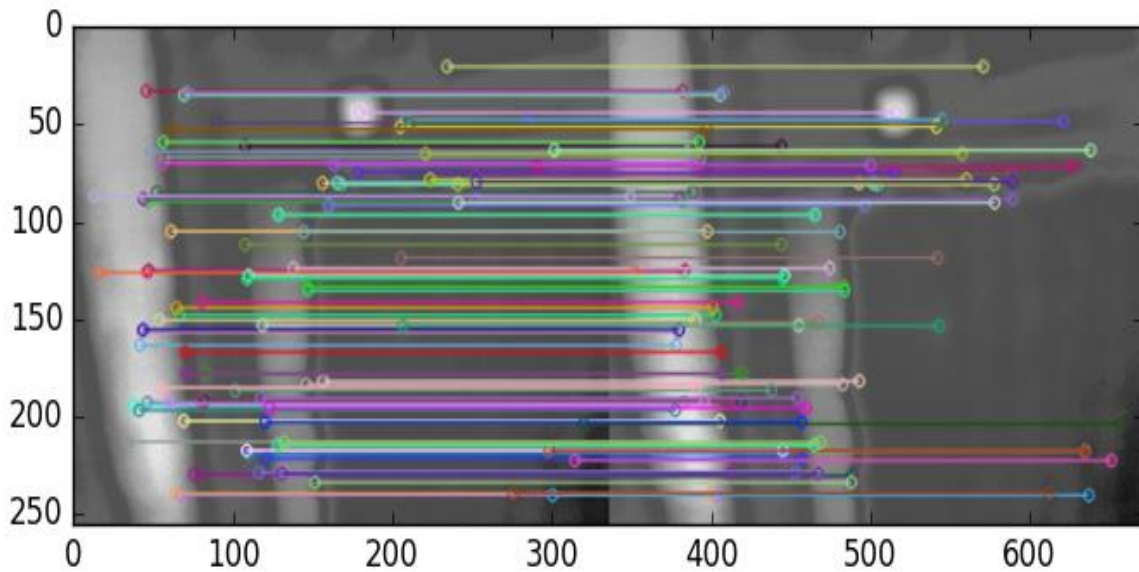


Figure 4.16. SURF features matching of thermal images

Table 4.4. SURF features recognition

		Number of SURF Features	Selected SURF Features (EKF, k=2)
Thermal Camera	Image1	481	249
	Image2	524	216

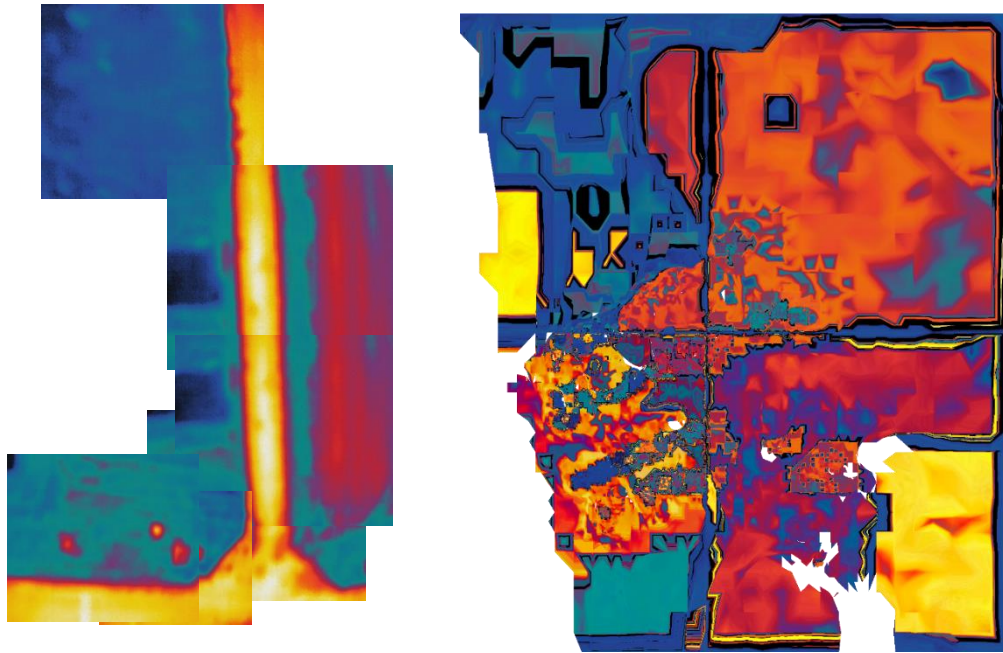
Table 4.5. SURF features matching accuracy

	Matching Features	Matching Correctly	Matching Accuracy
Thermal Camera	186	167	89.7%

4.4.3 Mosaicking of Thermal Images Using SURF Features

The results of thermal images mosaicking with multiple images using ORB features (**Figure 4.17**). The mosaicking results influenced by the matching error with ORB features for thermal images, it occurred chaotic image. The results of thermal images mosaicking with multiple images using SURF features could find from **Figure 4.18** and **Figure 4.19**. It could achieve

the ability of mosaicking multiple thermal images. Some problems were found when did the mosaicking image distortion caused by image channels changing (Thermal image - Grayscale image – RGB image) (**Figure 4.19**). And, drop frame and image radial distortion when mosaiced with more than 16 thermal images. Further research is needed to focus on dropping frames and mosaicking with multiple images and confirmation of estimating moistures from thermal images.



16 images

Figure 4.17. Mosaic of features in thermal imagery

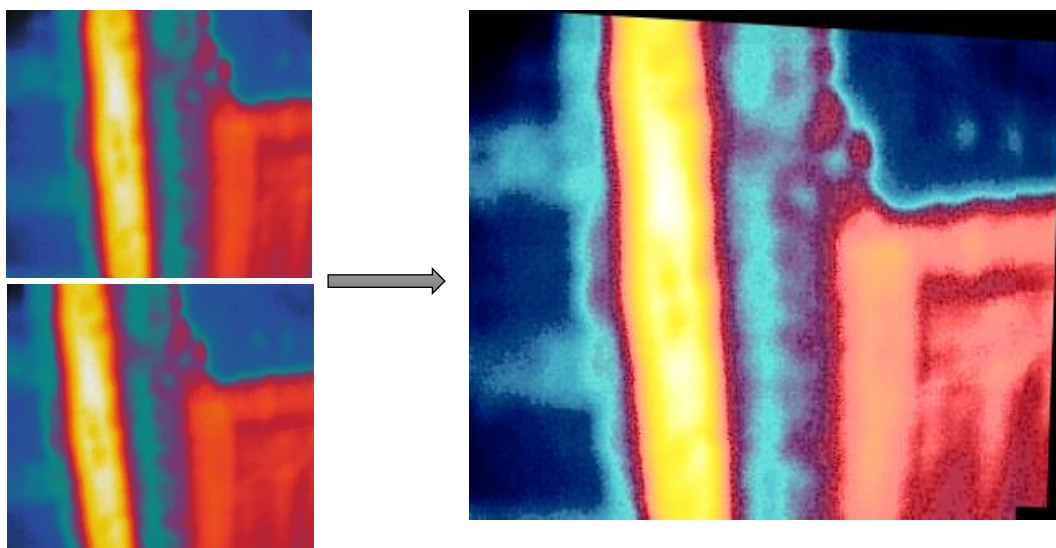


Figure 4.18. Mosaic of features in thermal imagery

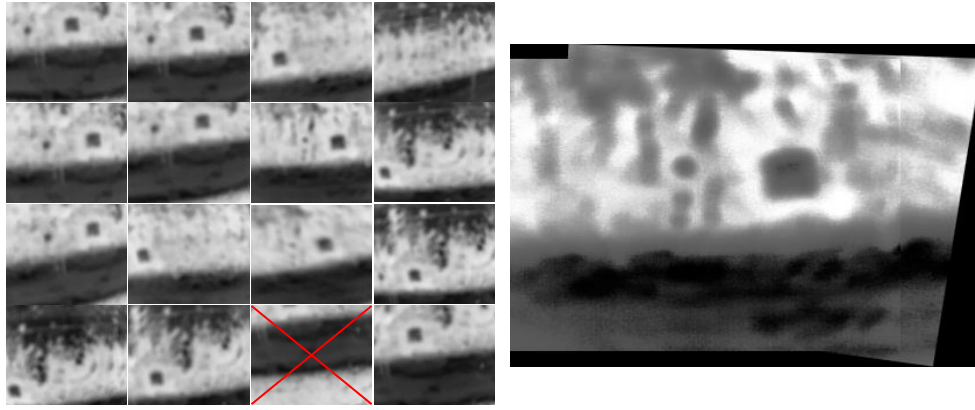


Figure 4.19. Multiple thermal images mosaicking using surf features

4.4.4 Mosaicking of RGB Images and Thermal Images of the Field



Figure 4.20. Mosaicking of RGB Images of the Field

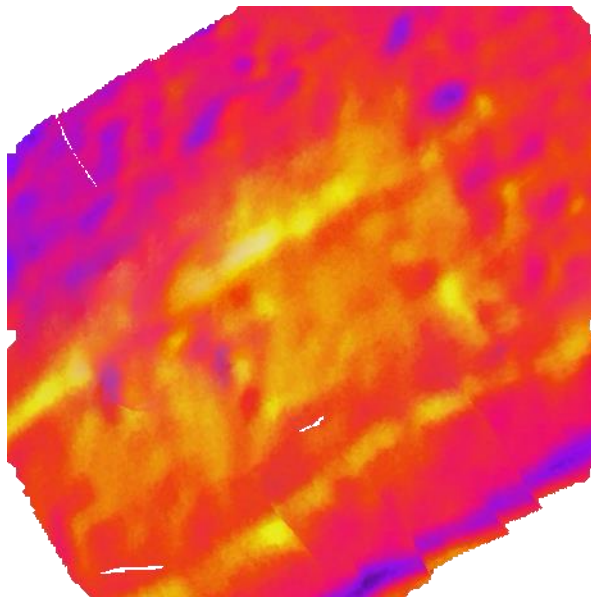


Figure 4.21. Mosaicking of Thermal Images of the Field

4.5 Discussion

The study aims to measure field moisture content using thermal image processing for precision agricultural management. Developed the calibration method for detecting soil moisture with thermal images. UAV images were collected with thermal camera. The mosaic was conducted for 16 images for thermal images. Imagery from each sensor was geo-referenced and mosaicked with a combination open source software open drone map. An algorithm was developed based on the surf. Soil moisture from ground reference direct measurement needs to correlate with thermal images digital numbers using the regression model with more accuracy. Soil moisture measurement using thermal imagery from UAV needs further confirmation. Mosaicking with multiple thermal images had the problems of dropping frames and image radial distortion. Dropping frames and mosaicking with multiple images need to be focused on.

4.6 Summary

The main purpose of this part of research is aimed to measure field moisture content using thermal image processing for precision agricultural management for helping farmers manage their irrigation systems more effectively with a small amount of water. Also, to improve the yield and quality of crops by improving the management of soil moisture during key plant growth stages. Developed the way estimated of surface soil moisture from thermal images using the calibration method. Soil samples were collected and added different amount of water for measuring the moisture percentage using a moisture sensor, as well, the thermal images were captured using a thermal camera, monotectic analysis method was chosen for recognizing the relation of soil moisture and the digital numbers of thermal images. Soil moisture measurement using thermal imagery from UAV needs further confirmation. Compared the performances of ORB features and SURF features for thermal images mosaicking. SURF features could easily detect from thermal images with high accuracy of matching. Developed a method of mosaicking multiple thermal images with SURF features using Python2.7® and OpenCV®. Dropping frames and mosaicking with multiple images need to be focused on. Further experiment will be conducted using wireless sensor network for confirmation of soil moisture information to train and test the datasets using machine learning approaches. In the applications of spray and nonspray area, including soil moisture information, would require a multi task robot platform. In the multi-task robot platform, UAV-based coordination has the high potential to lead the task for developing a navigation planner. In the following chapter, UAV-based navigation planner will be introduced with multi-task robot platform using

autonomous electrical platonic vehicle. In the multi-task system, feature recognition, edge detection and navigation planner system will be discussed. In the navigation planner, GIS mapping will be incorporated along mosaicking the ORB RGB image features for the large farms.

Chapter 5

Development of UAV-Follower based Multi-task Robots System Using Features Recognition and Navigation Planner

5.1 Background

With the reduction of new agricultural labor force and ageing intensifies, this creates inevitable problems of labor shortages in agricultural production. It reported that agricultural employment population decreased each year, and nearly half of labors over the age of 65 in Japan. More than 400 thousand ha. farmland was abandoned (**Figure 5.1**). Japanese Government has published a New Robot Strategy, which aims to achieve for implementation of automatic driving tractors to actual field until 2020 (New Robot Strategy, The Headquarters for Japan's Economic Revitalization, 2015).

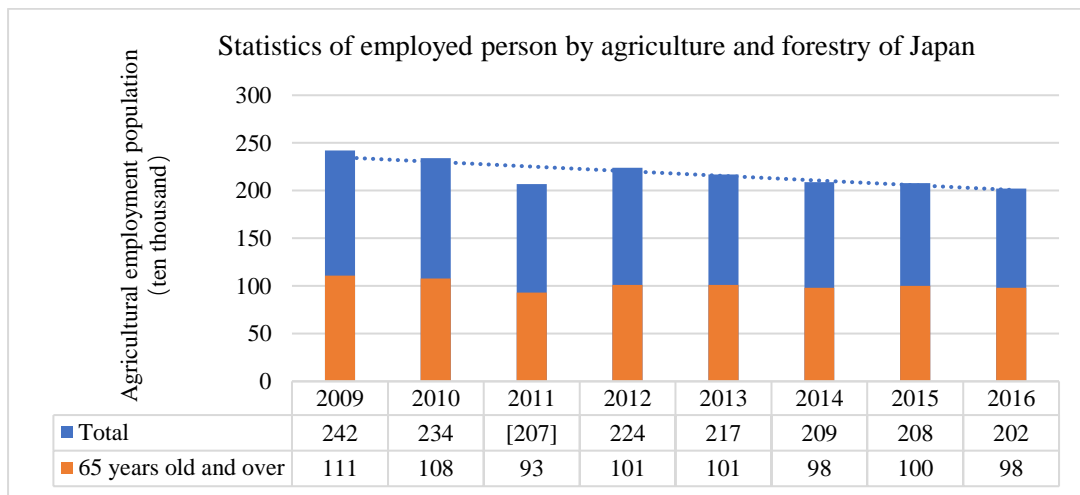


Figure 5.1. Statistics of employed person by agriculture and forestry of Japan

It is still a challenging subject for mobile robots operating in agricultural environments because of the changes in weather conditions and variations of the nature of the terrain and vegetation. Study of agricultural autonomous vehicle keeps popular for long time. Autonomous navigation systems could work for different tasks, such as planting, weeding, spraying, fertilizing, inspection, cultivating, harvesting and transportation. The visual sensors such as cameras have been widely used in robotic navigation system due to the cost effectiveness and capability to provide huge information. The using of mechanical sprayers, especially in conventional agriculture is the most common form of pesticide applications. It reported that over 98% of

insecticides sprayed and 95% of herbicides reach a destination other than their target species, because of sprayed or spread across entire farmlands. Nowadays, it is widely recognized that the abuse of agricultural chemicals is harmful to our environment. To reduce the use of pesticides and improve the efficiency, spray technology has become got importance topic in the field of precision agriculture. In the previous chapter, we have focused the potential of UAV in agricultural sensing system and application.

UAVs have the potential in agricultural applications and have ideal solution to enable precision agriculture compare to aerial mapping and satellite remote sensing. Not only use of UAVs is more efficient, but also more cost-effective compare to areal or high-resolution commercial satellite data sets. It helps farmers to monitor crops in real-time and provides high-resolution images of field and canopy for crop growth and production. For example, some researchers tried to create accuracy maps using the HD images acquisition with UAV for precision agricultural to monitor the crops growing and guided autonomous agricultural robotics for target operations (spraying, harvest transporting and weeding control). It could effectively improve the operational efficiency, guide the transportation vehicle and reduce dependence on agricultural labor force by collaborative work for autonomous agricultural robots with UAV.

Objectives

The aim of this part of research is to develop a UAV-follower based autonomous spray system using feature recognition for target spraying for precision agricultural practices. Further, coordination of UAV-follower vehicle. It is expected that the autonomous electrical vehicle with spraying system could follow the UAV (map-based or target tracking) for spraying inside the target field.

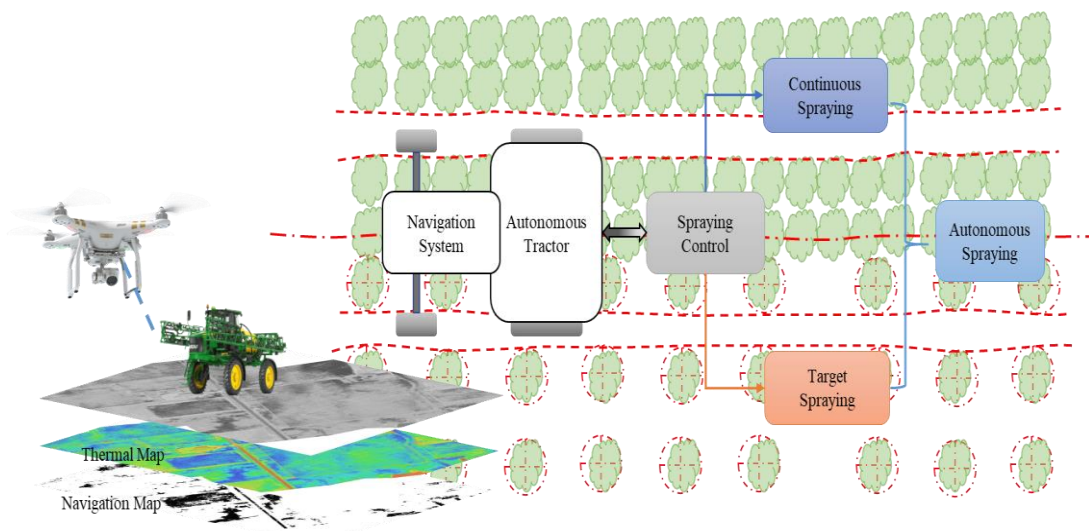


Figure 5.2. UAV-Follower based autonomous spray system

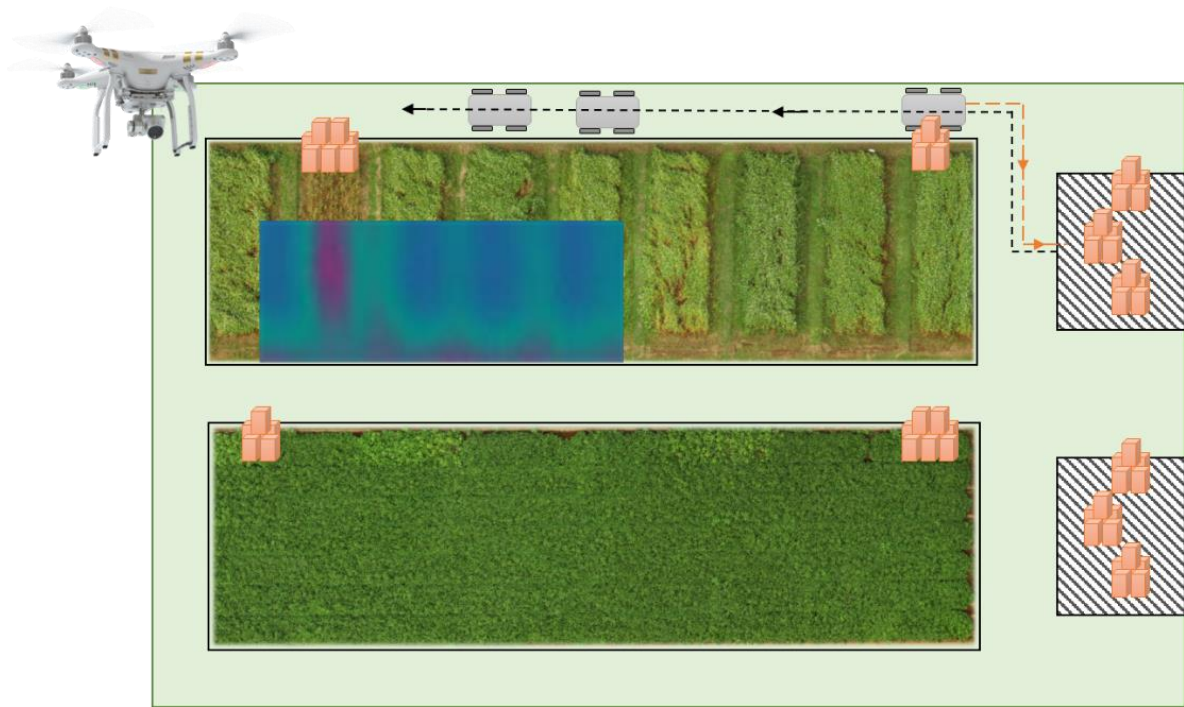


Figure 5.3. UAV-Follower based autonomous transportation system

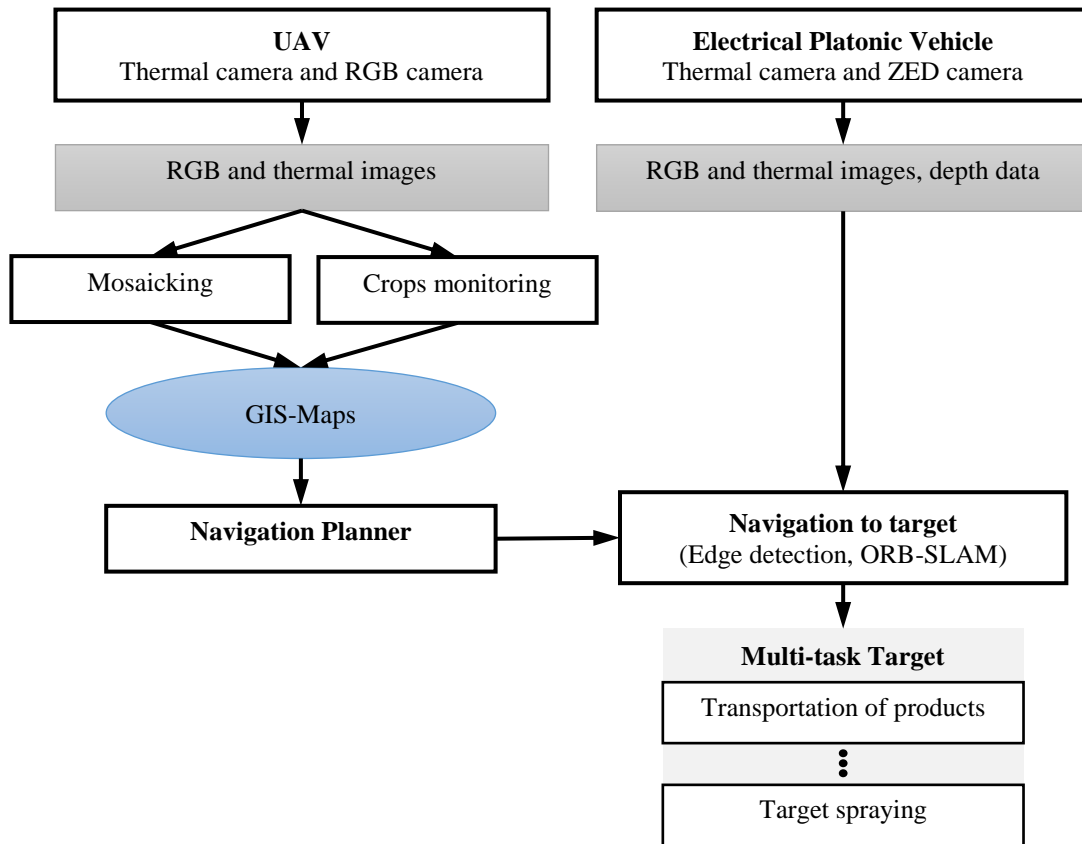


Figure 5.4. Flowchart to integrate UAV image and Electronic Platonic Vehicle (EPV) through Navigation Planner

5.2 Materials and Materials

5.2.1 ORB-SLAM

ORB-SLAM (Simultaneous Localization and Mapping) is a versatile and accurate SLAM solution for monocular, stereo and RGB-depth cameras. ORB-SLAM is based on the Oriented FAST and rotated BRIEF (ORB) features which is a fast-robust local feature detector, it is rotation invariant and resistant to noise, less affected by image noise, and is capable of being used for real-time performance. It operates in real time, in small and large, indoor and outdoor environments.

The ORB-SLAM use the same features (ORB) for all tasks (**Figure 5.5**): tracking, mapping, relocalization and loop closing. It makes the system more efficient, simple and reliable compare to the other SLAM systems.

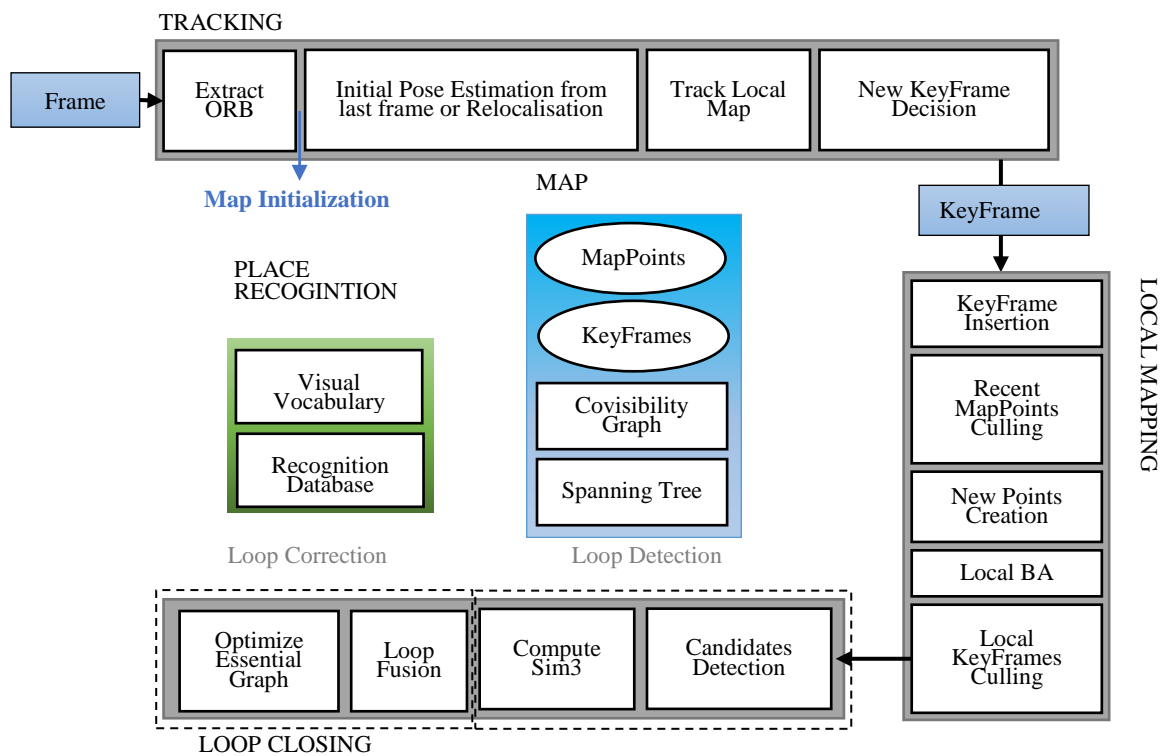


Figure 5.5. Overview of ORB – SLAM system

5.2.2 Image Edge Detection

Edge detection is a basic tool for image processing, computer vision and machine vision, especially in the areas of detection and extraction features. Edge detection includes various mathematical methods that are intended to identify points in a digital image that have sharp changes in brightness or more formal discontinuities. The point at which the brightness of the

image changes drastically is usually organized into a set of curved segments called edges. (Raman Maini, etc., 2009). Detecting sharp changes in image brightness is to capture changes in important events and world properties. It can be shown that under fairly general assumptions about the image forming model, the discontinuity of image brightness may correspond to: discontinuity in surface orientation, discontinuity in depth, changes in material properties, and changes in scene illumination. Commonly, it divided into two categories for most of the edge detection methods, search-based and zero-crossing based. The search-based method detects the edge by first calculating a measure of the edge strength, typically a first derivative expression, such as a gradient magnitude, and then uses the calculated estimate of the local direction to search for the local direction maximum of the gradient magnitude. The edge, usually the gradient direction. The zero-crossing method searches for a zero-crossing in the second-order derivative expression computed from the image to find the edge, usually the zero-crossing of the nonlinear difference expression or the zero-crossing of the Laplacian operator.

5.2.2.1 Sobel operator

It can be applied to estimate image gradients from the input image by using different gradient operators. Using central differences is the simplest approach, it could be found as:

$$L_x(x, y) = -\frac{1}{2}L(x - 1, y) + 0 \cdot L(x, y) + \frac{1}{2} \cdot L(x + 1, y) \quad (5.9)$$

$$L_y(x, y) = -\frac{1}{2}L(x, y - 1) + 0 \cdot L(x, y) + \frac{1}{2} \cdot L(x, y + 1) \quad (5.10)$$

The following filter mask is applied to the image data:

$$L_x = [-1/2 \quad 0 \quad 1/2] \quad (5.11)$$

$$L_y = \begin{bmatrix} +1/2 \\ 0 \\ -1/2 \end{bmatrix} \quad (5.12)$$

The Sobel operator is based on the filters as following:

$$L_x = \begin{bmatrix} -1 & 0 & +1 \\ -2 & 0 & +2 \\ -1 & 0 & +1 \end{bmatrix} \quad (5.13)$$

$$L_y = \begin{bmatrix} +1 & +2 & +1 \\ 0 & 0 & 0 \\ -1 & -2 & -1 \end{bmatrix} \quad (5.14)$$

Given this estimate of the first-order image derivative, the gradient magnitude is then calculated as:

$$|\nabla L| = \sqrt{L_x^2 + L_y^2} \quad (5.15)$$

where the gradient orientation is estimated like: $\theta = \text{atan2}(L_y, L_x)$

5.2.2.2 Robert's cross operator

The Roberts Cross operator performs simple, fast-calculated two-dimensional spatial gradient measurements on the image. It represents the estimated absolute magnitude of the spatial gradient of the input image of pixel value at each point in the output. The operator with a pair of 2×2 convolution kernels:

$$\begin{bmatrix} +1 & 0 \\ 0 & -1 \end{bmatrix} \text{ and } \begin{bmatrix} 0 & +1 \\ -1 & 0 \end{bmatrix} \quad (5.16)$$

One kernel is simply another core rotated by 90°. Gradient magnitude is calculated as:

$$\nabla I(x, y) = G(x, y) = \sqrt{G_x^2 + G_y^2} \quad (5.17)$$

where the gradient orientation can be estimated as:

$$\theta = \arctan\left(\frac{G_y}{G_x} - \frac{3\pi}{4}\right) \quad (5.18)$$

5.2.2.3 Canny Edge Detector

Canny edge detection is a technique for extracting useful structural information from different visual objects and significantly reducing the amount of data to be processed. (John C., 1986). The Canny edge detection algorithm contains 5 different steps: Apply a Gaussian filter to smooth the image to eliminate noise; find the intensity gradient of the image; apply non-maximum suppression to eliminate spurious responses to edge detection; apply double thresholds to determine potential edges; track the edges by hysteresis: edge detection is

ultimately determined by suppressing all other edges that are weak and not connected to strong edges.

5.2.2.4 Gaussian filter

Since all edge detection results are susceptible to image noise, noise must be filtered out to prevent false detections caused by noise. The Gaussian filter is applied to the image convolution to smooth the image. This step will make the image slightly smoother to reduce the effect of significant noise on the edge detector. The equation of the Gaussian filter kernel of size $(2k + 1) \times (2k + 1)$ is given by:

$$H_{ij} = \frac{1}{2\pi\sigma^2} \exp\left(-\frac{(i-(k+1))^2 + (j-(k+1))^2}{2\sigma^2}\right); 1 \leq i, j \leq (2k + 1) \quad (5.17)$$

Here is an example of a Gaussian filter with the size of 5×5 for creating the adjacent image, with $\sigma = 1.4$ (The asterisk indicates convolution operation).

$$B = \frac{1}{159} \begin{bmatrix} 2 & 4 & 5 & 4 & 2 \\ 4 & 9 & 12 & 9 & 4 \\ 5 & 12 & 15 & 12 & 5 \\ 4 & 9 & 12 & 9 & 4 \\ 2 & 4 & 5 & 4 & 2 \end{bmatrix} * A \quad (5.18)$$

The size of the selected Gaussian kernel will affect the performance of the detector. The larger the size, the lower the sensitivity of the detector to noise. Edge detection operators (such as Roberts, Prewitt, or Sobel) return the values of the first derivative of the horizontal (G_x) and vertical (G_y) directions. Thus, the edge gradient and direction can be determined:

$$G = \sqrt{G_x^2 + G_y^2} \quad (5.19)$$

$$\Theta = \text{atan2}(G_x, G_y) \quad (5.20)$$

Where G can be calculated using the Hypot function, atan2 is an arctangent function with two parameters.

5.2.2.5 Edge Tracking by Hysteresis

Some edge pixels are still caused by noise and color changes. To account for these spurious responses, edge pixels with weak gradient values must be filtered out and edge pixels with high gradient values must be preserved. This is achieved by selecting a high threshold and a low threshold. If the gradient value of the edge pixel is above the high threshold, it is marked as a strong edge pixel. If the gradient value of the edge pixel is less than the high threshold and greater than the low threshold, it is marked as a weak edge pixel. If the value of the edge pixel

is less than the low threshold, it is suppressed. The two thresholds are determined empirically, and their definition will depend on the content of a given input image.

5.2.3 Development of the Navigation System

In this study, we chose a 3D (ZED) camera for navigation. ZED camera is a 3D camera that provides depth sensing, position tracking and 3D graphics for any application. It could be used for robotics, VR (virtual reality) and 3D analytics. It contains dual 4MP camera for capturing 3D videos with high-resolution and high frame-rate. It could capture 110° wide-angle video and depth perception indoors and outdoors at up to 20m (0.5m-20m). The function of creating 3D dense map using Octomap was added to the system, because the ORB-SLAM generated sparse point clouds which is limitation for navigation and led to tracking lost easily. The Octomap was used for creating 3D dense map has little impact on real-time performance compared to sparse point clouds. And we send the motion and attitude signal $[V, a, \alpha, \delta]$ to the autonomous vehicle for guiding and navigation (Figure 5.6). The Octomap is projected on the GIS environment for mapping in the global positioning points. In case remote assisted autonomy of multiple coordinated UAV-based robot system GIS based navigation, planner is required.

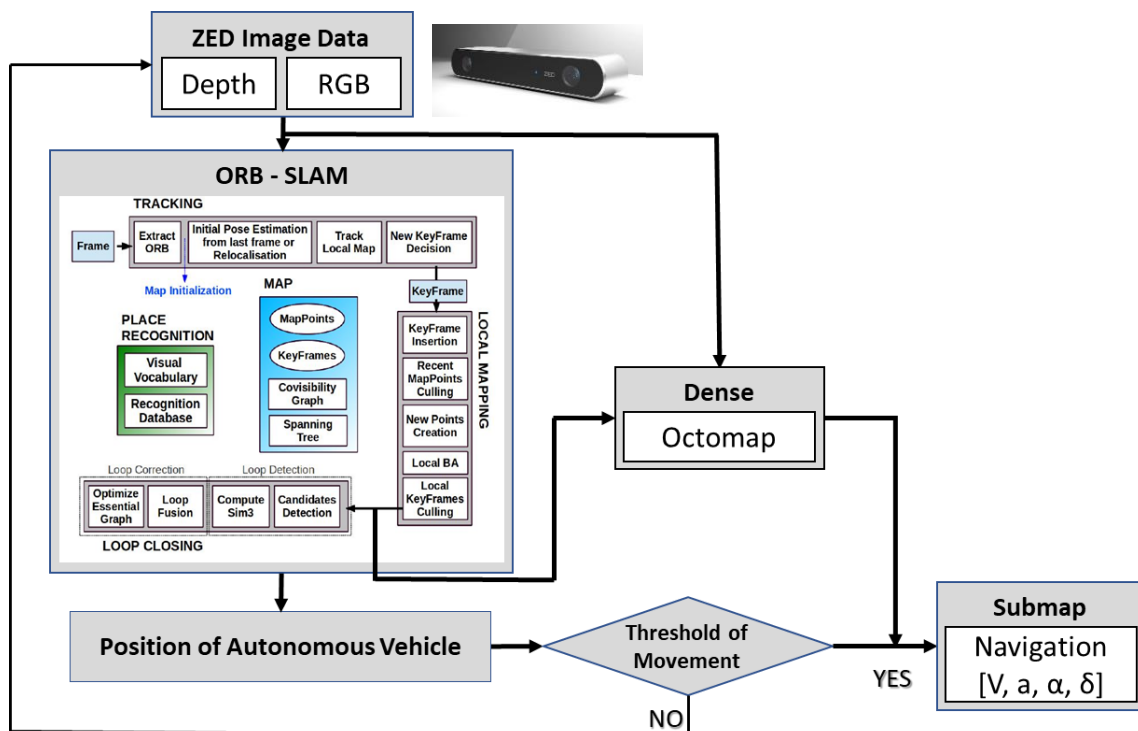


Figure 5.6. Create 3D dense map using Octomap

5.2.4 Development of Autonomous Electrical Vehicle

Two DC motors were installed in the autonomous electrical vehicle, one for driving and the other for steering. The DC motors was controlled by micro controller, it could execute moving and steering commands from the navigation system. One encoder was connected with the steering unit for monitoring the steering angle of vehicle. The other two encoders were equipped with the rear wheels for calculating the speed. The data was collected by an Arduino UNO. Again, a IMU sensor was used for detecting the attitude of the autonomous vehicle and feedbacking to the navigation for correcting controlling error. The IMU sensor (MPU – 6050 Module) is made with a 3-axis gyroscope and a 3-axis accelerometer on the same silicon die, which designed for the low power and cost, and high-performance requirements (**Figure 5.7**).

5.2.5 Development of Autonomous Spraying System

Spraying system contains two main parts, the main body and spraying actuator module. DC pump was for supporting presser of spraying and flowmeter was selected for controlling the amount of spray. The spraying actuator module contained 5 nozzles (**Figure 5.8**).

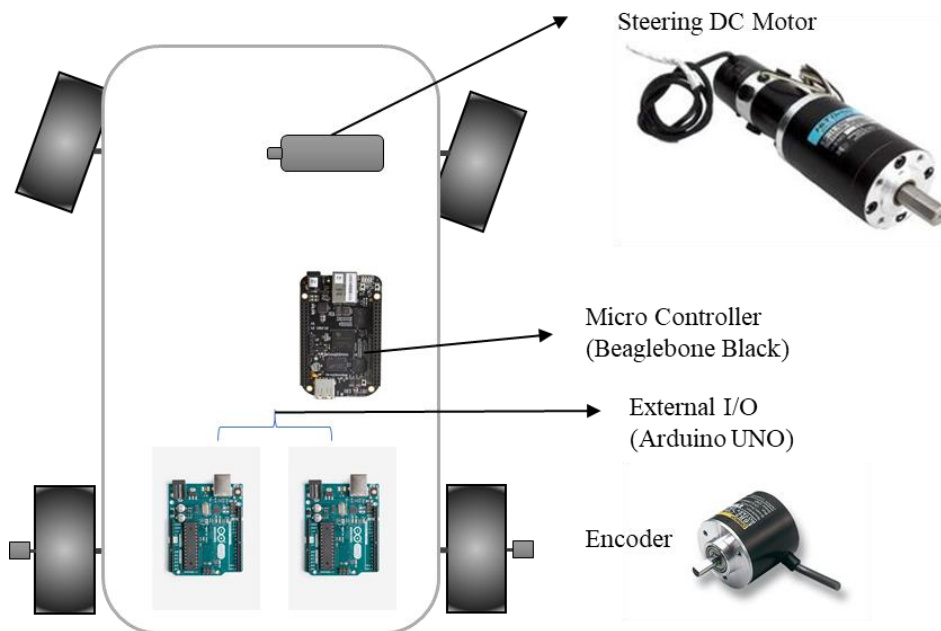


Figure 5.7. Development of autonomous electrical vehicle

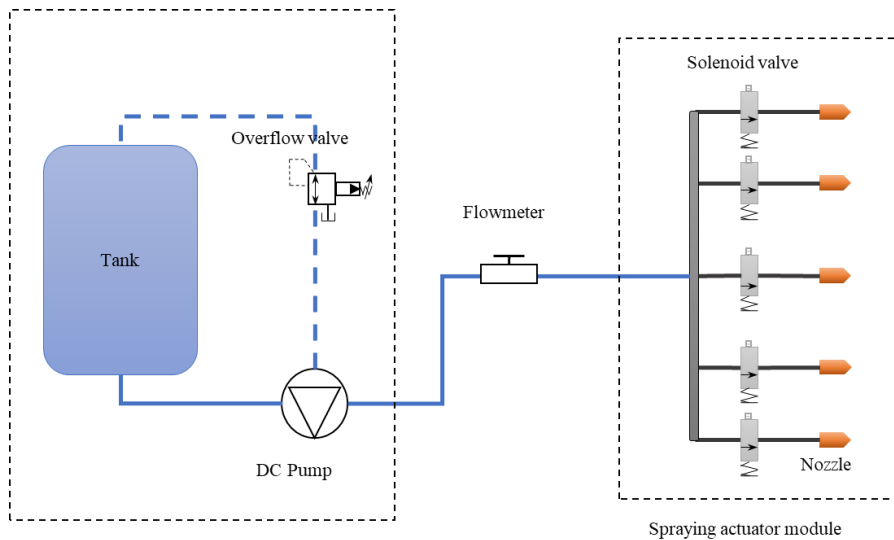


Figure 5.8. Development of Autonomous Spraying System

5.2.6 Choice of Work Patterns

1. Continuous Spraying

$$L/V < TT \quad (5.21)$$

2. Interval (target) Spraying

$$L/V > TT \quad (5.22)$$

Minimum operation time is less than moving time to adjacent plants, continuous spraying control strategy is adopted. Otherwise, target spraying control strategy will be used.

3. Mixed pattern

Including two work patterns above, judged by different plants spacing. Where, L is Adjacent plants spacing, V is the Velocity of spraying robot and TT is the Minimum operation time (threshold) (**Figure 5.9**).

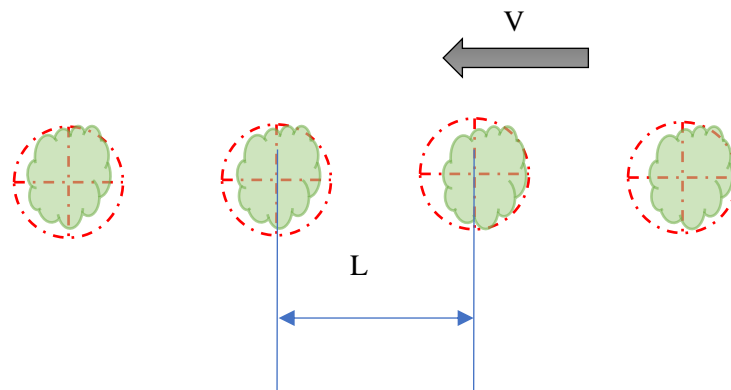


Figure 5.9. Choice of work patterns

5.2.7 Plants Edge Detection Using Canny Edge Detector

To achieve tart spraying, the position and size of plans should be detected. A plants edge detection system was developed using Canny edge detector, and Kalman filter was used for noise reduction, the k value for filtering was changeable for analyzing the best detecting results.

5.2.8 Images Mosaicking for Local Mapping

An open source software OpenDroneMap was selected for mosaicking aerial drone imagery. A typical drone uses a simple point-and-shoot camera, so images from drones, from different perspectives, are like any photos taken from a point-and-shoot camera, such as drones, balloons, kites and street view data. OpenDroneMap converts these simple images into 3D geographic data that can be used in conjunction with other geographic datasets. It uses ORB-SLAM to render texture meshes from video.

5.3 Results

5.3.1 ORB Features Extraction and Matching

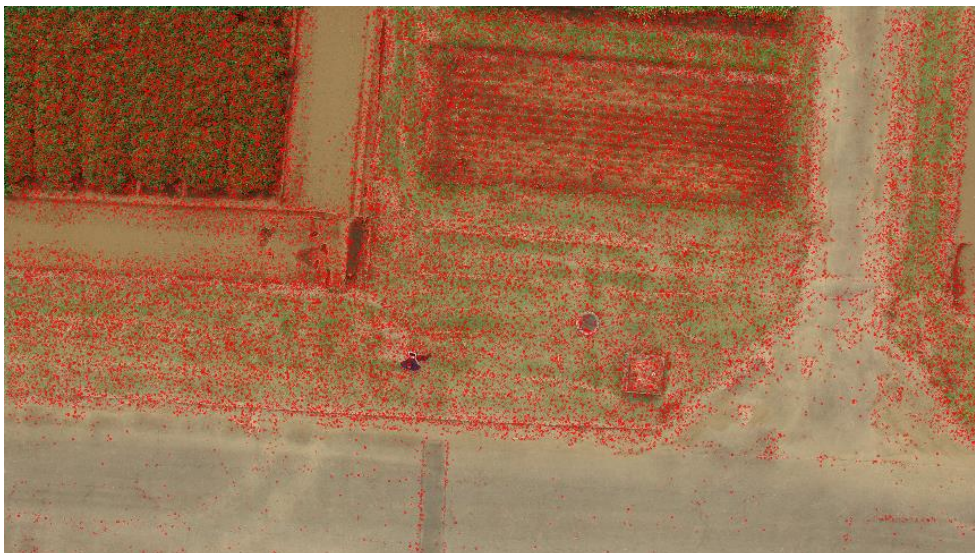


Figure 5.10. ORB features extraction without selected using EKF



Figure 5.11. ORB features extraction and selected using EKF

Table 5.1. ORB features extraction and selected using EKF

	Number of ORB Features	Selected ORB Features (EKF, k=2)	Reduction rate
RGB Camera	83961	53482	36.3%
	92767	58658	36.8%

5.3.2 ORB-SLAM Simulation

Large numbers of ORB features were extracted by the system, and many were invalid features (**Figure 5.11, Table 5.1**). In order to decrease the noise of images and increase calculating speed, EKF (Extended Kalman filter, $k=2$) was used for selecting good matching points at first step. The invalid features could reduce more than 36% after using EKF for selecting the ORB features (**Table 5.1**). The trajectory planning is shown while the large numbers of features are detected, and key features were selected for path generation (**Figure 5.11**).

5.3.3 Edge Detection Using Canny Edge Detector

Canny edge detector was used to detect the edge, soil and plants, which find the edge of the features; the edge of the features could help in navigation system as a map-based references

(Figure 5.12). In this case we, have used canny used detector for the EPV and UAV both to find out the edges of the features.

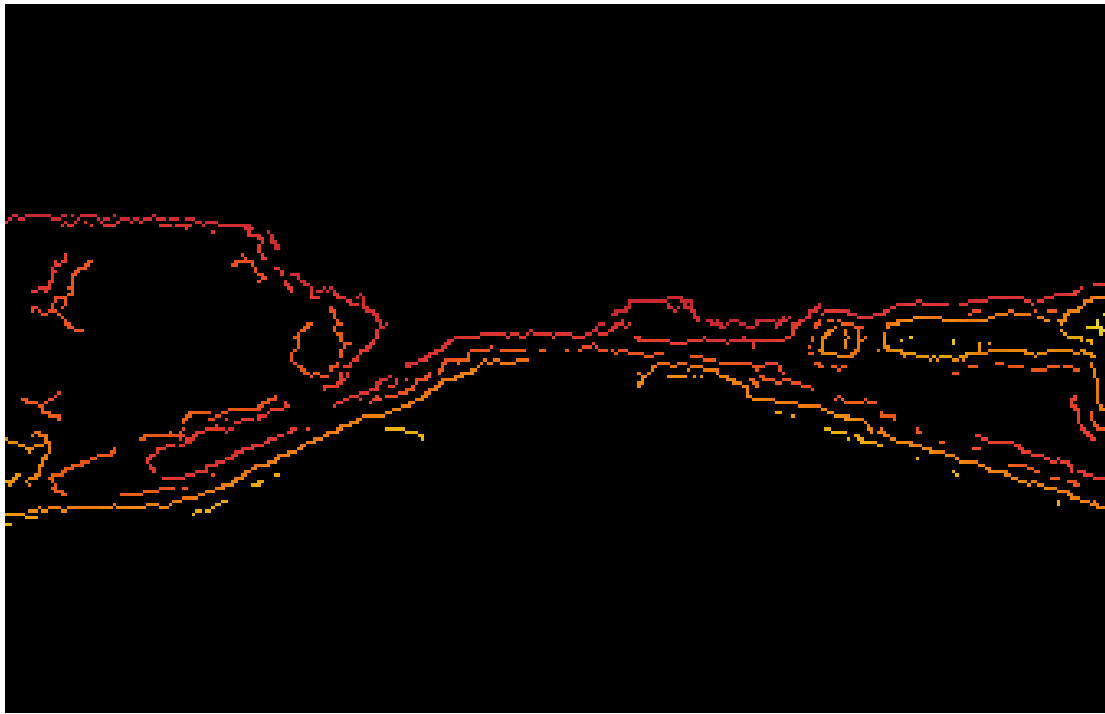


Figure 5.12. Road edge detection using Canny edge detector using EPV



Figure 5.13. ORB features detected by ORB-SLAM system using ZED camera to navigate the EPV

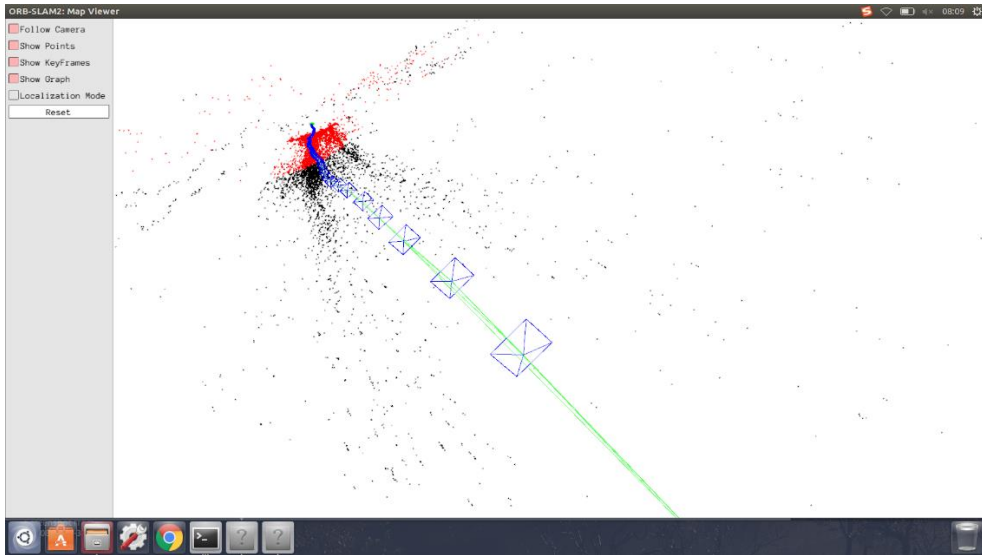


Figure 5.14. Simulation experiment results for navigation using ORB-SLAM using ZED camera system to navigate the EPV

5.3.4 UAV Features Mapping for Developing Navigation Planner

The UAV images system for crop plant growth and field condition was mapped to mosaic multiple images taken by the UAV at the T-PIRC farm. Total 81 images were taken with 30% overlap to develop the mosaic map for field 1 with crops (**Figure 5.15**) and 96 images were taken to develop the mosaic with same overlap percentage for field 2 (**Figure 5.16**). The GIS-based navigation planner map will be developed in our further research using ArcGIS and local ground trothing points.

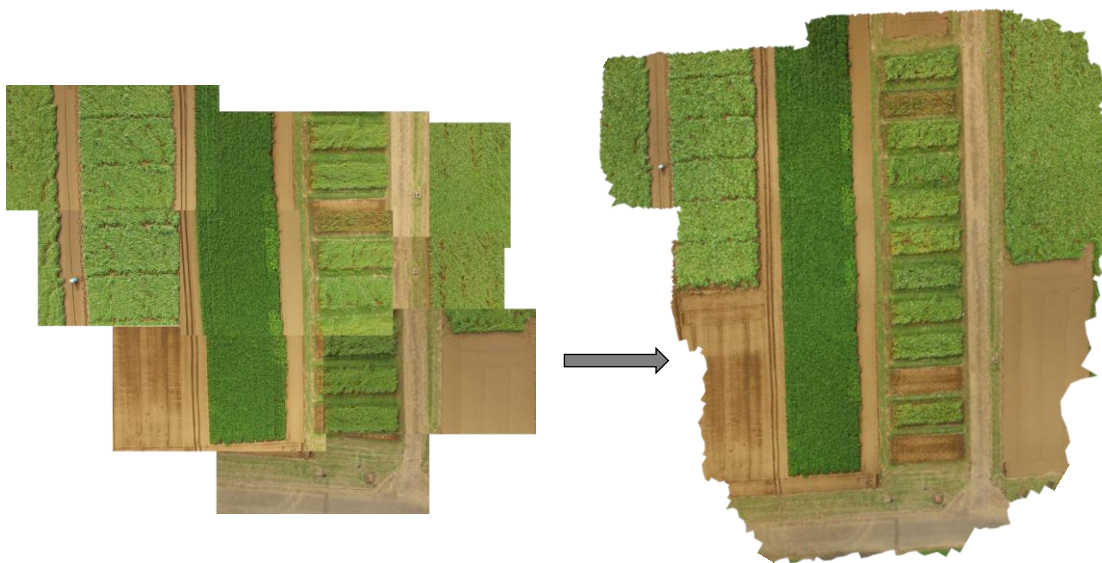


Figure 5.15. Images mosaicking for local mapping

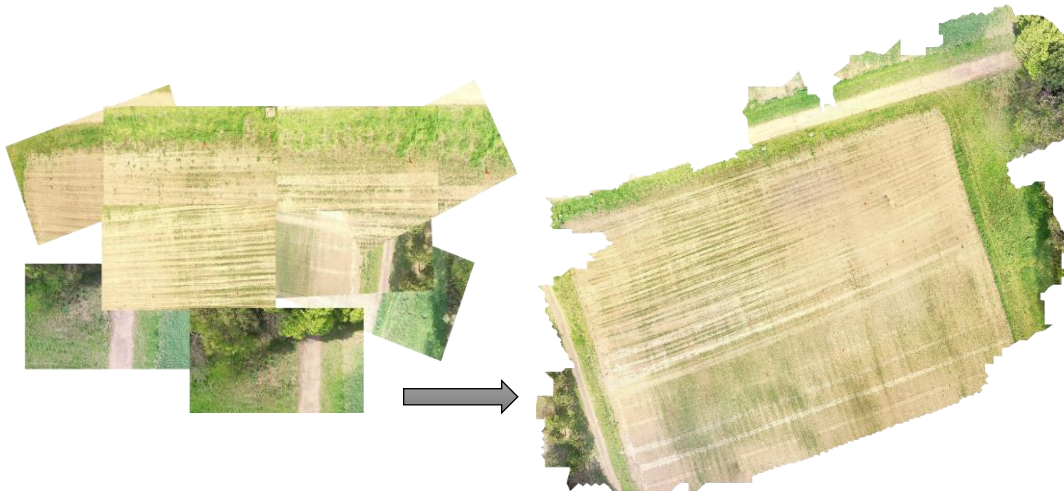


Figure 5.16. Images mosaicking of agricultural fields

5.4 Discussion

The coordination navigation system was the aim of the subjects. The coordination-based navigation could help in agricultural work to reduce with remote assistance for autonomous application of multiple robots. In this part of the research the attempts were taken to join feature recognition system for further application with aided in EPB and UAV. The UAV was considered as the leader of the multiple coordinated mobile robots. In the further research, field worked will be conducted based on the navigation planer with UAV leader for EPV vehicles.

5.5 Summary

This research was conducted to develop UAV-follower based multi-task robot's system using features recognition and navigation planner for working in the farm. In the present scenario, Japanese agricultural labor declining situation, multi-task robot planner is needed which is smaller in size and can work in rural farms. With this reason, this part of the research attempted to add navigation planer concept, some of the experimental and simulation data using ORB features. ORB features were collected from the UAV and mosaic map was developed to add in the navigation planer. In the navigation planer, the EPV robots-based operations are in lined for road navigation, transpiration of products, and target spraying. This chapter will be reported further after completion of the experiments for UAV-follower system. The EPV platform is built to test with feature recognition system. 3D-based image acquisition, ORB features extraction is completed along with edge detection. In further research, vision based EPV

mobile robots' experiments will be conducted to follow the UAV with the aid of navigation planner to complete multi-task inside the farm.

Chapter 6

Conclusions and Further Research

The research was aimed to develop a machine learning system to recognize the features from UAV platform for precision agricultural management. In the precision agricultural management, one of the targets about the spray and nonspray area recognition, moisture content information for irrigation and small-scale robot application to work in the field. The following major contributions are made to achieve the goal of this proposed research. Furthermore, the additional researches are also proposed in continuation of this thesis.

6.1 Development of a Machine Learning System with High Computational Speed for Agricultural Recognizing Features

The machine learning system was developed using MSM for images collected by a UAV in different types of farm fields. The machine learning system was developed to train and test the datasets for two classifiers of agricultural croplands and orchard areas for enabling autonomous spraying system in future. The classifiers were sub categorized as spray and non-spray areas. Datasets images were collected from low (5 m) and high altitude (15 m) respectively. The offline recognition system was noted as 70.4% and 80.5% for low and high-altitude systems respectively. On other hand, the online recognition system performance was reported with higher accuracy of 80% from low altitude and 71% from higher altitude image acquisition systems. The computation time for online recognition system was observed minimum with an average 0.004 s for reporting recognition of each of the frame for classifiers. The developed machine learning system for recognizing the classifiers can be implemented in the autonomous UAV spray system for recognizing spray and non-spray within the minimum computation in real-time.

6.2 Detection Soil Moisture Content from Thermal Images

The study aims to measure field moisture content using thermal image processing for precision agricultural management. Developed the calibration method for detecting soil moisture with thermal images. UAV images were collected with thermal camera. Soil moisture from ground reference was directly measured to correlate with thermal images digital numbers using the regression model. For measuring field moisture content using thermal camera, we have

collected soil samples to analyses the digital data of thermal images to find out the relation with soil moisture. Monotectic analysis was conducted to confirm the relation between soil moisture content information and thermal imagery. An algorithm was developed based on the ORB and SURF features for mosaicking images. The matching accuracy was just noted 61.7% for ORB features and 89% was observed using SURF features. Extended Kalman filter (EKF) was used for reducing the noise. SURF featured had better performance using thermal images. Soil moisture measurement using thermal imagery from UAV needs further confirmation.

6.3 Vision based Multi-task Robot System for Agricultural Farm

This research was conducted to develop vision system and integrate feature recognition procedure through UAV-based leader follower system. The Simultaneous Localization and Mapping (SLAM) approach are used to simulate the path planer for an autonomous spray system. This part of this research has the target to utilize the RGB image maps, which are targeted to develop the map-based system from drone image to navigate and apply chemical inside the field. While working inside the field it was also necessary to detect the road running and field edge detection. Canny edge detection was utilized to reduce the feature and identify the key features from ORB features. Further research will be conducted to map-based navigation system for UAV leading multi-task robot system to spray on the targeted areas, transportation of products and scouting in the field.

6.4 Further Research

To accomplish the goal and further application of this research, the following key areas will be conducted to work in leader follower system for UAV and autonomous small-sprayer.

6.4.1 Automated Field Moisture Determination using Wireless Sensor Network (WSN)

Cloud-based machine learning system will be developed for automated field moisture determination using WSN. UAV thermal imagery and WSN will be utilized for train the datasets for developing automated soil moisture information. Ground reference soil moisture sensors will be used to train the datasets. The soil moisture information from field and canopy moisture content information could help in understanding of irrigation management and leaf wetness or humidity.

6.4.2 UAV and Multi-robot SWARM Application

In the Japanese agricultural environment, the small-scale robot has the more opportunity in related safety points to utilize in the farm. In our future research, developed featured map from UAV and multi-robot application scenario will be developed. The cloud-based operation system and remote assistance simulation will be proposed for future application.

6.5 Outlook of Future Agriculture

The problem of aging population and insufficient agricultural labor force has become increasingly prominent, so that a large number of high-quality fields are abandoned. Particularly serious, these problems can lead to food safety and serious social problems. Urgently needed advanced technology to solve this problem. It urgently needed advanced technology to solve this problem, such like the agricultural applications of robotic, IoT technologies, ICT, remoting management skills, etc. Nowadays, with the development of computer sciences and sensors, it would be able to achieve autonomously working with the driverless tractors or agricultural autonomous machinery within 10 years. However, the autonomous tractors or autonomous agricultural machinery still appears to be insufficient for the whole agricultural production process from farmland preparation to harvesting and finally arriving at the table of the diners. This requires coordination of multiple technologies. For example, UAV would be used for cruise monitoring of the farmland or plantations, the IoT system could achieve precision management during crops growth, and the robotics would be used for target management and autonomous harvesting for realize the unmanned and smart management of whole agricultural production.

Acknowledgements

Firstly, I would like to express my profound gratitude and sincere appreciation to my academic advisor and research supervisor Dr. Tofael Ahamed, for his availability, expertise and advice, motivation, and encouragement to move forward. His kind advice, scholastic guidance, sympathetic supervision, and encouragement guided me to walk on this avenue.

It is my great pleasure to express indebtedness, deepest sense of gratitude, sincere appreciation to my research supervisor Professor Dr. Tomohiro Takigawa who introduced me to a most compelling research path. His kind advice and wealth of knowledge guided me to start the academic research.

I am pleased to express my cordial respects and gratitude to Associate Professor Ryoza Noguchi, Assistant Professor Takuma Genkawa, Professor Shusuke Matsushita and Professor Kota Motobayashi, members of the advisory and thesis evaluation committee for their kind comments, advice, and suggestions during the course of this study.

Special thanks should be expressed to staffs of Agricultural and Forestry Research Center, University of Tsukuba: Mr. Tsuyoshi Honma for fabricating experimental equipment's, Mr. Yasuhiro Matsumoto and Mr. Akira Saitoh for their helps on maintaining the experimental vehicle. I acknowledge my gratitude to the Embassy of Japan, for selecting as a candidate for MEXT scholarship. Also, thanks go to the Ministry of Education, Culture, and Science, Japan for granting the scholarship that covered my study and stay in Japan.

Sincere gratitude and thanks to my seniors Dr. Zhang Linhuan, and my research partner Yan Zhang for their great support during study. Special thanks are extended to sincere gratitude and thanks to my lab fellows, Md Monirul Islam, Munirah Hayati Hamidon and Ms. Juliet Ngo for their help and assistants during experiments and completion of thesis. I also thank Dr. Nazia Muhsin, Dr. Riska Ayu Purnamasari and Dr. M Monjurul Islam for their great camaraderie.

Sincere expression of gratitude is due to my family, their tolerance and understanding, companionship and support always motivate and encourage me. Especially, gratitude and thanks from the heart for my deeply loved wife, taking all the family responsibilities for taking care of parents and my son, enable me to focus more on research.

References

- Adão, T., et al. (2017). "Hyperspectral Imaging: A Review on UAV-Based Sensors, Data Processing and Applications for Agriculture and Forestry." *Remote Sensing* 9(11): 1110.
- Berni, J., et al. (2009). "Thermal and Narrowband Multispectral Remote Sensing for Vegetation Monitoring from an Unmanned Aerial Vehicle." *IEEE Transactions on Geoscience and Remote Sensing* 47(3): 722-738.
- Bishop, Christopher (2006). *Pattern recognition and machine learning*. Berlin: Springer. ISBN 0-387-31073-8.
- Carrio, A., et al. (2017). "A Review of Deep Learning Methods and Applications for Unmanned Aerial Vehicles." *Journal of Sensors* 2017: 1-13.
- Castro Jimenez, L. E. and E. A. Martinez-Garcia (2016). "Thermal Image Sensing Model for Robotic Planning and Search." *Sensors (Basel)* 16(8).
- English, A., et al. (2014). "Vision based guidance for robot navigation in agriculture." 1693-1698.
- Fukui, K. (2014). *Subspace methods*. Computer Vision, Springer: 777-781.
- Fukui, K. and O. Yamaguchi (2007). The kernel orthogonal mutual subspace method and its application to 3D object recognition. *Asian Conference on Computer Vision*, Springer.
- Fukui, K. and Yamaguchi O. The kernel orthogonal mutual subspace method and its application to 3D object recognition. *Asian Conference on Computer Vision*, Springer. 2007.
- Fukui, K. and O. Yamaguchi (2005). Face recognition using multi-viewpoint patterns for robot vision. *Robotics Research. The Eleventh International Symposium*, Springer.
- Fukui, K. and Yamaguchi O. Face recognition using multi-viewpoint patterns for robot vision. *Robotics Research. The Eleventh International Symposium*, Springer. 2005.
- González-Aguilera, D., et al. (2012). "Novel approach to 3D thermography and energy efficiency evaluation." *Energy and Buildings* 54: 436-443.
- Hung, C., et al. (2014). "Feature Learning Based Approach for Weed Classification Using High Resolution Aerial Images from a Digital Camera Mounted on a UAV." *Remote Sensing* 6(12): 12037-12054.
- Hornung, A., et al. (2013). "OctoMap: an efficient probabilistic 3D mapping framework based on octrees." *Autonomous Robots* 34(3): 189-206.
- Herbert Bay, Andreas Ess, Tinne Tuytelaars, and Luc Van Gool, (2008). *Speeded Up Robust Features*, ETH Zurich, Katholieke Universiteit Leuven.

- Iijima, T., et al. (1974). A theory of character recognition by pattern matching method. Learning systems and intelligent robots, Springer. 1973, 437-450.
- Jones, H. G., et al. (2009). "Thermal infrared imaging of crop canopies for the remote diagnosis and quantification of plant responses to water stress in the field." *Functional Plant Biology* 36(11): 978.
- John Canny, (1986). A Computational Approach to Edge Detection, *IEEE Transactions on pattern analysis and machine intelligence*, VOL. PAMI-8, NO. 6.
- Lagüela, S., et al. (2012). "Automation of thermographic 3D modelling through image fusion and image matching techniques." *Automation in Construction* 27: 24-31.
- Lee, D. H., et al. (2012). "Development of Autonomous Sprayer Considering Tracking Performance on Geometrical Complexity of Ground in Greenhouse." *Journal of Biosystems Engineering* 37(5): 287-295.
- Lagüela, S., et al. (2011). "Energy efficiency studies through 3D laser scanning and thermographic technologies." *Energy and Buildings* 43(6): 1216-1221.
- Majidi, B. and A. Bab-Hadiashar (2005). Real time aerial natural image interpretation for autonomous ranger drone navigation. *Digital Image Computing: Techniques and Applications*, IEEE.
- Maeda, E. and H. Murase (1999). Multi-category classification by kernel based nonlinear subspace method. *Acoustics, Speech, and Signal Processing, 1999. Proceedings., 1999 IEEE International Conference on*, IEEE.
- Maeda, K.-i. and S. Watanabe (1985). "A pattern matching method with local structure." *Trans. IEICE* 68(3): 345-352.
- Maeda K., Watanabe S. Pattern matching method with local structure. *Trans IEICE*. 1985, J68-D: 345–352.
- Nevalainen, O., et al. (2017). "Individual Tree Detection and Classification with UAV-Based Photogrammetric Point Clouds and Hyperspectral Imaging." *Remote Sensing* 9(3): 185.
- Peteinatos, G. G., et al. (2014). "Potential use of ground - based sensor technologies for weed detection." *Pest management science* 70(2): 190-199.
- Peña Barragán, J. M., et al. (2012). Object-based approach for crop row characterization in UAV images for site-specific weed management. *Proceedings of the 4th GEOBIA, May 7-9, 2012 - Rio de Janeiro - Brazil*. p.426.
- Pimentel, D. and M. Burgess (2011). "Small amounts of pesticides reaching target insects." *Environment, Development and Sustainability* 14(1): 1-2.
- Rebetez, J., et al. (2016). Augmenting a convolutional neural network with local histograms—a case study in crop classification from high-resolution UAV imagery. *European Symposium on Artificial Neural Networks, Computational Intelligence and Machine Learning*. Bruges (Belgium), 27-29.

- Rublee, Ethan; Rabaud, Vincent; Konolige, Kurt; Bradski, Gary (2011). ORB: an efficient alternative to SIFT or SURF. IEEE International Conference on Computer Vision (ICCV).
- Raman Maini, et al. (2009). Study and Comparison of Various Image Edge Detection Techniques, International Journal of Image Processing (IJIP), Volume (3): Issue (1).
- Sun, W., et al. (2015). "Preparation Analysis on Effect Factors of Spraying Quality for Boom Sprayer." 49-55.
- Salamí, E., et al. (2014). "UAV Flight Experiments Applied to the Remote Sensing of Vegetated Areas." Remote Sensing 6(11): 11051-11081.
- Sakano, H.; Mukawa, N.; Nakamura, T. Kernel mutual subspace method and its application for object recognition. Electronics and Communications in Japan (Part II: Electronics). 2005, 88(6): 45-53.
- Torres-Sánchez, J., et al. (2015). "An automatic object-based method for optimal thresholding in UAV images: Application for vegetation detection in herbaceous crops." Computers and Electronics in Agriculture 114: 43-52.
- Turner, D., et al. (2014). "Spatial Co-Registration of Ultra-High Resolution Visible, Multispectral and Thermal Images Acquired with a Micro-UAV over Antarctic Moss Beds." Remote Sensing 6(5): 4003-4024.
- Tellaache, A.; Xavier P.; et al. A vision-based method for weeds identification through the Bayesian decision theory. Pattern Recognition. 2008, 41(2): 521-530. Majidi, B. and A. Bab-Hadiashar (2005).
- Watanabe, S. and N. Pakvasa (1973). "Subspace method of pattern recognition." Proc. 1st. IJCP: 25-32.
- Watanabe, S. and Pakvasa N. Subspace method of pattern recognition. Proc. 1st. IJCP.
- Xue, J., et al. (2012). "Variable field-of-view machine vision-based row guidance of an agricultural robot." Computers and Electronics in Agriculture 84: 85-91.
- Yan Z., Pengbo G., Tofael A. Development of a rescue system for agricultural machinery operators using machine vision. Biosystems Engineering. 2018, 169: 149-164.
- Yamaguchi, O., et al. Face recognition using temporal image sequence. IEEE. 1998.
- Zhang, Y., et al. (2018). "A promising trend for field information collection: An air-ground multi-sensor monitoring system." Information Processing in Agriculture.
- Zhang, Y., et al. (2018). "A promising trend for field information collection: An air-ground multi-sensor monitoring system." Information Processing in Agriculture.

- Zhang, Y., et al. (2018). "A promising trend for field information collection: An air-ground multi-sensor monitoring system." *Information Processing in Agriculture* 5(2): 224-233.
- Zhang, Y., et al. (2018). "Development of a rescue system for agricultural machinery operators using machine vision." *Biosystems Engineering* 169: 149-164.
- Zhao, D., et al. (2016). "Theoretical Design and First Test in Laboratory of a Composite Visual Servo-Based Target Spray Robotic System." *Journal of Robotics* 2016: 1-11.
- Zarco-Tejada, P. J., et al. (2012). "Fluorescence, temperature and narrow-band indices acquired from a UAV platform for water stress detection using a micro-hyperspectral imager and a thermal camera." *Remote Sensing of Environment* 117: 322-337.